THE UNIVERSITY OF CALGARY

Block of the cGMP-gated Channels Found in the Outer Segment of Rod and Cone Photoreceptors by Internal and External Organic Cations

by

Stephanie Christine Stotz

A THESIS

SUBMITTED TO THE FACULTY OF GRADUATE STUDIES

IN PARTIAL FULFILMENT OF THE REQUIREMENTS FOR THE

DEGREE OF MASTER OF SCIENCE

DEPARTMENT OF NEUROSCIENCE

CALGARY, ALBERTA

JUNE, 1996

THE UNIVERSITY OF CALGARY

FACULTY OF GRADUATE STUDIES

The undersigned certify that they have read, and recommend to the Faculty of Graduate Studies for acceptance, a thesis entitled "Block of the cGMP-gated Channels Found in the Outer Segment of Rod and Cone Photoreceptors by Internal and External Organic Cations" submitted by Stephanie Christine Stotz in partial fulfilment of the requirements for the degree of Master of Science.

Supervisor, Dr. L.W. Haynes, Department of Neuroscience

Dr. R.J. French, Department of Neuroscience

Dr. K. Sharkey, Department of Neuroscience

Dr. B. Clark, Department of Cardiovascular / Respiratory Sciences

28 June 1995

Date

ABSTRACT

Using tetra-alkylammonium compounds and other organic cations as probes, structural properties of the cone and rod cGMP-gated channel pores have been deduced. Tetramethyl- through tetrapentylammonium block the channels from the intracellular side in a voltage-dependent fashion. Binding energy increased with the addition of one carbon to each of the alkyl side chains in a manner consistent with hydrophobic interactions occurring between the blocker and the pore. Block by tetrahexylammonium was voltage-independent, suggesting that pore size limits access to the channel's intracellular blocker site. Cone, but not rod, channels were blocked by millimolar concentrations of extracellular tetramethylammonium. Cone channels contain two blocker binding sites flanking the cation binding site proposed by Haynes (1995b). N-methyl-D-glucamine and the buffer Tris (2-amino-2-hydroxymethyl-1,3-propanediol) also blocked the cone channel in a voltage-dependent fashion at mM concentrations, but had lower affinity than similar sized tetra-alkylammonium blockers.

ACKNOWLEDGEMENTS

A special thanks to my supervisor, Dr. Larry Haynes, who took the time to teach me. You are a man from whom alot may be learned. I greatly appreciate the direction, suggestions and invaluable advise given during my Masters. I hope to achieve the potential you recognized. May the future contribute further collaborations.

Thank you to my supervisory committee, Dr. Keith Sharkey and Dr. Bob French, who were supportive from Day 1. You have shown by example what good research is all about. All of the hallway advise has been taken to heart, and will inevitably shape my future.

Thanks to Maria Polyak for her support and friendship in the lab. My sanity remains intact thanks to her. Speaking of the insane, thanks to the Barnes lab (Marshall, Dimetry, Todd, Jason and Bill) for making me laugh.

DEDICATION

Search me, O God, and know my heart;

test me and know my anxious thoughts.

See if there is any offensive way in me,

and lead me in the way everlasting.

Psalm 139: 23-24

This work is dedicated to my Grandmother, Eva Grant, who reminded me of my focus. I can't wait to see you again.

To my family (Mom, Dad, Jonathan and Stuart), Karen, and Ken - You're the best!! God couldn't have given me a better support system.

TABLE OF CONTENTS

LIST OF TABLES

LIST OF FIGURES

LIST OF EQUATIONS

LIST OF SYMBOLS, ABBREVIATIONS, NOMENCLATURE

cAMP	adenosine 3′, 5′-cyclic monophosphate
cDNA	complementary DNA
cGMP	guanosine 3′, 5′-cyclic monophosphate
COOH-terminal	carboxy-terminal
δ	fraction of transmembrane voltage drop crossed
GARP	glutamic-acid-rich protein
GCAP	guanylate cyclase-activating protein
GDP	guanosine 5′-diphosphate
GTP	guanosine 5′-triphosphate
IRBP	interstitial retinol-binding protein
I-V	current-voltage
$K_{D(0)}$	dissociation constant at 0 mV
nAChR	nicotinic acetylcholine receptor
NH_2-terminal	amino terminal
NMDG	N-methyl-D-glucamine
PDE	cGMP phosphodiesterase
TAA	tetra-N-alkylammonium
TBA	tetrabutylammonium
TEA	tetraethylammonium
TMA	tetramethylammonium
TPeA	tetrapentylammonium
TPrA	tetrapropylammonium
Tris	2-amino-2-hydroxymethyl-1,3-propanediol
V_{rev}	reversal potential

CHAPTER 1: INTRODUCTION & BACKGROUND

The visual transduction cascade, within the outer segment of both rod and cone photoreceptors, is responsible for capturing and transducing light energy into an electrochemical signal. This signal carries information about the incoming light levels to higher integration centers of the visual system and brain. An integral component of the visual transduction cascade is the cyclic GMP-gated channel, whose activity directly reflects changes in cytosolic guanosine 3′, 5′-cyclic monophosphate (cGMP) levels. Properties of this ligand-gated channel are better understood physiologically and structurally as a result of powerful new techniques. Patch-clamping, molecular cloning, and site-directed mutagenesis have enabled single-channel behaviour to be recorded, amino acid sequences to be derived, and specific parts of the sequence to be related to precise physiological functions of ion channels (Unwin, 1989). As continued research further links structural components of the protein to roles in channel selectivity, gating, and modulation, a clearer image of the three-dimensional channel structure is developing. The purpose of the research outlined in this thesis is to increase our understanding of the structural components within the pore of the cGMP-gated channel which contribute to ion selectivity and conduction.

The photoresponse

An overview of the phototransduction cascade

Photoreceptors within the retina of the eye are responsible for capturing the energy contained in a photon of light. Within the outer segment of the photoreceptor exists a G-protein coupled enzyme cascade (Fig. 1) which is activated by light energy. Activation

Figure 1 The vertebrate phototransduction cascade. A detailed description of the cascade components and their interactions is provided in the text. This enzyme cascade, found in the outer segments of rods and cones, is responsible for the efficient detection of light and transfer of information to higher visual centers.

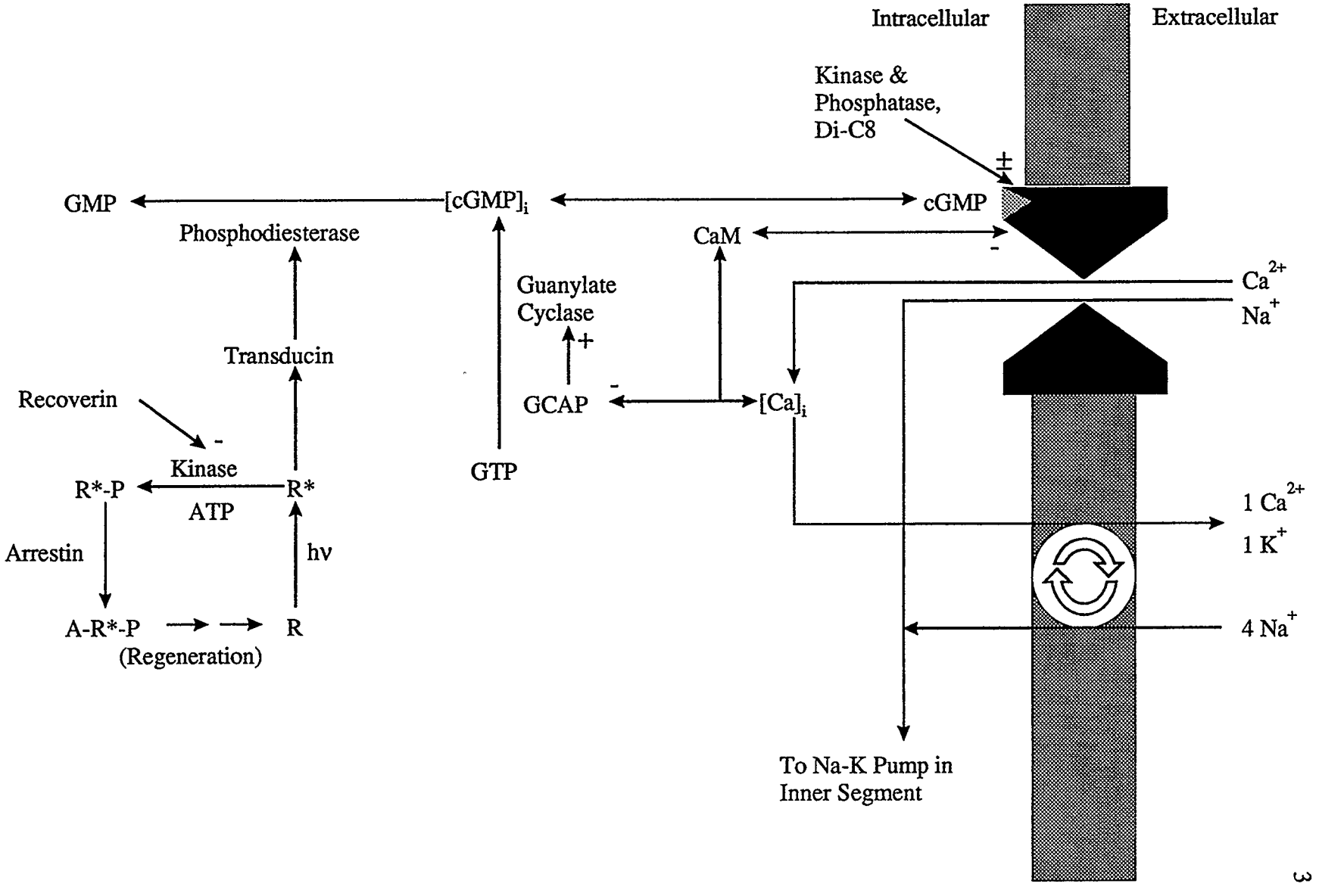
Intracellular
Extracellular
Kinase &
Phosphatase,
Di-C8
±
GMP
[cGMP]i
cGMP
Phosphodiesterase
CaM
-
Ca2+
Na+
Guanylate
Cyclase
+
Transducin
Recoverin
-
GCAP
-
[Ca]i
Kinase
R*-P
R*
ATP
GTP
1 Ca2+
1 K+
Arrestin
hν
A-R*-P
R
4 Na+
(Regeneration)
To Na-K Pump in
Inner Segment

of the enzyme cascade evokes changes in the concentration of free outer segment cGMP. cGMP is a cytoplasmic messenger that acts as a ligand, activating a non-specific cation conductance through channels in the plasma membrane. When the photoreceptor is in the dark, bound cGMP maintains the channel in its open state. The inward flow of cations through the open channels creates a depolarized transmembrane voltage across the outer segment. Light activation of the enzyme cascade leads to the hydrolysis of cGMP, and as ligand concentrations fall cGMP unbinds from the channel. As the channels close, cation conductance decreases and the photoreceptor hyperpolarizes. The change in photoreceptor potential regulates the amount of transmitter (glutamate) released at the cell's synaptic endings. Under depolarized conditions, a basal level of transmitter is released. As the membrane hyperpolarizes, less glutamate is released. The network of cells (bipolar, horizontal, amacrine, and ganglion cells) that transfer light information from the photoreceptors to the visual cortex infer from the level of transmitter levels whether light has been detected. The photoreceptor recovers from the photoresponse through the process of light adaptation, which includes termination of the G-protein coupled enzyme cascade, regeneration of cGMP, and possible modulation of channel activity (Stryer, 1986; Yau & Baylor, 1989).

The dark current

In the absence of light, a "dark current" flows through both the rod and cone photoreceptors. Open cGMP-gated channels contribute the majority of the ionic current flowing into the photoreceptor outer segment, with additional current contributed by a membrane exchanger. This Na^+/Ca^{2+}-K^+ exchanger is responsible for balancing calcium

influx, extruding a potassium and a calcium ion in exchange for four sodium ions (Cervetto *et al.*, 1989). Dark current into the rod outer segment is composed of 70% sodium, 15% calcium, 5% magnesium, and 10% Na^+/Ca^{2+}-K^+ exchanger (Lagnado *et al.*, 1992; Nakatani & Yau, 1988a), while current entering the cone is estimated to contain twice as much calcium (Perry & McNaughton, 1991). The inward flux of cations is carried through the photoreceptor outer segment into the inner segment, setting the cell membrane potential to a depolarized -40 mV (Tomita *et al.*, 1967; Fain & Lisman, 1981; Attwell *et al.*, 1982; Baylor *et al.*, 1984; Attwell, 1990).

The magnitude of the dark current is maintained at an equilibrium via a series of feedback loops reliant on sensitivity to calcium levels (Cohen *et al.*, 1978; Kilbride, 1980; Woodruff & Fain, 1982). A steady dark current is essential to reduce spontaneous low-frequency fluctuations in cGMP levels. Consistent levels of cGMP improve the reliability of light detection and prevent the potentially harmful influx of excess cations (Yau & Baylor, 1989).

Membrane depolarization activates several ion channels of the inner segment, one of these being the voltage-gated Kx channel which selectively extrudes potassium (Attwell & Wilson, 1980; Beech & Barnes, 1989). These ion channels, with the help of an ATP-dependent Na^+/K^+ pump, are responsible for controlling the levels of cytoplasmic ions (Fain & Lisman, 1981). Under dark conditions, cell depolarization promotes the continual release of glutamate from the photoreceptor synaptic endings. Second-order cells of the retina (bipolar and ganglion cells) relay this chemical signal to the visual cortex, reporting the absence of light (Sekuler & Blake, 1994).

Activation of the light response

Within the membrane of rod outer segment discs lies the visual pigment rhodopsin. Rhodopsin absorbs light energy with a peak absorbance of 502 nm, preferentially equipping the rod to gather information about the intensity and duration of light experienced rather than the wavelength (Sekuler & Blake, 1994). Photopigments of the cone are relatives of rhodopsin, and are found within invaginated lamellae of the outer segments. Each human cone contains one of three opsins that are selective for wavelengths within the ranges of 420 (blue-sensitive), 530 (green-sensitive), and 560 nm (red-sensitive). The combined light response of cones throughout the eye conveys information about color to the higher integrative centers of the brain (Sekuler & Blake, 1994). In the case of both the rod and cone, light energy induces the isomerization of the visual pigment to an enzymatically active intermediary molecule. Rhodopsin is a conjugate molecule formed in the combination of the membrane-bound protein opsin with retinal (the aldehyde of vitamin A). Retinal in the 11-cis configuration is transformed to all-trans retinal by the light energy contained in a single photon (Hubbard & Kropf, 1958). This isoform of rhodopsin spontaneously converts to metarhodopsin II, the active intermediary molecule capable of triggering the G-protein enzyme cascade (Yau & Baylor, 1989).

Amplification of the visual signal

Amplification of the visual signal occurs as a single active metarhodopsin molecule triggers the exchange of guanosine triphosphate (GTP) for bound guanosine diphosphate (GDP) on hundreds of transducin molecules (Fung & Stryer, 1980).

Transducin is a well known G-protein located in the photoreceptor outer segment. Three subunits, the Tα, Tβ and Tγ components, form a complex that makes up the complete transducin molecule (Stryer, 1983; Krapivinsky *et al.*, 1989). Association of GTP with the Tα subunit liberates it from the Tβγ transducin complex. The dissociated Tα-GTP is then capable of interacting with the enzyme cGMP phosphodiesterase (Fung *et al.*, 1981; Stryer, 1983, 1986). cGMP phosphodiesterase (PDE) is another heteromultimeric protein found in the photoreceptor outer segment. The complete enzyme is formed through tight associations between the PDEα, PDEβ, and two PDEγ subunits (Stryer, 1983; Stryer *et al.*, 1983). Interactions between Tα-GTP and the two PDEγ subunits removes restraints on the hydrolytic activity of the PDEα and PDEβ subunits (Fung et al., 1981; Hurley & Stryer, 1982). The active PDE subunits are then capable of rapidly hydrolysing essentially all of the free cGMP found in the cytoplasm of the photoreceptor outer segment (Morrison *et al.*, 1987).

The net effect of cascade activation

Up until this point the channels have been maintained in their open state by associations with cGMP. In response to the fall in the concentration of free cGMP, ligand bound to the cGMP-gated channel dissociates. As the channels close, the inward flow of current is terminated and the photoreceptors hyperpolarize (Fesenko *et al.*, 1985; Haynes & Yau, 1985; Karpen *et al.*, 1988a, 1988b; Haynes & Yau, 1990a, 1990b). A hyperpolarized membrane potential causes less transmitter to be released from the photoreceptor synaptic endings, communicating to connecting interneurons that light has been detected. These interneurons act as integrators and relayers of information about

light intensity and frequency to the higher processing levels of the retina and brain (Tessier-Lavigne, 1991).

Regeneration of free cytoplasmic cGMP

While the cGMP-gated channel is the only ion channel found in the outer segment of the photoreceptor, an electrogenic exchanger also lies in the plasma membrane. Even though the cGMP-gated channels close in response to light, this Na^+/Ca^{2+}-K^+ exchanger continues to run causing the cytoplasmic levels of calcium to fall (Yau & Nakatani, 1984, 1985). Termination of the light-induced response begins as guanylate cyclase, an integral membrane protein of the photoreceptor outer segment (Dizhoor *et al.*, 1994), is activated by a soluble factor sensitive to low calcium concentrations (Lolley & Racz, 1982; Koch & Stryer, 1988; Gorczyca *et al.*, 1994a, 1994b, Dizhoor *et al.*, 1994). This putative soluble factor has been identified as guanylate cyclase-activating protein (GCAP) (Gorczyca *et al.*, 1994b, 1995), a 20-kDa protein purified from bovine rod outer segments (Gorczyca *et al.*, 1994a). *In vitro*, GCAP is capable of sensing changes in calcium concentration in the sub-micromolar range (Koch & Stryer, 1988), and of activating guanylate cyclase (Gorczyca *et al.*, 1994a). Guanylate cyclase activity restores the concentration of cytoplasmic cGMP to levels normally present in the dark by catalyzing the conversion of 5′-GMP into cGMP (Koch & Stryer, 1988). Free cGMP re-associates with the cGMP-gated channel, triggering gating of the channel to the open state (Fesenko *et al.*, 1985). Increased production of cGMP may also play a role in photoreceptor light adaptation, decreasing the intensity of subsequent receptor responses to a photon of light (Yau & Baylor, 1989).

Termination of the G-protein enzyme cascade

As cGMP-gated channels begin to reopen, isomerized rhodopsin is phosphorylated by rhodopsin kinase, a covalent modification that reduces the efficiency of metarhodopsin II / transducin interactions (Stryer, 1986). Low cytoplasmic calcium concentrations also influence the activity of arrestin (Zuckerman *et al.*, 1985), a membrane protein which competitively inhibits interactions between the phosphorylated visual pigment and transducin (Kühn *et al.*, 1984; Zuckerman *et al.*, 1985). Concurrently, GTPase activity of the Tα transducin subunit slowly hydrolyses bound GTP to GDP, terminating the ability of Tα to activate PDE and promoting the binding of Tα with the Tβγ complex of transducin (Yau & Baylor, 1989). The cumulative effect of rhodopsin kinase, arrestin, and the GTPase activity of transducin is the regeneration of components of the G-protein enzyme cascade in their complex form, enabling the photoreceptor to detect a new light stimulus.

Regeneration of the photopigment

To complete the photoresponse cycle, rhodopsin must be regenerated. Isomerization of all-trans retinal to the 11-cis configuration requires transportation of the photopigment to the pigment epithelial cells. Transportation is arranged by a special retinal-binding protein, aptly named the interstitial retinol-binding protein (IRBP) (Bridges, 1976; Bridges *et al.*, 1984; Fong & Bridges, 1990). In the pigment epithelium, all-trans retinal is reduced to all-trans retinol (vitamin A), the precursor required for the synthesis of 11-cis retinal. Once 11-cis retinal has been resynthesized, it is transported back to the photoreceptor where it re-associates with opsin in the membrane of the outer

segment (rods) and lamellae (cones) (Aidley, 1989; Tessier-Lavigne, 1991).

The role of calcium as a cell regulator

So far the role of calcium in photorecovery has been implicated through interactions with GCAP (Koch & Stryer, 1988; Gorczyca *et al.*, 1994a) and arrestin (Zuckerman *et al.*, 1985). Calcium levels may also effect the rate of recovery by determining the rate of cGMP break down in the presence of light. The enzymatic activity of PDE is sensitive to levels of calcium, decreasing its activity as calcium concentrations fall (Torre *et al.*, 1986). Reduced PDE activity may prevent the rapid depletion of free cGMP expected to result from the activation of the light-induced enzyme cascade. As a result, the receptor would recover more rapidly from the photoresponse. Under conditions of low background illumination, calcium inhibition of PDE will also slow the fall of free cGMP levels, allowing the photoreceptor to detect stimuli over a wider range of light intensities (Torre *et al.*, 1986).

Calcium may also effect the speed of photorecovery through interactions with modulatory mechanisms. In the presence of calmodulin, the affinity of the rod cGMP-gated channel for its ligand has been shown to decrease as calcium levels increase (Hsu & Molday, 1993). This result has indicated that in the presence of physiological ligand concentrations and calcium-calmodulin, the channel open probability would decline (Hsu & Molday, 1993). If calcium-calmodulin interactions occur with the rod channel in the dark, the light-induced reduction of calcium levels would cause dissociation of the complex. As a result, the channel's affinity for its ligand would increase, promoting entry of the channel into the open state. Phosphorylation of the rod channel has been shown

to have an opposite effect. Protein phosphatase activity increases the apparent ligand affinity of the rod cGMP-gated channel (Gordon *et al.*, 1992). Under conditions promoting dephosphorylation, the rod channel would achieve the open state with greater ease. These mechanisms modulating channel affinity for its ligand have yet to be verified in the native system. However, calcium-calmodulin, nitric oxide (generated from sodium nitroprusside), and inositol triphosphate have had no effect on the affinity cone cGMP-gated channels have for cGMP (Haynes & Stotz, 1996).

Similarities and differences between rods and cones

Physiological factors

Comparisons between the light-induced enzyme cascades of rods and cones indicate that many similarities and a few important differences exist between the two systems (Yau & Baylor, 1989). Components within the cascades are complementary though not identical, as are mechanisms for light adaptation (Nakatani & Yau, 1988b; Yau & Baylor, 1989). However, it is evident that the time scale upon which components of these two cascades work is different. Under physiological conditions, cones are approximately a hundred times less sensitive to light than are rods (Schnapf & McBurney, 1980; Cobbs *et al.*, 1985), respond more quickly to changes in light levels, and adapt to a wider range of illumination intensities (Nakatani & Yau, 1986; Miller *et al.*, 1994). Measurements of channel density on the membrane surface of the rod and cone photoreceptors indicate that the density of channels on the cone membrane is about ten times lower than on the rod membrane (Haynes *et al.*, 1986; Zimmerman & Baylor, 1986; Cook *et al.*, 1987; Haynes & Yau, 1990a). However, since the surface area of the cone

outer segment is about ten times larger than the rod outer segment, both cell types have approximately the same number of channels (Haynes & Yau, 1990a). Differences in the speed of signal transduction may be explained by the larger surface-to-volume ratio of the cone in comparison to the rod. Since the cytoplasmic volume of the cone is 25-fold less than the rod, the rates of all enzymatic activity may be increased by as much as 25-fold (Pugh & Lamb, 1993), decreasing cone reaction time in both response and recovery. For the cone, this translates into an advantage in efficiency when dealing with a photoresponse.

Electrophysiological factors

With the introduction of cellular electrophysiological techniques, it has been possible to investigate properties of the cGMP-gated channel in both rods and cones. In a voltage-clamp experiment, the membrane voltage of a cell is controlled while the transmembrane current required to maintain that voltage is measured. A specialized version of the voltage clamp, the patch clamp, allows currents through single ion channels to be resolved (Hamill *et al.*, 1981). Although both the cGMP-gated channels of the rod and cone are non-specific cation conductors (Fesenko *et al.*, 1985; Furman & Tanaka, 1990; Menini, 1990; Colamartino *et al.*, 1991; Zimmerman & Baylor, 1992; Picones & Korenbrot, 1992; Haynes, 1995a, 1995b), differences exist in how ions interact with the pore region as they pass through.

Experimental measures of current flow through the channel as a function of voltage show that while the rod channel demonstrates only strong "outward" rectification under physiological conditions, the cone channel shows both "inward and outward"

rectification (Yau *et al.*, 1986). Outward rectification of current describes a conductance that is greater at positive voltage potentials than at negative potentials. In the case of cone conductance, the current increases exponentially with voltage in both the depolarizing and the hyperpolarizing directions while maintaining a plateau at potentials around 0 mV (Haynes & Yau, 1985). Rectification in both channel types is the result of a voltage-dependent block of the channels by permeant divalent cations; when divalent cations are removed both current voltage relations become almost linear (Yau *et al.*, 1986; Haynes, 1992).

In the absence of divalent cations, the single channel conductance of the cGMP-gated channel may be evaluated. Under these conditions, the conductance through the cone channel is twice that of the rod channel (unit conductance of 50 pS in cones: Haynes & Yau, 1990a; 25 pS in rods: Haynes et al., 1986; Zimmerman & Baylor, 1986; Matthews & Watanabe, 1987; Matthews & Watanabe, 1988). Permeability sequences, determined from shifts in reversal potential that are apparent under symmetrical bi-ionic conditions (Hille, 1992), indicate the relative ease with which monovalent cations pass through the individual channels. Comparisons of the cone cGMP-gated channel permeability sequence, $P_{NH4}>P_K>P_{Li}>P_{Rb}=P_{Na}>P_{Cs}$ (Haynes, 1995a), with the rod channel sequence, $P_{Li}>P_{Na}=P_K>P_{Rb}>P_{Cs}$ (Menini, 1990), indicate that slight differences in pore structure may allow certain ions to pass with greater ease. Divalent cations have also been shown to permeate rod and cone channels with different selectivity patterns (Perry & McNaughton, 1991; Haynes, 1995b). Differences in selectivity, conductance, and rectification suggest that ions passing through the pore region of the cGMP-gated channel

are interacting with distinct structural features that are characteristic of either the rod or the cone pore (Haynes, 1992, 1995a, 1995b).

Structure determination

Techniques of ion channel structure determination

Many techniques have been developed in the last 20 years in order to elucidate the molecular structure of ion channels. Work began in the 1970's with classical methods of protein chemistry and progressed in the 1980's to cloning and sequencing with methods gained from molecular genetics (Hille, 1992). Advances made within the realms of protein imaging, molecular biology, histochemistry, and electrophysiology have improved our ability to determine ion channel structure. Once the structure of an ion channel has been fully determined, our understanding of how channels function within the native system will become much clearer.

Protein imaging techniques

Transmission electron microscopy, three-dimensional (3-D) electron image analysis, and X-ray crystallography have provided important insights into channel structure at the macromolecular level. The general shape of many kinds of ion channels has been determined by shadowing proteins lying within the plasma membrane with heavy metals or outlining them with negative stain, and then viewing them under the transmission electron microscope (Alberts *et al.*, 1983). To determine the precise location of each atom in a molecule, however, crystals made from the protein under consideration must be analyzed by either X-ray crystallography or 3-D electron imaging. These crystals may be obtained by rapidly freezing the specimen in a thin film of solution. This type

of preparation provides the protein of interest in a static position while maintaining the protein's association with the surrounding lipid and ionic environment (Unwin, 1989). The crystals can then be viewed under the electron microscope at low resolution in their hydrated, unfixed, and unstained state at very low temperature (temperature less than -196 °C is required for the ice to remain stable) (Darnell *et al.*, 1990). With the use of X-ray crystallography, the 3-D structure of the crystallized protein can be deduced from the diffraction pattern; photon radiation scattered by the crystal produces a set of discrete spots captured by photographic film that correspond to the protein's form (Darnell *et al.*, 1990). X-ray crystallography has certain advantages over 3-D electron imaging, providing greater resolution and greater penetrating power so thicker specimens can be used. However, the basic problem preventing wider use of these imaging methods for ion channel structure determination lies with the production of protein crystals. Large, highly ordered crystals lying on a regular lattice are required for high-resolution studies (Alberts *et al.*, 1983). The process of crystallization tends to disrupt the association of ion channels with the lipid bilayer, destabilizing the quaternary structure of the protein. As a result, a single bacterial photosynthetic center is the only integral membrane protein that has been crystallized and whose protein structure has been completely determined at the atomic level (Deisenhofer & Michel, 1989). In order to work around this problem, crystals have been formed from purified channel proteins highly concentrated in artificial lipid bilayers. Under these conditions, the crystallized proteins form relatively regular two-dimensional (2-D) lattices that can be analyzed by X-ray diffraction or electron microscopy at more modest resolutions (Hille, 1992).

Crystallographic analysis of cryo-images has led to the development of 3-D contour maps for two ion channels: the gap junction channel and the nicotinic acetylcholine receptor (nAChR) channel. Analysis of the gap junction channel through combined imaging methods has portrayed the channel as a ring formed from six identical connexins; cylindrical proteins approximately 75Å in length. Images of the conducting channel predict that the pore is a minimum of 16Å in diameter (Schwartzmann *et al.*, 1981), accounting for the nonspecific conductive properties of the gap junction channel (Unwin, 1989). The second channel studied by cryo-methods was the nAChR channel. Compared to the gap junction channel, the open pore of this cation-selective channel is much smaller, approximately 7Å in diameter (Dwyer *et al.*, 1980). The structural ring of the nAChR is formed from five rod-shaped subunits; two identical α polypeptides complexed with single β, γ, and δ polypeptides (Changeux *et al.*, 1984; Karlin *et al.*, 1986; McCarthy *et al.*, 1986). With continued improvements in crystallization procedures and imaging techniques, these methods may one day be responsible for the determination of many ion channel structures. However, until 3-D imaging at low resolution is possible for these membrane bound proteins, other techniques of structure determination must be developed and used in order to form a comprehensive picture of the ion channel.

Use of molecular biology in channel structure determination

The most commonly used tools for investigating structure / function relationships in ion channels have come from molecular biology. Many similarities and differences between the components forming ion channels have been identified by sequencing the proteins. Among different ion channels, regions of common amino acid sequence may

delineate structures responsible for important catalytic functions (Watson *et al.*, 1992). The hydropathy plot is an example of a technique developed to predict structure based on sequence characteristics. This technique is based on information gathered from imaging of the bacterial photosynthetic center (BPC). Transmembrane segments of the BPC are formed from hydrophobic spans, 20 to 27 amino acids in length, that traverse the membrane at angles 10 to 20° off the perpendicular (Deisenhofer & Michel, 1989). Knowing this, other channel sequences have been analyzed for spans of twenty or more amino acids that are hydrophobic in nature. Sequences that fit these prerequisites are labelled as putative transmembrane segments (Hille, 1992). Further studies investigating the relation of particular amino acid residues to proper channel function may verify the position of certain sequences.

When modelling the structure of an ion channel, it is important to identify the orientation of an amino acid sequence with respect to the plasma membrane. Monoclonal *antibodies, made against short synthetic peptides of known channel sequence and labelled* with radioactive markers, have been used to determine whether target sequences are exposed to the intracellular or extracellular medium (Lindstrom *et al.*, 1987). Residues, such as serine, threonine, and tyrosine, are subject to phosphorylation by intracellular protein kinases. Labelled phosphates bonded to the channel protein indicate that segments containing these residues may be located on the cytoplasmic surface. In the same manner, residues modified by reactive derivatives of channel blockers or toxins can be targeted within an amino acid sequence (Huganir & Greengard, 1990). Since all ion channels are glycoproteins, glycosylation studies have been used to identify residues

subject to high mannose glycosylation. Glycoproteins are proteins with branching oligosaccharide chains attached to specific extracellular residues. These carbohydrate moieties, added to the protein channel while it is still being processed in the endoplasmic reticulum and Golgi apparatus, are thought to aid the channel in achieving proper orientation in the membrane bilayer (Armstrong, 1989). Evidence of glycosylation indicates that the residue must be positioned on the extracellular surface of the protein (Noda *et al.*, 1983; Poulter *et al.*, 1989). While none of the methods mentioned above are able to definitively assign the position of an amino acid sequence, the combination of information from several techniques can provide enough information to develop a putative model of ion channel structure.

Application of molecular techniques to the cGMP-gated channel

Isolation of the rod cGMP-gated channel

In order to isolate the protein which forms the rod cGMP-gated channel, bovine rod outer segments were solubilized in CHAPS detergent. Red-dye affinity chromatography was used to purify a 63 kilodalton (kDa) polypeptide believed to encode for the rod cGMP-gated channel (Cook *et al.*, 1987). Reconstitution of the purified protein into a lipid bilayer system allowed electrophysiological comparisons to be made with the native rod channel properties. Under controlled conditions, the 63 kDa polypeptide was shown to conduct current in a manner similar, but not identical, to the native rod cGMP-gated channel (Cook *et al.*, 1987; Hanke *et al.*, 1988). Using radioactive cGMP, direct photoaffinity labelling studies were performed, showing the specific binding of the labelled ligand to proteins with molecular masses similar to the

63 kDa polypeptide (Cook *et al.*, 1987). A monoclonal antibody produced against the polypeptide was also found to specifically label the putative channel in both rod outer segments and in purified channel preps (Cook *et al.*, 1987). Using this antibody, both cGMP-gated channel activity and a protein complex consisting of a 63 kDa and a 240 kDa polypeptide were quantitatively immunoprecipitated (Molday *et al.*, 1990). Another monoclonal antibody, generated against a peptide corresponding to the NH_2-terminal segment of the 63 kDa polypeptide, also labelled the functionally active form of the channel complex (Molday *et al.*, 1991).

Cloning and expression of the 63 kDa polypeptide

To provide further evidence that the 63 kDa polypeptide formed the rod cGMP-gated channel, the polypeptide was cloned, the primary amino acid sequence deduced, and expression studies performed (Kaupp *et al.*, 1989; Kangawa *et al.*, 1989). Tryptic peptide sequences of the 63 kDa polypeptide were used to produce oligonucleotide probes for screening a bovine retinal cDNA library. These probes identified a full-length cDNA clone which encoded a 79.6 kDa polypeptide in a bacterial system (Kaupp *et al.*, 1989). This polypeptide was thought to corresponded to the putative cGMP-gated channel polypeptide, with the difference in molecular weight being accounted for by uncleaved introns. mRNA derived from cloned cDNA was introduced into the *Xenopus* oocyte expression system in order to determine the functional properties of the translated protein.

Electrophysiological properties of the cloned rod cGMP-gated channel

Investigation of the electrophysiological properties of the expressed cGMP-gated channel (Kaupp, 1989) and comparison with the known properties of the native rod

cGMP-gated channel (Zimmerman & Baylor, 1986; Haynes *et al.*, 1986; Matthews, 1986, 1987; Matthews & Watanabe, 1987, 1988; Sesti *et al.*, 1994), demonstrated that many channel traits, such as ionic selectivity and blockage by divalent cations, were quite similar (Kaupp *et al.*, 1989; Kaupp, 1991). However, single-channel recordings of the cloned channel showed well-resolved openings up to 10 ms in duration (Kaupp *et al.*, 1989; Nizzari *et al.*, 1993), while the native channel is characterized by continuous flickering between the open and closed states that are difficult to resolve (Zimmerman & Baylor, 1986; Haynes *et al.*, 1986; Matthews, 1986, 1987; Matthews & Watanabe, 1987, 1988). L-*cis*-diltiazem is a potent blocker of native rod cGMP-gated channel activity when present in low micromolar concentrations (Koch & Kaupp, 1985; Stryer *et al.*, 1986; Haynes, 1992), yet even relatively large concentrations of the antagonist had little effect on the reconstituted channel (Cook *et al.*, 1987), or on the expressed channel (Kaupp *et al.*, 1989). The similarities and differences between the properties of the native rod cGMP-gated channel and the cloned cGMP-gated channel formed from only the 63 kDa polypeptide indicated that while the molecular structures of the channel pores are similar, they are not identical (Nizzari *et al.*, 1993).

Identification of a second subunit

Given the inability of the 63 kDa polypeptide to form a channel with properties identical to the rod cGMP-gated channel, it seemed possible that other subunits may complex with this putative α-subunit to form the complete native channel. The 240 kDa protein, which typically purifies in association with the α-subunit (Molday *et al* 1990), was proposed as this second subunit. Coexpression of the α-subunit with the 240 kDa

protein produced single channel activity resembling that of the native rod cGMP-gated channel (Molday *et al* 1991). Interactions between the 240 kDa protein and the α-subunit confer characteristics of L-*cis*-diltiazem sensitivity, flickering fast channel gating (Chen *et al.*, 1993), and calmodulin-binding ability (Chen *et al*, 1994; Molday & Hsu, 1995) to the native rod cGMP-gated channel. Based on the results of these expression studies, the native rod cGMP-gated channel is thought be a heteromeric channel composed of at least 2 different subunits, the 63 kDa α-subunit and the 240 kDa protein, complexed to form a conducting pore (MacKinnon, 1995).

Assigning structure to the rod α subunit

Identifying the transmembrane segments

To determine the selectivity of the ligand-binding domain, chimeras were made by replacing the rod channel cGMP-binding sequence with the olfactory channel cAMP-binding sequence. This change in ligand-binding domain enabled the rod channel, which normally binds cGMP, to select cAMP as the ligand required for channel gating (Goulding *et al.*, 1994). Another domain, located at the NH_2-terminal, also influences channel transitions between the open and closed state. Interactions with cGMP at this position determines the ease with which the channels open (Goulding *et al.*, 1994; Gordon & Zagotta, 1995). In addition to locating positions within the rod cGMP-gated channel where interactions with ligand are possible, this study showed that specific features of the domains are responsible for influencing agonist efficacy and selectivity.

Glycosylation studies

To confirm the location of amino acid loops connecting transmembrane segments

in relation to the membrane, glycosylation studies were carried out on the rod cGMP-gated channel. Gels, run before and after the deglycosylation of the purified channel, indicated that the channel was N-glycosylated at a single site (Wohlfart *et al.*, 1989). However, analysis of the rod α-subunit primary amino acid sequence identified five consensus sequences of Asn-X-Thr or Asn-X-Ser where N-linked glycosylation to an asparagine (Asn) was possible (Wohlfart *et al.*, 1989). The number of possible glycosylation sites was reduced as residues located within transmembrane segments were eliminated from consideration, since oligosaccharide branches are attached exclusively to residues on the extracellular surface of a protein (Armstrong, 1989). With only two possible sites remaining, antibodies were generated against synthetic peptides in position 327, confirming that the loop between the fifth and sixth transmembrane segments was located on the extracellular surface of the rod cGMP-gated channel (Wohlfart *et al.*, 1992).

Structural hints obtained from protein homology

Although the cyclic nucleotide-gated channels are functionally classified as ligand-gated channels, comparison of the primary amino acid sequence of the rod α-subunit with sequences of voltage-gated channels has indicated that several structural features are maintained between the two classes (Kaupp, 1991; Bönigk *et al.*, 1993). Similarities in structure include a putative transmembrane topography of six membrane-spanning segments (Kaupp *et al.*, 1989), a voltage-sensor sequence motif within the fourth transmembrane segment (Numa, 1989; Jan & Jan, 1990), and a putative pore region located between the fifth and sixth transmembrane segments (Fig. 2) (Goulding *et al.*,

1992; Heginbotham *et al.*, 1992; Bönigk *et al.*, 1993). Despite pore regions with a difference of only two amino acid residues, a glycine and a tyrosine which are present in the voltage-gated potassium channel and absent in the rod cGMP-gated channel (Heginbotham *et al.*, 1992), conductance properties of the two channel types are quite different. The rod cGMP-gated channel is a non-specific cation conductor blocked by divalent cations (Fesenko et al., 1985; Furman & Tanaka, 1990; Menini, 1990; Colamartino et al., 1991; Zimmerman & Baylor, 1992), while the potassium channel conductance is highly selective for potassium over any other cations (Hille, 1973; Gay & Stanfield, 1978; Reuter & Stevens, 1980; Yellen, 1987). Expression of potassium channel cDNA containing a deletion of the glycine and tyrosine residues from the pore region created a channel with non-specific cation conductance capabilities which were blocked by divalent cations (Heginbotham *et al.*, 1992). This result suggests that the pore regions of the ligand-gated cGMP channel and the voltage-gated potassium channel are very similar in structure, with only two amino acid residues accounting for the major functional differences that exist in permeation. Based on the extensive sequence homology that exists between the ligand-gated family and the voltage-gated family, links to an ancestral channel have been proposed for the two groups (Jan & Jan, 1990).

Putative structure of the 240-kDa protein

Analysis of the primary amino acid sequence obtained from cloned cDNA of the rod 240-kDa protein has identified two separate domains. The cytoplasmic NH_2-terminal is identical to a glutamic-acid-rich protein (GARP) (Sugimoto *et al.*, 1991), while the COOH-terminal exhibits high sequence homology with the rod α-subunit (Körschen *et al.*,

Figure 2 A schematic model of the bovine rod cGMP-gated channel α-subunit organization within a lipid bilayer. This α-subunit, whose structure is similar in cone cGMP-gated channels and potassium channels, includes six transmembrane segments, a voltage-sensor sequence motif within the fourth transmembrane segment, a pore region between segments six and seven, and a glycosylation sequence between the fifth and sixth segments.

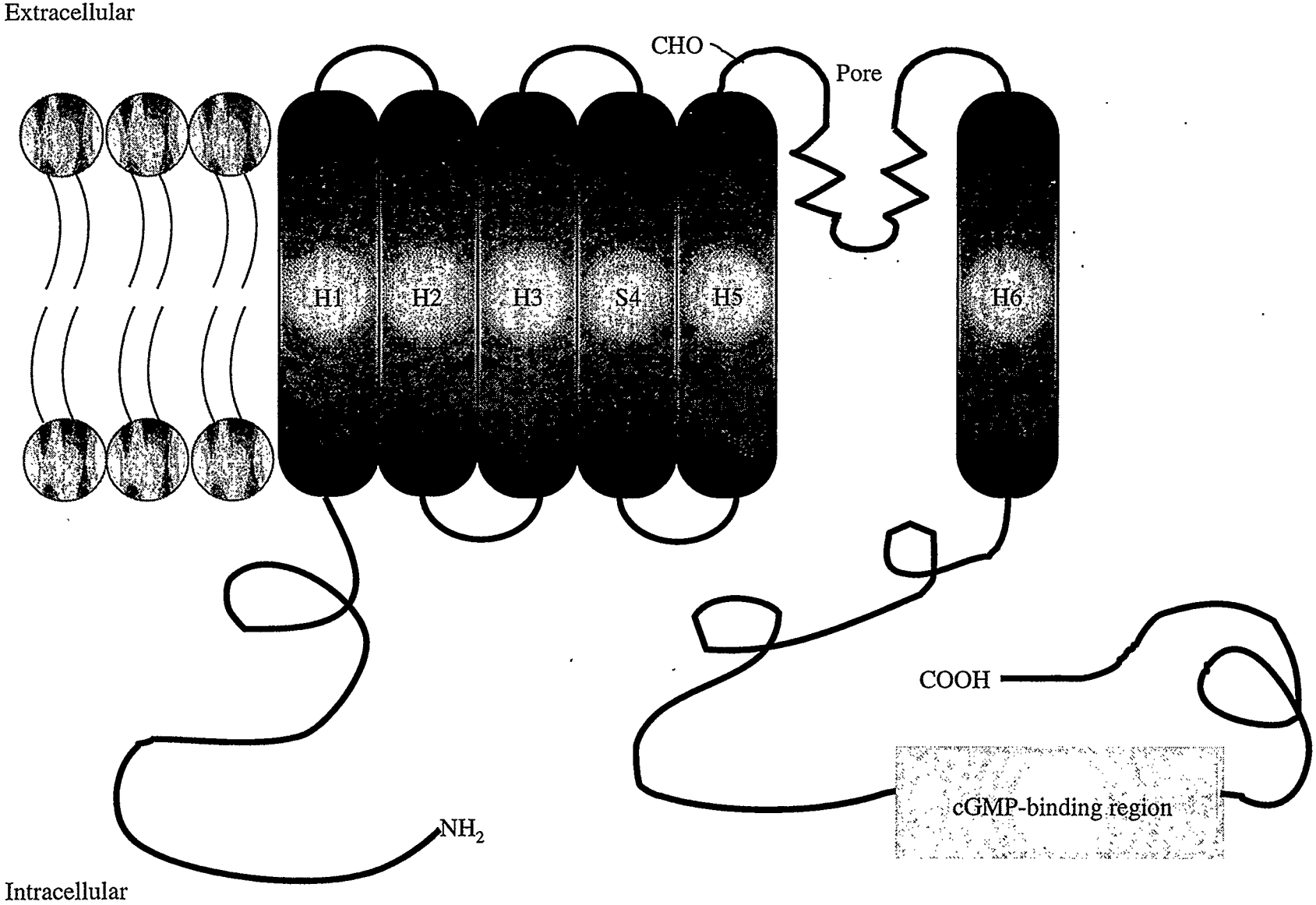
Extracellular
CHO
Pore
H1
H2
H3
S4
H5
H6
COOH
cGMP-binding region
NH_2
Intracellular

1995; Kaupp, 1995). While the function of GARP within the photoreceptor has yet to be determined, it has been proposed to aid interactions between the rod cGMP-gated channel and other proteins such as the Na^+/Ca^{2+}-K^+ exchanger (Bauer & Drechsler, 1992), or to serve as a targeting sequence for orientation of the channel in the plasma membrane (Kaupp, 1995). The COOH-terminal of the 240 kDa protein, formerly referred to as the β-subunit, shares 30% sequence identity with the rod α-subunit. Similarities between the two subunits are greatest within the respective cGMP-binding domains, where 50% of the sequences are identical (Chen *et al.*, 1993). Hydropathy analysis of this second subunit has suggested that putative α-helices traversing the plasma membrane are less hydrophobic than those of the α-subunit. Sequence analysis has also determined that a negatively charged glutamic acid residue within the channel pore region and the consensus sequence for N-linked glycosylation present within the α-subunit (Wolfart *et al.*, 1989) are absent from the 240 kDa protein (Molday & Hsu, 1995). Unique to the 240 kDa protein is a domain responsible for interactions with calmodulin (Chen *et al.*, 1994; Hsu & Molday, 1994). It is proposed that this characteristic enables the native rod channel to modulate affinity for its ligand (Molday & Hsu, 1995). Despite slight differences in amino acid sequence, homology between the COOH-terminal of the 240 kDa protein and the rod α-subunit suggests that the subunits may be similar in overall structure (Chen *et al.*, 1993).

The complexed structure of the rod cGMP-gated channel

The use of molecular biology, immunocytochemistry and biochemistry in structure determination have allowed for the development of a model of the rod cyclic nucleotide-

gated channel which attributes 3-D structure to a linear amino acid sequence. Functional evidence suggests that the rod cGMP-gated channel is formed through the associations of the α-subunit with the 240 kDa protein (Molday & Hsu, 1995). Four subunits have been proposed to come together to form the complete channel, yet the stoichiometric ratio of α-subunit to 240 kDa protein has yet to be confirmed (MacKinnon, 1995). These subunits are thought to have similar topologies consisting of six transmembrane segments, with a voltage sensor motif in segment four, a pore region located between segments five and six extending into the membrane, and a cGMP binding domain located at the carboxy-terminus (Fig. 2) (Jan & Jan, 1990; Chen *et al.*, 1993; Molday & Hsu, 1995). Based on information obtained from electrophysiological studies, gating of the channel to the open state is thought to require binding of cGMP to at least three ligand binding sites (Haynes *et al.*, 1986; Zimmerman & Baylor, 1986; Haynes & Yau, 1990a). Modulation of channel affinity for its ligand may be regulated through interactions between the 240 kDa subunit and calmodulin (Chen *et al.*, 1994; Hsu & Molday, 1995). Both of the putative subunits are thought to contribute their pore regions to the formation of a central canal which conducts ions in a non-selective manner (Fig. 3) (Molday & Hsu, 1994). Details of the rod cGMP-gated channel structure are sketchy with many characteristics yet to be determined in order to fill out the overall picture.

Putative structure of the cone cGMP-gated channel

Recently, a 63 kDa protein corresponding to the cone cGMP-gated channel was cloned from the chicken retinal cDNA library (Bönigk *et al.*, 1993). The polypeptide sequence of this putative cone channel shares high homology with the sequence of the

Figure 3 A schematic model of the bovine rod cGMP-gated channel complex. Two subunits, the 63 kDa α-subunit and the 240 kDa β-subunit, interact to form the pore of the native channel. Both subunits contain sites for binding cGMP, while the β-subunit exclusively contains sites for calmodulin interactions. The channel mouth is widest intracellularly, capable of containing blockers as large as TPeA. The permeant ion binding site narrows to approximately the size of methyl guanidinium, while the extracellular mouth contains a TMA binding site that is absent from the cone.

Extracellular

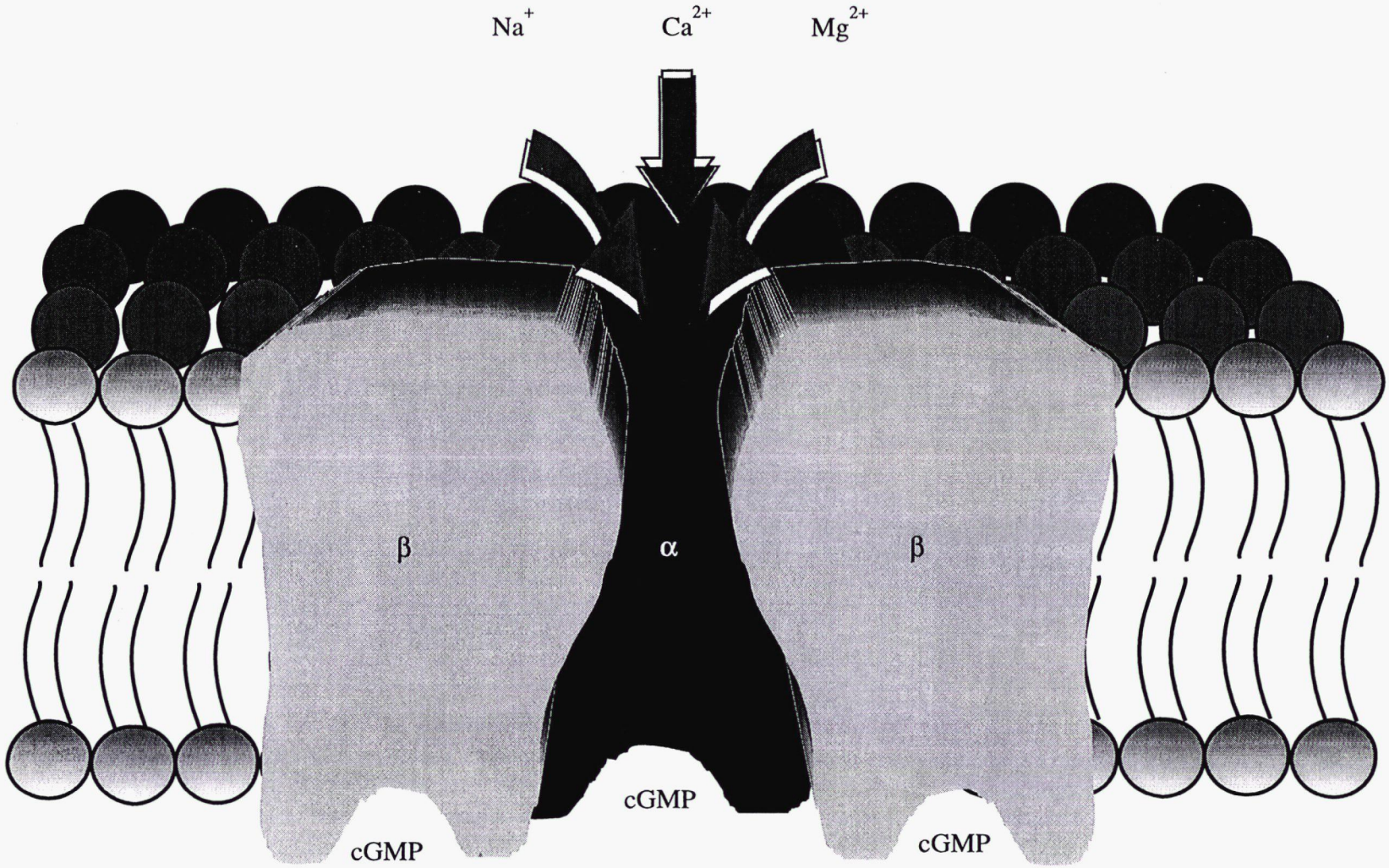

Intracellular

chicken rod cGMP-gated channel α-subunit. Deviations are most apparent over the first 15% of the amino acid sequence or first 70-80 residues at the NH_2-terminal (Miller *et al.*, 1994). Comparison of sequences thought to form the rod and cone channel pore regions identified a difference of only a single amino acid, an isoleucine residue in the cone which has been replaced by a valine in the rod (Bönigk *et al.*, 1993). Studies have yet to determine if this amino acid, located on the extracellular surface of the channel mouth, is responsible for rectification differences between the rod and cone or if other factors are involved. High sequence homology between the rod α-subunit and the cone 63 kDa protein once again suggests that the cone protein will form a structure similar to the rod α-subunit. As of yet, no β-subunit has be indentified.

Expression of the cloned cone cGMP-gated channel in *Xenopus* oocytes has demonstrated that while the relative ion permeabilities of the cloned cone 63 kDa protein are similar to those determined for the native cone channel (Perry & McNaughton, 1991; Picones & Korenbrot, 1992; Haynes, 1995a), the current-voltage (I-V) curve of the expressed cone channel deviates from that of the native channel (Bönigk *et al.*, 1993). The I-V relation for the cone cGMP-gated channel in striped bass or catfish is nearly linear in the absence of divalent cations (Haynes & Yau, 1990; Picones & Korenbrot, 1992), and is inwardly and outwardly rectifying in the presence of divalent cations (Haynes & Yau, 1985, 1990a). Since the expressed cone channel has a non-linear I-V relation under all conditions, additional factors, possibly even a polypeptide homologous to the rod β-subunit, may be required to form a reconstituted channel corresponding to the wild-type cone cGMP-gated channel (Bönigk *et al.*, 1993).

Identification of other cyclic nucleotide-gated channels

Oligonucleotide probes, formed from conserved regions of the rod channel α-subunit, have been used to clone cDNAs encoding related proteins. The olfactory cAMP-gated channel was the first related cyclic nucleotide channel to be identified by this method (Dhallan *et al.*, 1990; Ludwig *et al.*, 1990; Goulding *et al.*, 1992; Dhallan *et al.*, 1992). Sequence comparison of aligned segments between the rod cGMP-gated channel and the olfactory cAMP channel showed that 57% of the amino acids are identical and another 15% are conservative substitutions (Bönigk *et al.*, 1993). Other cyclic nucleotide-gated (CNG) channels that share sequence homology with the rod cGMP-gated channel have since been identified in other cells and tissues, such as the pineal (Dryer & Henderson, 1991), aorta (Biel *et al.*, 1993), kidney (Ahmad *et al.*, 1990; Light *et al.*, 1990), bipolar cells (Nawy and Jahr, 1990), and testis (Biel *et al.*, 1994). The roles that many of these members of the CNG channel family play within their respective systems have yet to be determined.

Electrophysiological contributions to ion channel structure determination

Keys from permeation and block

While molecular techniques have furthered our understanding of which structures are formed by various amino acid sequences, our knowledge of the functioning channel structure is still limited. Electrophysiological studies examine the conductance of an ion channel with the use of the patch clamp technique (Hamill *et al.*, 1981). Permeability studies, investigating the ease with which metallic and organic cations pass through the open channel, have provided evidence for diameter and length of the pore formed by the

protein. Significant features lining the mouth and pore of the conducting channel have been identified with the use of impermeant cations that get stuck in the channel. The combination of information gained from what can pass through the channel and what cannot has contributed to our view of what the region responsible for the passage of ions looks like.

Permeant alkali metal cations

Although the cGMP-gated channel of both the rod and cone is relatively non-selective as to which cations it will conduct (Fesenko *et al.*, 1985; Furman & Tanaka, 1990; Menini, 1990; Colamartino *et al.*, 1991; Zimmerman & Baylor, 1992; Picones & Korenbrot, 1992; Haynes, 1995a, 1995b), a small variance in permeability sequences is apparent between the rods and cones (Menini, 1990; Haynes, 1995a). Alkali metal cations up to the size of cesium, whose ionic radius is approximately 1.69 Å, are able to squeeze through the narrow pore with varying degrees of ease (Furman & Tanaka, 1990; Haynes, 1995a). A fit of the ion selectivity sequences to the Eisenman electrostatic model, which estimates the field strength of the ion binding site (Eisenman & Horn, 1983), indicates that despite any variance, both channels contain a similar high-field-strength ion binding site within their pore regions (Menini, 1990; Picones & Korenbrot, 1992; Haynes, 1995a).

Permeant organic cations

Organic cations, whose size and properties are easily varied, have been employed as structural probes of channel conductance pathways (Miller, 1982). The cross-sectional areas of the narrowest pore region within the sodium channel, potassium channel (Hille,

1971, 1973, 1975), and rod cGMP-gated channel (Picco & Menini, 1993), have been estimated with the use of small, permeant organic cations. Methyl guanidinium, with dimensions of 0.38 by 0.59 nm, was the largest ion to permeate the rod cGMP-gated channel (Picco & Menini, 1993). This rough estimate of rod channel pore size partially explains the channel's non-selective properties. The slightly smaller, yet more selective sodium channel pore was estimated to form a cylinder with dimensions of 0.3 by 0.5 nm (Hille, 1971), while the cross-section of the highly selective potassium channel pore was estimated to be 0.3 nm in diameter (Hille, 1973). By determining the largest metallic and organic cations capable of permeating the ion channel pore, estimates of dimensions corresponding to the putative selectivity filter have been made.

Organic channel blockers

Large organic cations, which block conduction through various open channel pores, have been used to determine the dimensions and properties of the wider mouth leading to the channel pore (Armstrong, 1975a; Miller, 1982). The binding affinity with which many of these organic cation blockers adhere to the channel is voltage-dependent, indicating that the blockers sense the electrical potential that exists across the channel pore (Yellen, 1987). In its simplest form, the Woodhull model can be used to analyze data obtained from blockage studies (see Theory of block). This model provides estimates of the dissociation constant of the blocker in the absence of a potential ($K_{D(0)}$), and the fraction of the transmembrane voltage drop crossed by the blocker in reaching its binding site (δ) (Woodhull, 1973). $K_{D(0)}$ indicates how tightly the blocker binds within the channel pore, while the δ estimates the position of the blocker binding site within the

electrical field. Attempts have been made to link electrical distance with physical distance using bis-quaternary ammonium blockers of varying length (e.g., Miller, 1982). These compounds contain two charged groups, one which marks the blocker binding site within the conduction pathway while the other is positioned at varying locations within the voltage drop, depending on the chain length. By monitoring the effective valence of block, the electrical field length has been estimated for both the SR and Ca^{2+}-activated potassium channels (Miller, 1982; Villarroel *et al.*, 1988).

The intracellular mouth region of many potassium channels, such as the squid axon delayed rectifier potassium channel (French & Shoukimas, 1981), the rabbit t-tubule calcium-activated potassium channel (Villaroel *et al.*, 1988), and the rabbit sarcoplasmic reticulum potassium channel (Coronado & Miller, 1982), have been systematically investigated with the use of alkylated ammonium derivatives as probes. Although the absolute values of $K_{D(0)}$ and δ vary for each channel type, several traits of blockage are maintained when intracellular organic blocker is present. Each potassium channel is reported to have a single tetra-alkylammonium binding site within the transmembrane voltage drop which interacts with a range of differently sized organic compounds. The largest TAA compound capable of blocking the potassium channel in a voltage-dependent manner is tetrapentylammonium (French & Shoukimas, 1981), indicating the relative size of the vestibule proceeding the potassium channel pore. The affinity channels have for their blockers increases as the number of possible hydrophobic interactions between the channel and blocker increases (Swenson, 1981; French & Shoukimas, 1981; Villaroel *et al.*, 1988; Coronado & Miller, 1982), indicating that the blocker binding site is very

hydrophobic. Studies to determine whether hydrogen bonding is important in stabilizing channel / blocker interactions have shown that addition of hydroxyl groups to the organic blocker decreases binding affinity for the delayed rectifier potassium channel (Swenson, 1981; French & Shoukimas, 1985).

The delayed rectifier potassium channel and the calcium-activated potassium channel are also blocked in a voltage-dependent manner by extracellular tetraethylammonium. This external blocker binding site is separate from the internal TAA binding site (Armstrong & Hille, 1972), selectively interacting with only tetraethylammonium (Villaroel *et al.*, 1988).

The key characteristic that sets electrophysiological investigations apart from other methods of structure determination is the ability to reconcile structure with function. The potassium channel is classically characterized as a selective conductor of a large volume of cations (Armstrong & Hille, 1972). Combining the attributes of a large inner vestibule (holds ions of at least the size of TPeA; French & Shoukimas, 1981) for collecting ions and a small pore for permeation selection (diameter estimated to be 0.3 nm; Hille, 1973) enables the potassium channel to conduct a large number of ions while choosing between ions that differ in diameter by only a fraction of an angstrom.

CHAPTER 2: BLOCK OF cGMP-GATED CHANNELS BY ORGANIC CATIONS

Introduction

Use of organic blockers as probes of the cGMP-gated channel

The purpose of the experiments described in the remainder of this thesis is to characterize the pore and mouth of the cGMP-gated channel in both the rod and cone photoreceptors. Organic cation blockers have previously been used to provide a variety of information about the structure and dimensions of the conducting region for potassium channels (French & Shoukimas, 1981; Coronado & Miller, 1982; Villaroel *et al.*, 1988). These same techniques will be applied to the ligand-gated cGMP channel in order to delineate the dimensions of the channel mouth region as well as the properties of structures lining the ion channel pore.

Theory of block

The process of ion permeation is similar to an enzymatic reaction. Ions free in solution correspond to the substrate (S), interacting sporadically with selective residues lining the channel pore, the enzyme (E). These interactions result in conduction and a measurable current, with the translocated ions as the product (P).

$$E + S \rightleftharpoons ES \rightarrow E + P \qquad (1)$$

When impermeant ions occupy the channel, the possibility of conduction is eliminated. The number of interactions between the ions and channel are reduced to those described by

$$E + S \underset{k_{-1}}{\overset{k_1}{\rightleftharpoons}} ES \tag{2}$$

where k_1 is the forward rate constant and k_{-1} is the reverse rate constant of transition. The equilibrium between the blocker binding and unbinding rates is described by the dissociation constant (K_D).

$$K_D = \frac{k_{-1}}{k_1} \tag{3}$$

Further description of the enzymatic process has been provided by the Michaelis-Menten equation. This equation calculates the initial velocity (v) of an enzymatic reaction relative to the maximal velocity (V_{max}) for a given substrate concentration (S):

$$\frac{v}{V_{max}} = \frac{[S]}{K_D + [S]} \tag{4}$$

Under conditions of equilibrium, v relative to V_{max} is equivalent to the fraction of conductance blocked (fractional block) by a known concentration of blocker [B]. Therefore, the Michaelis-Menten equation can be used to describe fractional block.

$$\textit{Fractional block} = \frac{1}{1+\frac{K_D}{[B]}} \tag{5}$$

If block is voltage-dependent, then the rates of blocker binding and unbinding are also influenced by voltage. As a result, K_D will be voltage-dependent. The effect of voltage on K_D is described by the Boltzman relation:

$$K_{D(V)} = K_{D(0)}\, e^{\frac{-z\delta FV}{RT}} \qquad (6)$$

where $K_{D(0)}$ is the dissociation constant of the blocker at 0 mV, δ is the fraction of the transmembrane voltage drop crossed by the blocker in reaching its binding site, and V is the voltage at which fractional block is being assessed. z, R, T, and F represent the ion valence, ideal gas constant, absolute temperature, and Faraday constant respectively. This relation predicts the relative probability of finding a particle in a high energy state, given the energy difference between the two states at equilibrium (Hille, 1992). Incorporation of the voltage-dependent K_D into the Michaelis-Menten equation provides a description of the fractional block brought about through associations of the intracellular blocker with the channel pore. This amended relation is now called the Woodhull equation (Woodhull, 1973):

$$Fractional\ Block = \frac{1}{1 + \frac{K_{D(0)} e^{-\frac{z\delta FV}{RT}}}{[B]}} \qquad (7)$$

Assessing blockage

In order to characterize block of the rod and cone cGMP-gated channels by organic cations, currents through the channels in the absence and presence of blocker were measured using the patch-clamp technique. Current traces obtained before, during, and after the application of organic cation blocker to the cytoplasmic surface of an excised inside-out membrane patch indicated the ability of the blocker to reversibly impede ion conduction. Organic blockers presented to the extracellular surface of a patch

using a pipet perfusion system enabled the assessment of external channel block. Data acquired in this study concerning the concentration- and voltage-dependence of channel block by various organic cations has facilitated the characterization of this ligand-gated channel properties.

Assumptions of the Woodhull model

Properties of channel structure can be inferred from the description of fractional block by the Woodhull model, provided two criteria are met. First, the organic cations must block the open channel by occluding the pore. If the organic cations are interacting with an allosteric or regulatory binding site on the protein surface, possibly stabilizing the channel's closed conformation (Hille, 1992), then the Woodhull description of the resulting decrease in conductance will provide no information about the structure of the channel pore. Therefore, evidence suggesting the mechanism of block must be procured before an adequate description of the block can be provided. Voltage-dependent block, competitive interactions with permeant ions, and block reversal by ions from the opposite side of the membrane (Hille, 1992), are all indicators of organic blocker interactions occurring within an open channel pore.

The second criteria that must be met is that the organic cations must be impermeant. If the blockers are capable of passing through the open channel, then estimates of δ (the blocker binding position within the electrical field) will be biased. Organic cations, such as tetramethylammonium (TMA) and tetraethylammonium (TEA), were shown to be impermeant blockers of both the rod (Hodgkin *et al.*, 1985; Furman & Tanaka, 1990; Menini, 1990; Picco & Menini, 1993) and the cone cGMP-gated channels

(Picones & Korenbrot, 1992; Haynes, 1993) in biionic permeability studies. In this type of experiment, sodium ions on the cytoplasmic side of the excised, inside-out patch are replaced with organic cations and the ability of the organic cation to permeate the channel is assessed. Because sodium ions are present in the extracellular solution, a negative electrochemical gradient will carry sodium through the channel across the membrane to the intracellular side. However, in the presence of a positive electrochemical gradient, only cytoplasmic organic cations capable of passing through the open channels will form the outward current. If the organic cations are impermeant, then there will be no outward current. Tetrapropylammonium (TPrA), choline and N-methyl-D-glucamine (NMDG) were also reported to be impermeant blockers of the cone cGMP-gated channel (Haynes, 1993).

Application of the Woodhull model

Description of fractional block as a function of voltage by the Woodhull model provides estimates of two important variables. These two variables, $K_{D(0)}$ and δ, indicate properties of the channel that can be used to construct electrical and physical structure models. Values for δ describe the position of the blocker binding site within the electrical field across the channel pore. While this electrical position does not directly translate to physical dimensions, various blockers can be used to determine whether multiple binding sites are present within the pore and their relative positions. Values for $K_{D(0)}$ provide estimates of blocker affinity for its binding site within the channel pore. Slight modifications to the blocker may affect binding affinity, suggesting the nature of the binding site. Knowing whether a particular binding site prefers to interact with

hydrophobic or hydrophillic blockers helps predict which amino acid groups form associations with the blocker.

A novel study

Although evidence exists for block of the rod and cone cGMP-gated channels by organic cations, characterization of blocker interactions with the channel pores has not previously been carried out in detail. The purpose of this study is to further our knowledge of ion channel structure. In this investigation, symmetrical tetra-alkylammonium compounds were used as organic probes to characterize the internal and external pore region of the cGMP-gated channel found in both the rod and cone photoreceptors of catfish. The fraction of conductance blocked by each organic cation was fit with the Woodhull model to provide estimates of the blocker's binding affinity and binding site location within the electrical field. To assess the importance of hydrophobic and hydrophillic interactions between blockers and channel binding sites, block by organic cations with hydroxyl groups available for hydrogen bond formation was investigated. In future studies, information about the electrical structure of the two cGMP-gated channels can be coupled with information obtained from molecular biology to develop a model of the physical structure of the channel pore. The electrical structures of the rod and cone cGMP-gated channel may contain variations that explain differences in permeation that exist between the two photoreceptor channel subtypes. Further comparison of the ligand-gated cGMP channel electrical structure with the voltage-gated potassium channel structure may demonstrate how slight differences in primary amino acid sequence can have large effects on functional pore properties and structure.

CHAPTER 3: METHODS AND MATERIALS

Experimental preparation

To obtain the unbleached photoreceptor cells of the channel catfish, *Icatalurus punctatus*, the fish was dark adapted for 30 minutes before decapitation, enucleation was performed under dim red light, and isolation of the retina was done under infrared light. After the eyes had been removed, each eye was coronally hemisected and the posterior portion divided into halves. In Ringer's solution (see "Solutions used in preparation" below), the retina of each half was gently peeled from the pigment epithelium and transferred to an enzyme bath of Ringer's solution containing 0.5 mg ml^{-1} hyaluronidase (type IV; Sigma Chemical Co., St. Louis, MO) and 0.05 mg ml^{-1} collagenase (type IV; Sigma Chemical Co.). 30 minutes in the enzyme bath ensured clean catfish photoreceptors free of tissues from the neighbouring interphotoreceptor matrix. This enzyme treatment has previously been shown to have no effect on channel properties (Haynes & Yau, 1990a). After the enzyme treatment, the pieces of retina were transferred to an ice-cold Ringer's solution and kept in the dark until use. To obtain a mixture of isolated rod and cone photoreceptors, a piece of retina was transferred to a Sylgard-bottomed petri dish containing a buffered sodium chloride (NaCl) solution (see "Solutions used in preparation" below) and finely chopped with a razor blade under normal room light. The dissociated cells and broken outer segments were collected with a 200 µl pipette and transferred to the experimental chamber. Once the cells had settled, the chamber was perfused with NaCl solution to remove the last traces of Ringer's solution.

Electrodes used in Dose-response experiments

Patch pipettes used to study block of cGMP-gated channels with internal organic cations were pulled from thick-walled Corning 7740 borosilicate glass capillaries of 1.2 mm outer diameter and 0.6 mm inner diameter (A-M Systems, Everett, WA).

Electrodes used in Perfused pipette experiments

The perfusion system used to expose the extracellular surface of a membrane patch to blocker required that electrodes of a larger diameter be used. These pipettes were pulled from Corning 7740 borosilicate glass capillaries with an outer diameter of 1.5 mm and an inner diameter of 0.8 mm (A-M Systems, Everett, WA). Quartz canulas (ALA Scientific Instruments, New York) were pulled to a fine point so they were able extend within the glass electrode up to 1 mm from the tip without touching the surrounding walls.

Treatment of the electrodes

The glass electrodes were pulled to a fine tip, approximately 1 μm in diameter, by a Flaming / Brown micropipette puller (Sutter Instrument Company, Novato, California). Electrode capacitance was reduced by applying a coat of Sylgard 184 (Dow Corning Co., Midland, MI) near the tip. Electrode tips were smoothed and cleaned by brief fire-polishing. When filled with NaCl solution, the tip resistance of the glass electrodes was between 20 and 25 MΩ.

Membrane patches

To obtain a membrane patch containing cGMP-gated channels, a glass pipette was pressed against either the tip of a cone outer segment or the side of a rod outer segment. Gentle suction was applied until a gigaohm seal was formed. Once the seal had formed,

the micro-manipulator was given a tap causing the electrode to rip the patch away from the outer segment of the photoreceptor. In this excised, inside-out configuration the cytoplasmic surface of the patch is exposed to the bath solution. The detached membrane patch was carefully moved to a position directly within the path of solution flow to facilitate rapid solution exchange. The recording chamber had a volume of 0.2 ml and was continuously perfused with solution. Various solutions could be selected via a rotary valve. Solutions flowed through the experimental chamber at a rate of 1.61 ml min^{-1}. At this rate, the solution bathing the membrane patch was fully exchanged within 100 ms of solution selection. However, 30 s typically expired before the commencement of recordings after a solution change in order to ensure complete replacement of the bath.

Perfused pipette experiments

To dialyse the extracellular surface of the membrane patch with a solution containing either blocker or low sodium, the patch electrode had to be perfused. A mini-perfusion system (2PK+, Adams & List Associates, Westbury, NY), illustrated in Figure 4, was attached to the quartz canula within the patch electrode. This mini-perfusion system consists of a pressure regulator, a perfusion bomb (or vial) containing blocker, and polyethylene tubing connecting the bomb to the quartz canula. After current had been measured under control conditions, solution within the bomb was perfused through the quartz canula into the patch electrode. As the solution diffused through the patch electrode, the extracellular surface of the excised inside-out patch was exposed to either low sodium or blocker. Currents could then be measured in the presence of the extracellular compound.

Figure 4 A schematic model of the perfused pipette system. A pressure regulator controls the flow of blocker from the perfusion bomb through the polyethylene tubing and quartz canula to the patch electrode. Diffusion of blocker through the patch electrode solution exposes the extracellular surface of the patch to blocker.

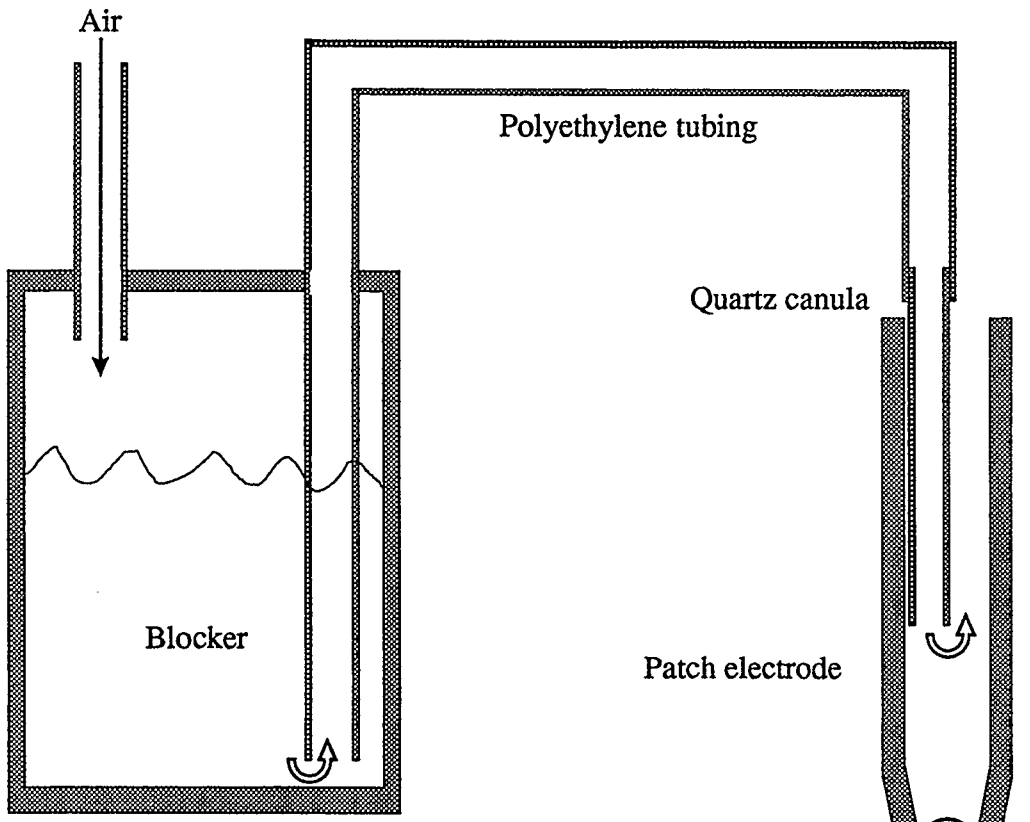

Perfusion Bomb

Membrane patch in the
excised inside-out configuration.

Solutions used in preparation

Ringer's solution contained (in mM): 110 NaCl, 2.5 KCl, 1.6 MgCl, 1.0 CaCl, 5.0 glucose, and 5.0 NaHEPES (pH 7.6).

NaCl solution contained (in mM): 120 NaCl, 0.1 NaEGTA, 0.1 NaEDTA, and 5.0 NaHEPES (pH 7.6).

Solutions used in dose-response experiments — internal block

The patch electrode contained the NaCl solution. The bath could be rapidly changed to contain either the NaCl solution or a solution in which one of the blockers had been substituted for sodium on an equimolar basis. For each additional carbon added to the chain length of a tetra-alkylammonium compound, the concentration of the blocker was decreased by approximately four fold to compensate for the increase in blocker efficacy. The concentration of individual blockers used are as listed in the figures. Channels were maximally activated by the addition of 1 mM cGMP to the bath solution, both in the presence and absence of blocker.

Solutions used in perfused pipet experiments — sucrose and external block

For the low sodium experiment, the perfusion bomb contained (in mM): 10 NaCl, 220 Sucrose, 0.1 NaEGTA, 0.1 NaEDTA, and 5.0 NaHEPES (pH 7.6). The bath was alternated between the NaCl solution and a blocker solution containing (in mM): 119.8 Na, 0.2 TBA, 0.1 NaEGTA, 0.1 NaEDTA, and 5.0 NaHEPES (pH 7.6). 1 mM cGMP was added to the bath solution to maximally activate the channels. The patch electrode contained the NaCl solution.

For the external block experiment, the perfusion bomb contained a solution of (in mM): 20 NaCl, 100 TMA-Cl, 0.1 NaEGTA, 0.1 Na EDTA, and 5.0 NaHEPES (pH 7.6). Both the patch electrode and the bath contained the NaCl solution. 1 mM cGMP was added to the bath solution to maximally activate the channels.

Data Acquisition

Electrical recordings

Current flowing through cGMP-gated channels within a membrane patch was measured under voltage clamp by an Axopatch 1D patch clamp amplifier (Axon Instruments, Inc. Foster City, CA). The signal from the patch clamp was fed through a PCM adaptor (Medical Systems, Inc), and two cascaded 4-pole Bessel filters whose front panel settings were at 5 kHz. The bandwidth for this arrangement was DC-2.8 kHz. According to the Nyquist theory, the sampling frequency should be at least twice the cut-off frequency, which for this arrangement would be 5.6 kHz. However, since the signal of interest is in the form of a slow wave and transient signals provide no added information, hard disk storage space was minimized by sampling at a lower frequency. The signal was digitized to the computer at 1 kHz and stored on the computer's hard disk.

Eliminating the capacitive transients from currents

An illustration of the protocol used to obtain the data reported in these experiments is provided in Fig. 5. Currents through a membrane patch were measured as pairs of voltage ramps were generated between ±80 mV. In the first ramp, the voltage was stepped from the holding potential of 0 mV to the most negative potential (-80 mV) and then ramped at 120 mV s^{-1} to the most positive potential (+80 mV). The voltage was

Figure 5 Voltage protocol used to assess cGMP-dependent currents. Pairs of ramps were run between ±80 mV in opposite directions. The equal magnitude and opposite polarity of the capacitive currents allowed for their elimination by averaging the resulting traces. The net cGMP-dependent current was determined by subtracting the averaged currents obtained before and after cGMP application from the traces obtained in the presence of cGMP.

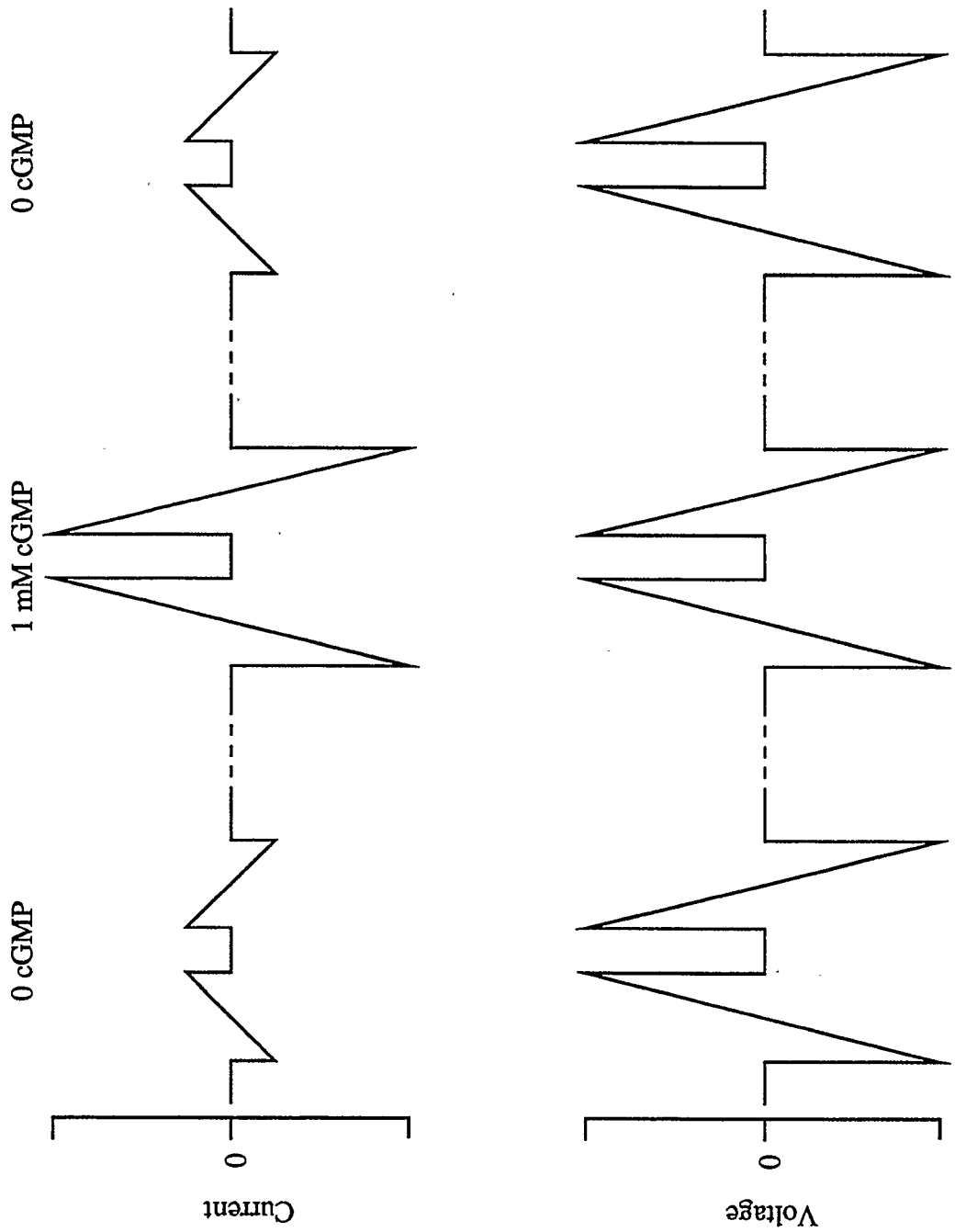
0 cGMP
1 mM cGMP
0 cGMP
Current
0
Voltage
0

returned to the holding potential (0 mV) for 500 ms before a second ramp was run. This time the voltage was ramped from the most positive potential (+80 mV) to the most negative potential (-80 mV) at 120 mV s^{-1}. Since the capacitive component of current recorded in each pair of ramps was of equal magnitude but of opposite polarity, the capacitive currents were eliminated by averaging the pairs together at each voltage.

Determination of the net cGMP-dependent current

cGMP-gated channels within membrane patches could be maximally activated by a saturating concentration of cGMP (determined in previous studies to be any concentration over 100 μM). The resulting current, however, contains a leakage component contributed by small gaps in the seal formed between the membrane and the electrode. To determine the net cGMP-dependent current through a membrane patch, currents were measured before, during, and after the addition of cGMP to the bath. Currents obtained before and after cGMP application were averaged and subtracted from the currents obtained in the presence of cGMP, eliminating the leakage component and rendering the net cGMP-dependent current. These net cGMP-dependent currents, obtained in the presence and absence of organic compounds, were plotted as a function of voltage in a current-voltage (I-V) relation. According to convention, current flowing from the cytoplasmic to the extracellular surface of the detached patch is referred to as outward in direction and is assigned positive values.

Data Analysis

Justifying the shift in reversal potential with the Nernst equation

According to the Nernst equation (Eq. 8), fractional replacement of sodium with an impermeant cation will cause a shift in the reversal potential. The shift in reversal potential apparent in current traces recorded in the presence of various TAA compounds is accounted for by the Nernst equation.

$$V_{Rev} = \frac{RT}{zF} \ln \frac{[Na]_o}{[Na]_i} \tag{8}$$

Calculating conductance

Currents were measured from the I-V relations at 10 mV intervals using a ruler. Using Ohm's law (Eq. 9), conductance (g) was calculated from the current (I) measured at each voltage (V), in order to take into account any shift in the reversal potential (V_{rev}) caused by replacing sodium with blocker.

$$g = \frac{I}{(V - V_{rev})} \tag{9}$$

When the concentration of sodium in solution is significantly reduced, as it is in dose-response experiments using TMA, TEA, Tris and NMDG, there is a concentration-dependent decrease in conductance (Fig. 6 in Haynes, 1995a). To correct for the conductance decrease unrelated to block, conductance was normalized to saturating concentrations of sodium in the TMA, TEA, Tris and NMDG experiments.

Fractional block and the Woodhull equation

Fractional block was calculated as the decrease in conductance elicited by a known concentration of blocker using:

$$Fractional\ block = \frac{g_{max} - g_b}{g_{max}} \quad (10)$$

where g_{max} is the cGMP-dependent conductance measured in the presence of saturating ligand and g_b is the conductance measured after the addition of blocker. The fraction of conductance impeded by the blockers was then plotted as a function of voltage. Fits of fractional block with the Woodhull equation (Eq. 7) have values for $K_{D(0)}$ and δ. $K_{D(0)}$ is a measure of the strength with which the blocker occupies the channel pore. δ is an estimate of the position of the blocker binding site within the pore electrical field.

Three different methods were used to fit fractional block with the Woodhull model. This was done to ensure that block could be consistently described by the electrical values. In the first method, fractional block as a function of voltage was simultaneously fit with the Woodhull equation (Eq. 7) at all blocker concentrations. In the second method, fractional block as a function of blocker concentration was simultaneously fit the Woodhull equation at all voltages. These two methods of fit provide electrical values that describe overall blocking effect of a compound on channels in a patch, and verify the internal consistence of the fitting paradigm. The mean electrical values recorded in Tables I (cones) and II (rods) for each blocker are the average of values from multiple patches. The third method fit the block elicited by a single concentration of blocker as a function of voltage with the Woodhull equation. $K_{D(0)}$ and δ values determined at each concentration were then averaged together to ascertain the mean values for a patch and to ascertain the overall effect of a compound on multiple cone or rod patches. Fits of the data by methods 1 and 2 were done within Mathcad

while fits by method 3 were carried out in the curve fitting program Dfits. Data are presented throughout as mean ± standard deviation.

Determining the energy involved in blocker binding

The free energy (ΔG) used to facilitate interactions between the blocker and its binding site within the channel pore was calculated using

$$\Delta G = RT\ln(K_{D(0)}) \tag{11}$$

Statistical tests

Statistical tests were used to compare the electrical values obtained for patches exposed to the same blocker and patches exposed to different blockers. To compare electrical values obtained by two different methods for equality, a two-tailed, two-sample Student's t-test was used. This same test was used to compare the mean δ values describing different blocker binding positions. To compare the location of blocker binding to the location of the permeant ion binding site, a one-tailed, two-sample Student's t-test was applied (Zar, 1984: Chapter 8, p. 97-101). To test whether the slope of a linear regression was significantly different from zero, variance was analyzed and an F value obtained (Zar, 1984: Chapter 17, p. 268). To determine whether slopes describing distinct data sets were similar, an ANOVA was carried out, yielding an F value (Zar, 1984: Chapter 18, p. 300). For all the statistical tests performed, the null hypothesis was rejected if $p < 0.05$.

CHAPTER 4: RESULTS

Internal block by Tetraalkylammonium compounds

Do Tetraalkylammonium compounds block conductance?

To determine the effect tetraalkylammonium (TAA) compounds have on conductance through open cone and rod cGMP-gated channels, each of TMA through TPeA were substituted for sodium on the cytoplasmic side of the channels. As the symmetrical carbon chains attached to the central ammonium group of the compound were increased in length, both the size and hydrophobicity of the compound increased. The current-voltage (I-V) relations obtained for cone and rod patches exposed to various concentrations of the TAA compounds are shown in Figures 6A and 7A respectively. Each TAA compound tested here blocked currents through an open cone or rod cGMP-gated channel in a voltage- and concentration-dependent manner.

How do TAA compounds interfere with conductance?

Since replacement of internal sodium with TAA compounds causes a Nernstian shift in current reversal potential (most apparent in the presence of TMA), a quantitative evaluation of blocker effect is more accurately made by assessing conductance. To clearly illustrate the voltage- and concentration-dependence of block, the fraction of conductance blocked by the TAA compounds was calculated for each concentration and plotted as a function of voltage (Fig. 6B, cones; Fig. 7B, rods) (see "Data Analysis" for equations). The data in these figures were fit with the Woodhull model according to method 1 (a simultaneous fit of the fractional block over all concentrations and voltages tested on a patch) to provide a summary view of how the blockers interact with the

Figure 6 Symmetrical TAA compounds block the cone cGMP-gated channel from the inside. **A.** I-V relations. Each plot represents data obtained from a single patch. These patches were chosen to illustrate a typical response of cone cGMP-gated channels to blocker. The blockers used were (from left to right) TMA, TEA, TPrA, TBA, and TPeA. For each blocker, a series of solutions containing increasing amounts of blocker were mixed so the concentration dependence of block could be determined. As blocker length was systematically increased, the concentrations of blocker used were decreased by approximately four fold. In these experiments, TMA was mixed in concentrations of 0, 5, 10, 20, 50, and 100 mM; TEA in concentrations of 0, 1, 2, 5, 10, and 20 mM; TPrA in concentrations of 0, 0.2, 0.25, 1, 2, and 5 mM; TBA in concentrations of 0, 0.05, 0.1, 0.2, 0.5, and 1 mM; and TPeA in concentrations of 0, 0.02, 0.05, 0.1, 0.2, and 0.5 mM. The shift in reversal potential observed in the I-V for TMA can be accounted for by the Nernst potential for sodium (see Data analysis). **B.** Block as a function of voltage. Data contained in each plot was obtained from the corresponding I-V functions directly above. The fraction of conductance blocked by each concentration of blocker is represented by a distinct symbol. (○, □, △, ▽, and ☆ are the blocker concentrations from lowest to highest.) The solid lines represent a fit of the Woodhull equation to the data by method 1. Data obtained in the presence of 100 mM TMA was considered unreliable due to a change in patch seal resistance and was not included in the fits. The electrical constants ($K_{D(0)}$ and δ) describing block of channels in each patch were 91 mM and 0.40 (TMA), 7 mM and 0.37 (TEA), 6.5 mM and 0.50 (TPrA), 0.47 mM and 0.41 (TBA), and 0.089 mM and 0.43 (TPeA).

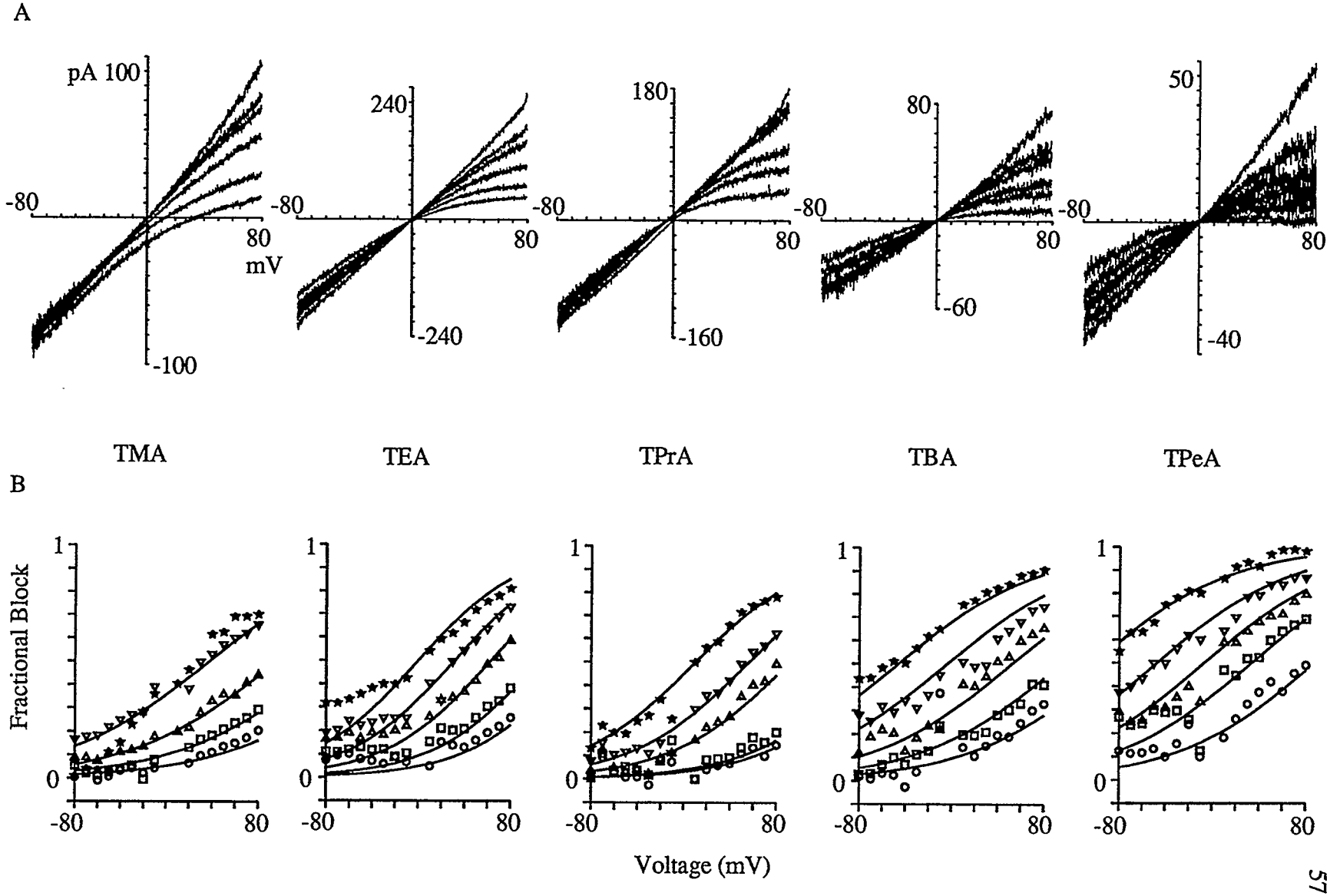
A
pA 100
-80
80
mV
-100
240
-240
180
-160
80
-60
50
-40
TMA
TEA
TPrA
TBA
TPeA
B
Fractional Block
1
0
-80
80
Voltage (mV)

Figure 7 Symmetrical TAA compounds also block the rod cGMP-gated channel from the inside. **A.** I-V relations. Each plot represents data obtained from a single patch. These patches were chosen to illustrate the typical response of rod cGMP-gated channels to blocker. The blockers used were (from left to right) TMA, TEA, TPrA, TBA, and TPeA. For each blocker, a series of solutions were mixed containing a increasing amounts of blocker so the concentration dependence of block could be determined. As blocker length was systematically increased, the concentrations of blocker used were decreased by approximately four fold. In these experiments, TMA was mixed in concentrations of 0, 5, 10, 20, 50, and 100 mM; TEA in concentrations of 0, 1, 2, 5, 10, and 20 mM; TPrA in concentrations of 0, 0.2, 0.25, 1, 2, and 5 mM; TBA in concentrations of 0, 0.05, 0.1, 0.2, 0.5, and 1 mM; and TPeA in concentrations of 0, 0.02, 0.05, 0.1, 0.2, and 0.5 mM. The shift in reversal potential observed in the I-V for TMA can be accounted for by the Nernst potential for sodium (see Data analysis). **B.** Block as a function of voltage. Data contained in each plot was obtained from the corresponding I-V functions directly above. The fraction of conductance blocked by each concentration of blocker is represented by a distinct symbol. (O, □, ▵, ▿, and ☆ are the blocker concentrations from lowest to highest.) The solid lines represent a fit of the Woodhull equation to the data by method 1. The electrical constants ($K_{D(0)}$ and δ) determined for block of each patch were 50.9 mM and 0.33 (TMA), 4.7 mM and 0.44 (TEA), 3.8 mM and 0.57 (TPrA), 0.48 mM and 0.49 (TBA), and 0.054 mM and 0.20 (TPeA).

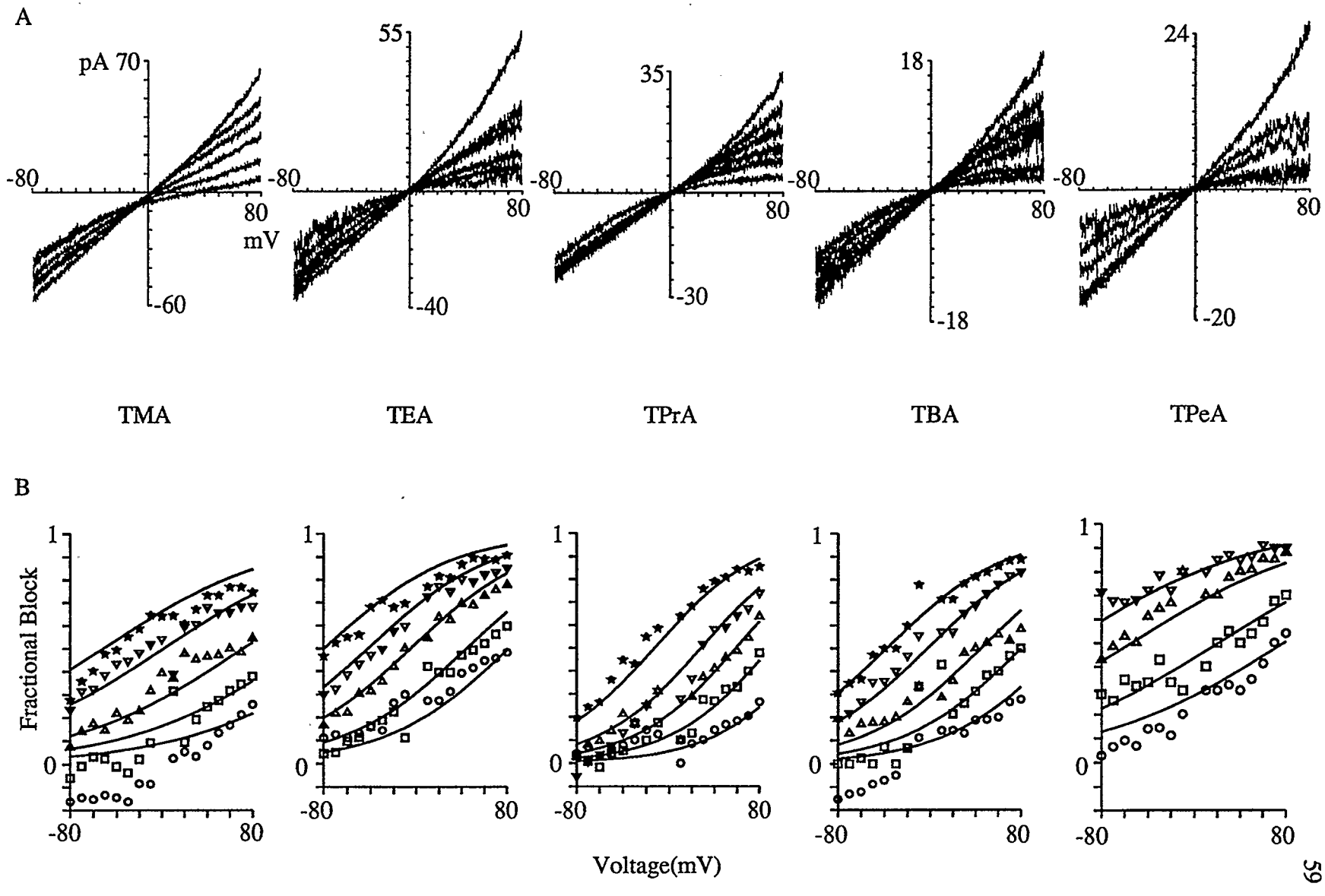
A
pA 70
-80
80
mV
-60
55
-40
35
-30
18
-18
24
-20
TMA
TEA
TPrA
TBA
TPeA
B
Fractional Block
1
0
-80
80
Voltage(mV)

channels. As the potential across each membrane patch was made more positive, the amount of block increased regardless of which TAA compound was present. Positive potentials increase the entry rate and decrease the exit rate of an ion entering the open pore from the cytoplasmic solution, and the same is true for the effect negative potentials have on ions entering from the extracellular solution. Voltage-dependent block of the channels indicates that the transmembrane potential controlling ion permeation also effects the ability of the TAA compounds to block the channel. The applied membrane potential is influencing the entry and exit rates of the blocker into the open channel. Since block increases with no relief even at the most positive potentials tested, these data suggest that the organic cations entering the open channels are unable to pass through completely. This observation supports the conclusion of previous bi-ionic experiments that these organic cations are impermeant to both the rod and cone cGMP-gated channels (Hodgkin *et al.*, 1985; Furman & Tanaka, 1990; Menini, 1990; Picco & Menini, 1993; Picones & Korenbrot, 1992; Haynes, 1993). Although voltage-dependent block could be explained through other mechanisms, the interaction of the TAA compounds with the channel pore will be further substantiated later in this chapter.

The fraction of conductance blocked by the TAA compounds also increased in a concentration-dependent manner. The Woodhull equation predicts this, for as the concentration of blocker increases the probability of channel occupancy by the blocker also increases. The fits obtained with the Woodhull model are consistent with a single molecule of blocker occupying the channel. This was confirmed by fitting the concentration-dependence of block at a given voltage by the Hill equation (Table I). In

Table I. Description of internal TEA block of an individual cone patch with the Hill equation.

Voltage (mV)	$K_{1/2}$	N
-80	104.79	0.538
-70	135.24	0.479
-60	89.39	0.502
-50	73.37	0.562
-40	48.14	0.653
-30	36.74	0.744
-20	46.01	0.657
-10	32.57	0.758
10	13.61	1.05
20	18.97	0.586
30	11.01	0.774
40	8.96	0.873
50	6.99	0.853
60	5.31	0.856
70	4.49	0.857
80	3.39	0.873

all cases, the Hill coefficient (the minimum number of binding sites available for blocker interactions) was ≤ 1, consistent with a single molecule of blocker occluding the channel.

What else do the I-V curves indicate?

As the size of the blocker was systematically increased, a concentration-dependent decrease in current at negative potentials became more apparent despite the lowering of actual blocker concentration (Fig. 6A: TPrA, TBA, TPeA; Fig. 7A: TEA, TPrA, TBA, TPeA). More extreme negative potentials than used here may be required to fully relieve the block, suggesting that stronger interactions are occurring between the pore and the blockers as size increases. Since block at negative potentials in the presence of identical blocker concentrations is seen more frequently in rod patches than cone patches, this may imply that the blockers adhere more tightly to the rod channel pore than to the cone.

Voltage-independent block at negative voltages was also occasionally observed as the blockers increased in size (e.g., cone TEA patch illustrated in Figure 6B). Whether this observation is an artifact of improper leakage compensation or holds significance was difficult to determine as it was not consistently observed. Since the Woodhull model exclusively describes voltage-dependent block, only the data at positive potentials was fit with the equation when voltage-independent block was observed.

Noise levels observed within the current traces obtained for both the rod and cone patches also increased as the blocker size increased. The noise levels may reflect an increase in block duration as the strength of binding interactions between the pore and bulky blockers increases. Noise levels in the rod I-V traces are generally larger than in the cone I-V traces, consistent with the suggestion that the blockers are adhering more

tightly within the rod pore than the cone. Since the noise observed in the traces was non-stationary, it was not analyzed further.

After current measurements in the presence of blocker had been made, currents in the absence of the blocker were reassessed. The TMA I-V relations shown in Fig. 6 and 8 are from the same cone patch. Included in Fig. 8, however, is the cGMP-dependent current measured in the absence of blocker after the concentration series had been run. Although there was some evidence of current run-down, blockage of current flow by TMA was reversible. A decrease in current as a result of channel loss can be differentiated from channel block by analyzing for voltage-dependence. Block could be reversed after the application of each of the organic cations tested.

Does the Woodhull model accurately describe fractional block?

Mean electrical values, describing block of multiple patches by each of the TAA compounds, were obtained by averaging fits made with method 1 of the Woodhull model. These values (Table II, cones; Table III, rods) have large standard deviations associated with them. The variability in $K_{D(0)}$ and δ could be the result of one of two processes: an artifact of model fitting or an intrinsic mechanism attributable to the cGMP-gated channels of both rods and cones. To check the consistency of fit, block as a function of voltage was fit with two other forms of the Woodhull model (see "Data Analysis" for details). $K_{D(0)}$ and δ, were obtained with each method for the series of TAA compounds used as blockers. $K_{D(0)}$ (the dissociation constant for the blocker at 0 mV) measures the affinity between the binding site and blocker, while δ measures the approximate location of the binding site within the membrane electric field. A summary of the values obtained

Figure 8 I-V relation for a cone patch exposed to TMA. cGMP-dependent current in the absence of blocker was reassessed after a series of TMA concentrations had been presented to the patch. The recovery of current and absence of voltage-dependent block indicate that block is fully reversible.

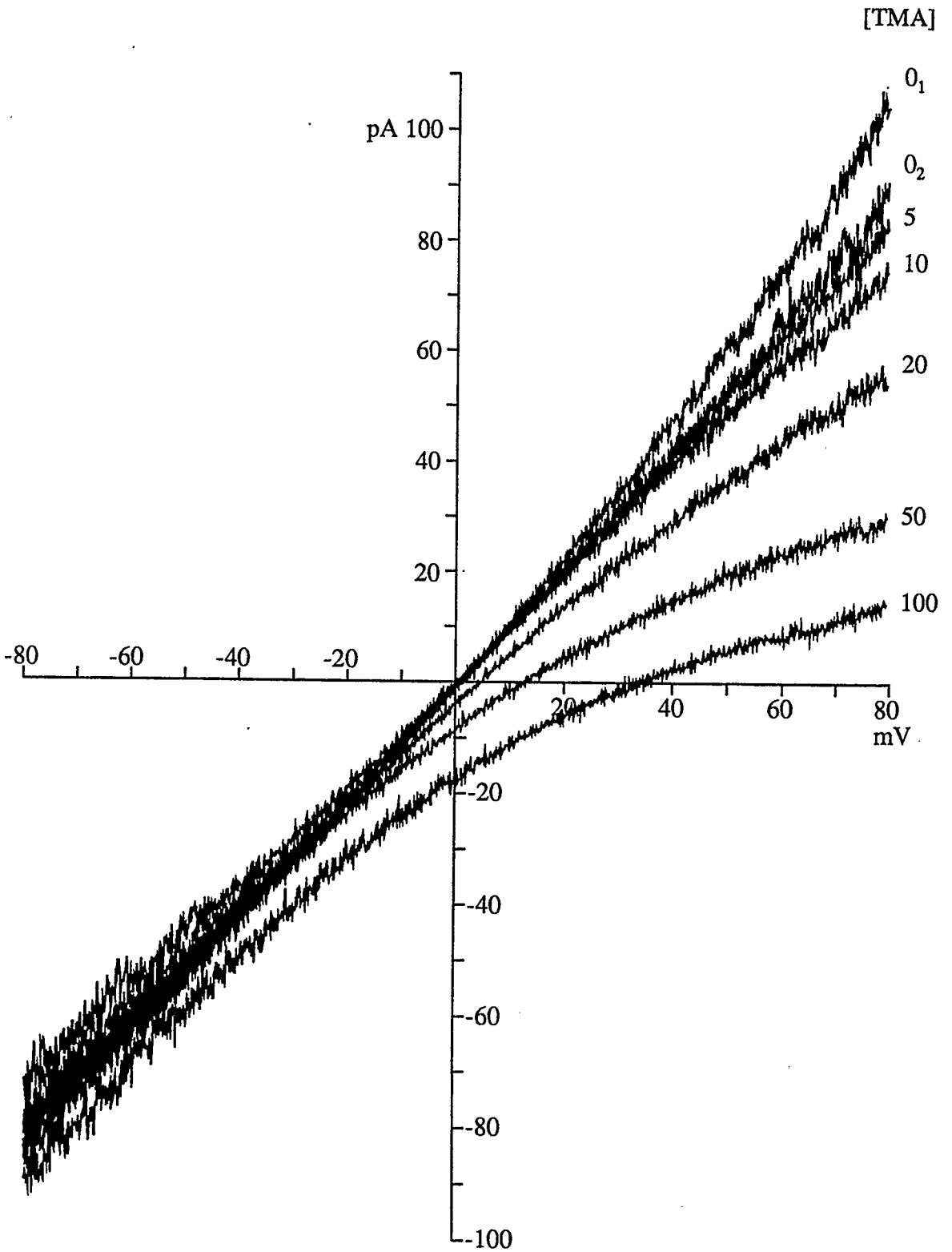
[TMA]
pA 100
80
60
40
20
-20
-40
-60
-80
-100
-80
-60
-40
-20
20
40
60
80
mV
0₁
0₂
5
10
20
50
100

Table II. Electrical values describing block of the cone cGMP-gated channel. Values are mean ± standard deviation.

	Method 1			Method 2			Method 3		
Blocker	$K_{D(0)}$ (mM)	δ	N‡	$K_{D(0)}$ (mM)	δ	N‡	$K_{D(0)}$ (mM)	δ	N§
TMA_i	75 ± 35	0.38 ± 0.16*	7	82 ± 44	0.40 ± 0.18*	7	63 ± 28	0.34 ± 0.13*	28
TEA_i	11 ± 8	0.41 ± 0.16*	9	12 ± 8.7	0.43 ± 0.20*	9	11 ± 7.5	0.38 ± 0.17*	40
$TPrA_i$	4.7 ± 2.7	0.42 ± 0.14*	9	5.3 ± 3.0	0.42 ± 0.17*	9	4.8 ± 2.7	0.43 ± 0.17*	38
TBA_i	0.57 ± 0.12	0.48 ± 0.12*	4	0.59 ± 0.15	0.45 ± 0.12*	4	0.54 ± 0.21	0.42 ± 0.14*	15
$TPeA_i$	0.08 ± 0.02	0.35 ± 0.09*	5	0.09 ± 0.02	0.33 ± 0.1*	5	0.085 ± 0.021	0.35 ± 0.10*	24
$Tris_i$	32 ± 14	0.47 ± 0.19*	4	32 ± 14	0.48 ± 0.22*	4	N.D.		
$NMDG_i$	85 ± 51	0.59 ± 0.26	11	79 ± 60	0.56 ± 0.28	11	N.D.		
TMA_o	N.D.			N.D.			144 ± 91	0.13 ± 0.05†	3

‡ - number of patches
§ - number of trials
* significantly different from the permeant ion binding site δ = 0.61 from the intracellular side at $p < 0.05$
† significantly different from the permeant ion binding site δ = 0.39 from the extracellular side at $p < 0.05$
N.D. not determined

Table III. Electrical values describing block of the rod cGMP-gated channel. Values are mean ± standard deviation.									
	Method 1			Method 2			Method 3		
Blocker	$K_{D(0)}$ (mM)	δ	N‡	$K_{D(0)}$ (mM)	δ	N‡	$K_{D(0)}$ (mM)	δ	N§
TMA_i	44 ± 40	0.28 ± 0.11	8	65 ± 89	0.30 ± 0.15	8	68 ± 75	0.37 ± 0.18	27
TEA_i	3.1 ± 1.5	0.32 ± 0.13	5	3.0 ± 1.4	0.30 ± 0.11	5	3.8 ± 1.9	0.37 ± 0.19	20
$TPrA_i$	3.6 ± 1.3	0.58 ± 0.09	6	3.6 ± 1.3	0.56 ± 0.11	6	3.8 ± 2.1	0.54 ± 0.17	27
TBA_i	0.29 ± 0.13	0.33 ± 0.17	6	0.29 ± 0.12	0.32 ± 0.17	6	0.28 ± 0.13	0.31 ± 0.12	30
$TPeA_i$	0.024 ± 0.006	0.30 ± 0.05	4	0.023 ± 0.003	0.29 ± 0.05	4	0.023 ± 0.01	0.29 ± 0.11	16

‡ - number of patches

§ - number of trials

with all methods of fit is provided in Table II (cones) and Table III (rods). The electrical constants obtained for a given blocker by each method were not statistically different from one another, indicating that block can be consistently described by different forms of the Woodhull model.

Is fractional block accurately described by the electrical values?

Since the Woodhull model determines the values of both $K_{D(0)}$ and δ describing block, it is important to ascertain whether the fitting process could be biased. (It is possible that achieving the best fit of the data requires $K_{D(0)}$ and δ values that compensate for each other, i.e., variables that are not independent.) As a part of the Levenberg-Marquardt algorithm used by the curve fitting program (Press *et al.*, 1992), the cross-correlation between electrical variables was determined (data not shown). While the degree of correlation varied from patch to patch, the electrical variables were all negatively correlated regardless of the blocker used or patch type. The negative dependence of $K_{D(0)}$ on the value of δ suggests that the Woodhull model requires $K_{D(0)}$ values to increase as δ values decrease in order for the best fit to be obtained. If the fitting process causes a bias in values, then the correlation between $K_{D(0)}$ and δ determined by the fit should be reflected in a data plot of $K_{D(0)}$ as a function of δ.

To determine if the bias of the model would be reflected in the data, the electrical constants determined by method 1 of the Woodhull model for each patch exposed to a TAA compound were plotted as a function of one another in Fig. 9 (A for cones; B for rods). For each blocker tested on cone patches, the correlation between $K_{D(0)}$ and δ was positive. This positive correlation, emphasized by the linear regression drawn through

Figure 9 A positive correlation exists between electrical constants describing TAA compound block of cone and rod channels, with the exception of rod channel block by TPeA. The electrical constants plotted in this figure were obtained by fitting fractional block as a function of voltage with method 1 of the Woodhull model. Values obtained from all cone patches (A) and all rod patches (B) were plotted as a function of one another on a semi-logarithmic scale. A distinct symbol was assigned to each TAA compound used as a blocker (○ TMA, □ TEA, △ TPrA, ▽ TBA, and ◇ TPeA). The logarithmically transformed data were fit by linear regression.

A. TAA compounds dissociate with greater ease the further across the cone membrane voltage drop they bind. The parameters of slope, y-intercept and Pearson's correlation coefficient (r values) for the linear regressions were 0.934, 1.49, and 0.81 (TMA); 1.973, 0.13 and 0.93 (TEA); 1.71, −0.126, and 0.86 (TPrA); 0.688, −0.583, and 0.97 (TBA); 1.21, −1.52 and 0.74 (TPeA).

B. TAA compounds, with the exception of TPeA, dissociate with greater ease the further across the rod membrane voltage drop they bind. The parameters of slope, y-intercept and Pearson's correlation coefficient (r values) for the linear regressions were 3.69, 0.41, and 0.82 (TMA); 1.72, -0.123, and 0.71 (TEA); 1.83, −0.548 and 0.94 (TPrA); 0.81, −0.856 and 0.63 (TBA); −2.17, −0.997, and 0.86 (TPeA).

A

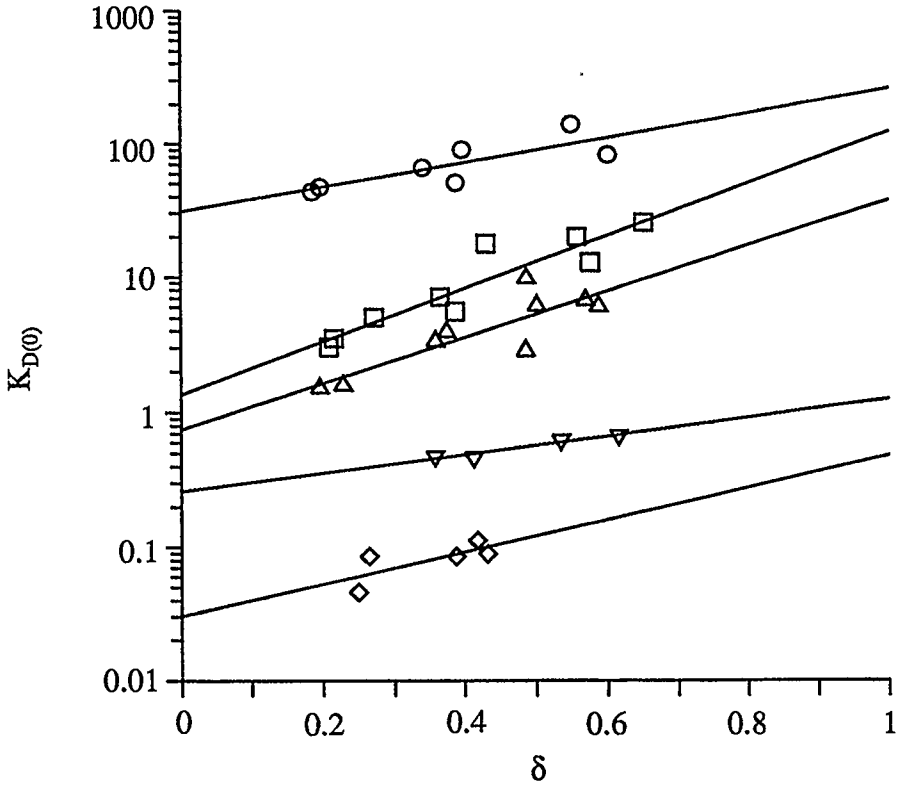
1000
100
10
1
0.1
0.01
$K_{D(0)}$
0
0.2
0.4
0.6
0.8
1
δ

B

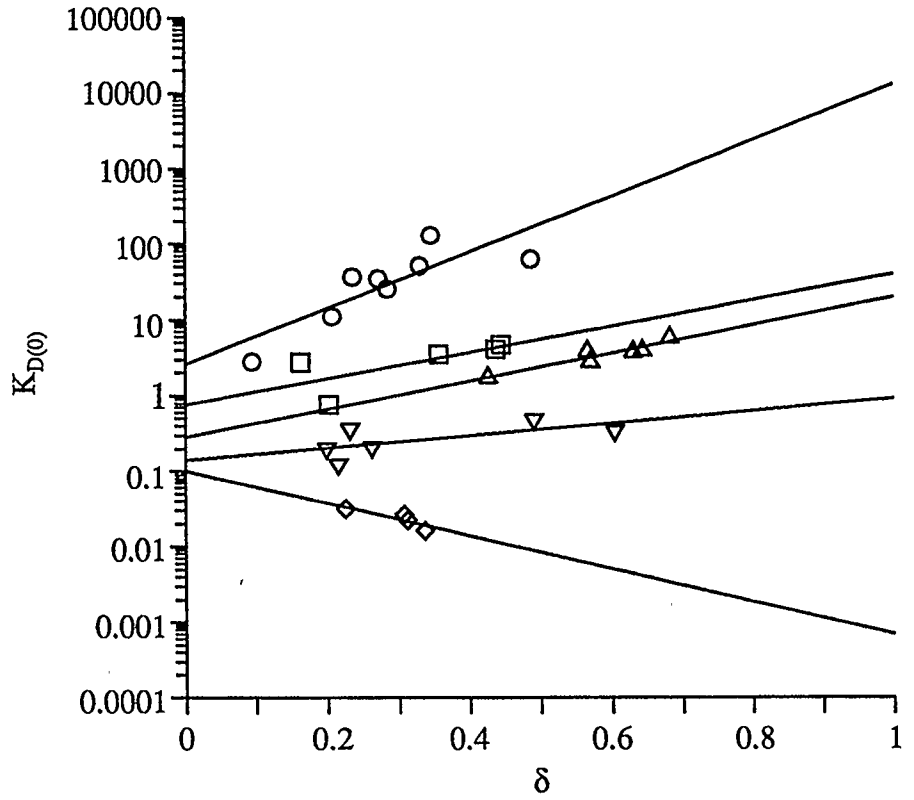
100000
10000
1000
100
10
1
0.1
0.01
0.001
0.0001
$K_{D(0)}$
0
0.2
0.4
0.6
0.8
1
δ

each data set, indicates that as δ increases, $K_{D(0)}$ follows. Each blocker tested on a rod patch, with the exception of TPeA, also demonstrated a positive correlation between the electrical constants. The positive correlation implies that the blockers dissociate from the cone and rod channels with greater ease the further into the membrane voltage drop they have moved. The exception is seen in the presence of TPeA. As TPeA moves further into the rod electric field the more difficult dissociation becomes. Since this observation was made exclusively in rod patches exposed to TPeA, the data suggests that the internal mouth of the rod pore may have unique properties not apparent in the cone pore. It is possible that size constraints of the larger blocker force a change in rod pore conformation in a manner that prevents the blocker from dissociating the further into the pore it moves. Since the negative correlation predicted to occur as an artifact of the fitting process is not generally reflected in the data, the variability in electrical values is likely to be accounted for by processes intrinsic to the rod and cone cGMP-gated channels.

Is the variability in block due to changes within a patch or between patches?

If the variability in electrical values is due to an intrinsic channel process, pinpointing the mechanism would be advantageous for understanding this ligand-gated channel. If every patch exposed to a TAA compound has different degrees and position of block, then the variability in electric values could be due to differences between patches. Using the rod patches exposed to TPrA as an example, a comparison of the electrical values obtained by method 1 of the Woodhull model is made in Table IV. Patch values for $K_{D(0)}$ ranged between 1.7 and 5.7 mM, while δ values ranged between

Table IV. Electrical values determined by Method 1 for individual rod patches exposed to internal TPrA.

Patch	$K_{D(0)}$	δ
060795c	5.7	0.68
300895a	2.8	0.57
010995a	1.7	0.43
200995b	3.9	0.64
280995a	3.7	0.63
280995c	3.8	0.57
mean ± sd	3.6 ± 1.3	0.58 ± 0.09

0.43 and 0.68. This variability in electrical values between patches was noted for rods and cones alike, regardless of which organic cation was used as a blocker. If variability was only observed between patches, slow changes in channel structure occurring over several minutes may be responsible for the effects on the pore electrical field. If changes are occuring on a faster time scale, diverse electrical values should also be apparent within a patch as time progresses. Since each patch was exposed to a maximum of five TAA concentrations, the block elicited by each concentration could be individually fit with the Woodhull equation using method 3. If channels within a patch are static over several minutes, then the electrical constants describing fractional block should be consistent over the entire concentration range. Table V lists the electrical values obtained by method 3 of the Woodhull model for each rod patch exposed to TPrA. TPrA consistently evoked block described by different values for $K_{D(0)}$ and δ, not only for the same concentration of blocker between patches, but for different concentrations of blocker within the same patch. This same phenomenon was noted for rod and cone patches alike, regardless of which organic cation was used as a blocker. When a single cone patch was repeatedly exposed to 20 mM TEA over 23 minutes, the electrical values describing block were also found to vary (Table VI). Therefore, the variability in electrical constants is likely due to continual conformational changes occurring within a patch which effect the membrane electric field. Whether channel conformational changes are affected by factors in the surrounding environment has yet to be determined.

Table V. Electrical values determined by Method 3 for individual rod patches exposed to TPrA.

Patch	060795c		300895a		010995a		200995b		280995a		280995c		Mean ± SD‡	
[B], mM	$K_{D(0)}$	δ	$K_{D(0)}$	δ	$K_{D(0)}$	δ	$K_{D(0)}$	δ	$K_{D(0)}$	δ	$K_{D(0)}$	δ	$K_{D(0)}$	δ
0.2	3.1	0.59	0.72	0.34	0.54	0.34	1.8	0.46	4.7	0.75	4.1	0.65	2.5 ± 1.8	0.52 ± 0.17
0.5	6.2	0.85	3.4	0.40	6.9	0.85	1.7	0.39	2.1	0.49	3.2	0.54	3.9 ± 2.2	0.59 ± 0.21
1	10.6	0.81	3.2	0.57	1.9	0.36	3.8	0.52	4.9	0.65	3.0	0.46	4.6 ± 3.1	0.56 ± 0.16
2	6.3	0.68	2.87	0.44	1.9	0.27	5.5	0.66	N/A	N/A	5.0	0.66	4.3 ± 1.9	0.54 ± 0.18
5	4.5	0.58	3.06	0.42	2.8	0.31	N/A	N/A	N/A	N/A	3.3	0.57	3.4 ± 0.8	0.47 ± 0.13
mean ± sd§	6.1 ± 2.8	0.70 ± 0.12	2.7 ± 1.1	0.43± 0.09	2.8 ± 2.4	0.43 ± 0.24	3.2 ± 1.8	0.51 ± 0.11	3.9 ± 1.6	0.63 ± 0.13	3.7 ± 0.83	0.58 ± 0.08		

‡ - determined for each blocker concentration

§ - determined for each patch

Table VI. Electrical values describing internal TEA block of a single cone patch vary with time.

Time (min)	$K_{D(0)}$ (mM)	δ
3	20.46	0.565
10	22.62	0.597
16	18.62	0.677
23	15.38	0.524

Do the TAA compounds interact with a common site in the channel pore?

The mean δ values recorded in Tables II and III suggest that there is a single position within the electric field of the cone or rod pore to which the TAA compounds bind. This position is located 41% of the way into the cone electrical field (n = 34) and 36% of the way into the rod (n = 29)(values are not significantly different from each other). However, the variance associated with these mean δ values also suggests that this position is not achieved by the blockers all of the time. δ values were plotted as a function of the number of carbons per blocker side chain in Figure 10 (A for cones; B rods). These plots illustrate that the fraction of the voltage drop crossed by a blocker in reaching its binding site within the pore of the channel is independent of the blocker size. Fits of the data with a linear regression again illustrated that average binding positions are located at 0.40 in the cone electrical field and 0.33 in the rod (values correspond to the y-intercepts of the linear regression). The slopes of both lines were found to be not significantly different from zero using a Student's t-test. The plots also illustrate that blockers of all sizes are capable of binding to any electrical position between 0.19 and 0.65 within the cone field or between 0.095 and 0.68 within the rod field. The apparent variability of the blocker binding sites within a distinct portion of the channel electrical field could be interpreted in two ways. The first interpretation would predict the existence of a single blocker binding site in the cGMP-gated channel pore. The position of the binding site within the electrical field would be determined by the conformation of the channel. Since it has been previously suggested that the channel is continuously changing shape, it is possible that the blocker's binding position within the membrane

Figure 10 TAA compounds bind to a single mean binding site independent of blocker size. δ values were determined for each patch exposed to blocker and plotted as a function of the number of carbons on each blocker side chain.

A. TAA compounds bind to a single site in the cone cGMP-gated channel pore. Each TAA compound was found to vary its binding position within 19% to 65% of the voltage drop. A fit of the data with a linear regression determined the average site of blocker interaction. The parameters of the line were 0.0016 (slope), 0.402 (y-intercept), and 0.0155 (r value).

B. TAA compounds bind to a single site in the rod cGMP-gated channel pore. Each TAA compound was found to vary its binding position within 9.5% to 68% of the voltage drop. A fit of the data with a linear regression determined the average site of blocker interaction. The parameters of the line were 0.014 (slope), 0.33 (y-intercept), and 0.122 (r value).

A

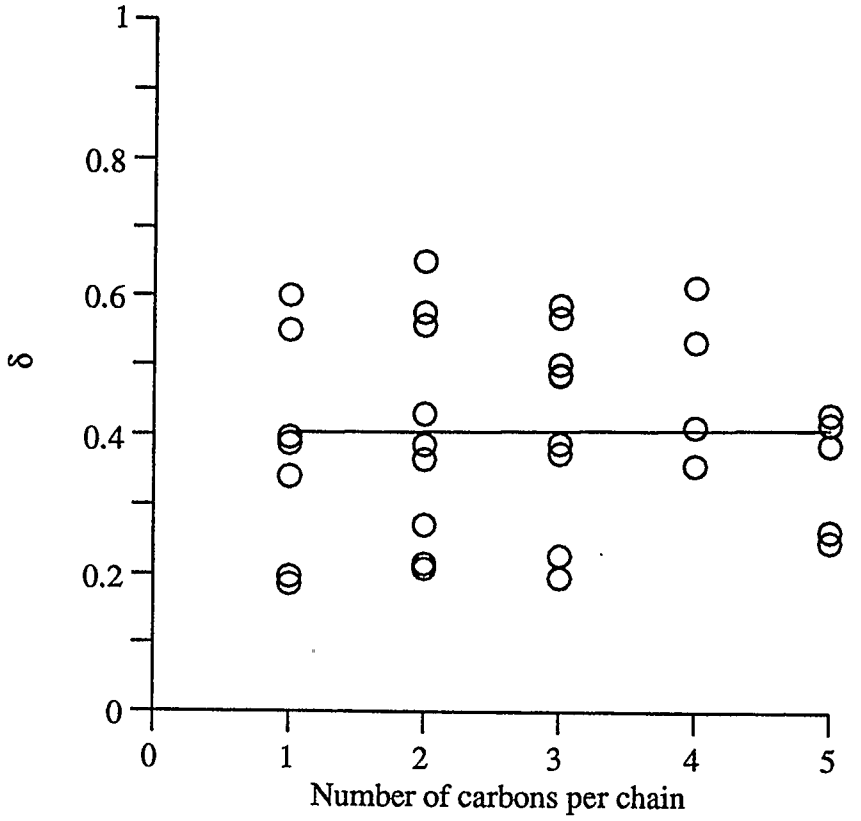
1
0.8
0.6
0.4
0.2
0
δ
0
1
2
3
4
5
Number of carbons per chain

B

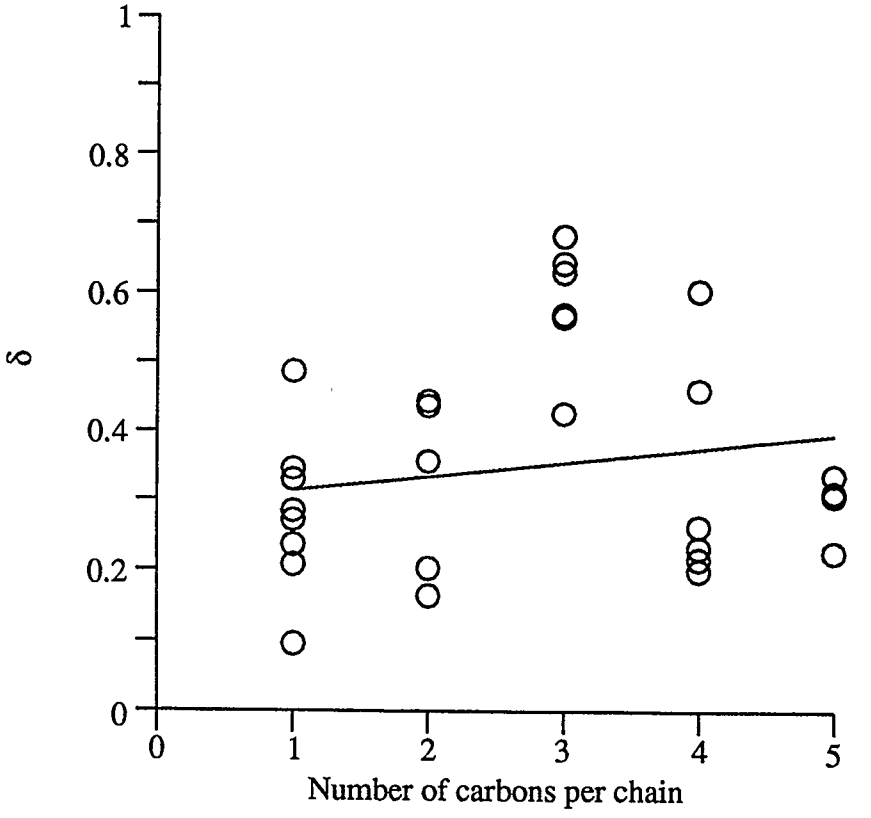
1
0.8
0.6
0.4
0.2
0
δ
0
1
2
3
4
5
Number of carbons per chain

electrical field is determined by the particular conformation of the channel at that moment. The second interpretation would predict that the channel contains multiple binding sites within the pore to which the cations randomly associate. However, an ion entering the membrane electric field experiences a constant driving force with which it overcomes the intervening energy barriers. This driving force determines that binding will not be random and that the blocker will ultimately reach the same site each time it enters the pore. Therefore, the model predicting a single flexible binding site within the pore of cone and rod channels best explains the range of δ values obtained for the TAA compounds.

Do the TAA compounds bind to a location distinct from other topographical sites?

The mean positions for blocker binding within the cone channel were compared to the permeant ion binding position predicted by Eyring rate models to occur at $\delta = 0.61$ (Haynes, 1995b). For each blocker, a Student's t-test determined that the TAA compounds bound on average to a position within the cone channel pore which was significantly different ($p < 0.05$) from the site responsible for permeant ion interactions. However, individual patches demonstrated that the TAA compounds were occasionally capable of reaching a comparable position within the cone membrane electric field (e.g., patch 080594c exposed to TMA $\delta = 0.601$, patch 040794b exposed to TEA $\delta = 0.652$, patch 310894b exposed to TBA $\delta = 0.616$).

How does TAA compound size effect binding interactions?

As the carbon chains of the TAA compounds were increased in length, $K_{D(0)}$ values decreased (Table II and III). A comparison of the mean $K_{D(0)}$ values revealed that

identical blockers bound to the cone channels with 51% lower affinity than they did to the rod channels. This observation supports inferences drawn from the I-V curves suggesting that TAA compounds dissociate with greater ease from the cone channel pore than from the rod. To determine the effect TAA compound size had on blocker / pore interactions, binding energy was calculated from the $K_{D(0)}$ values obtained by method 1 for each patch exposed to TAA compounds (see Data analysis). A plot of binding energy as a function of the number of carbons each symmetrical TAA compound contained on a side chain is shown in Fig. 11 (A for cones; B rods). As the hydrophobicity of the blocker increased, the energy with which the blocker bound to the channel pore of both the rod and cone also increased. This suggests that interactions with the pore are modified as the TAA compound side chains increase in length. Support for this implication is provided in the observations made while assessing the dependence of $K_{D(0)}$ on δ in Fig. 9. A comparison of the linear regressions using an analysis of variance in the cone (A) and rod (B) plots determined that the slopes are not identical. This implies that the interactions between the TAA compounds and the cone and rod channel pores change as blocker size changes. The lack of an apparent trend in the manner the slopes shift suggests that the change is not systematic. However, as the blockers increase in size, the longer chain lengths can occupy more surface area along the pore walls. Depending on the configuration of the blocker in solution and as it interacts with the channel, associations with a greater variety of amino acids lining the pore may occur. As the number of possible interactions increase, the type of associations formed may change.

Figure 11 TAA compounds bind to cone and rod channel pores with increased energy as their carbon chain length is increased. Binding energy was calculated using Eq. 11 from the mean dissociation constants ($K_{D(0)}$) determined by fits of fractional block with method 1 of the Woodhull equation. The binding energy of each patch was then plotted as a function of the number of carbons each symmetrical TAA compound had on a chain.

A. Cone cGMP-gated channels bound TAA compounds with greater energy as the blocker tails increased in length by a carbon. The linear increase in binding energy can be described by a regression formed with a slope of −3.97, a y-intercept of −2.88, and a r value of 0.95.

B. Rod cGMP-gated channels also bound TAA compounds with greater energy as the blocker tails increased in length by a carbon. The linear increase in binding energy can be described by a regression formed with a slope of −4.01, a y-intercept of −4.71, and a r value of 0.92.

A

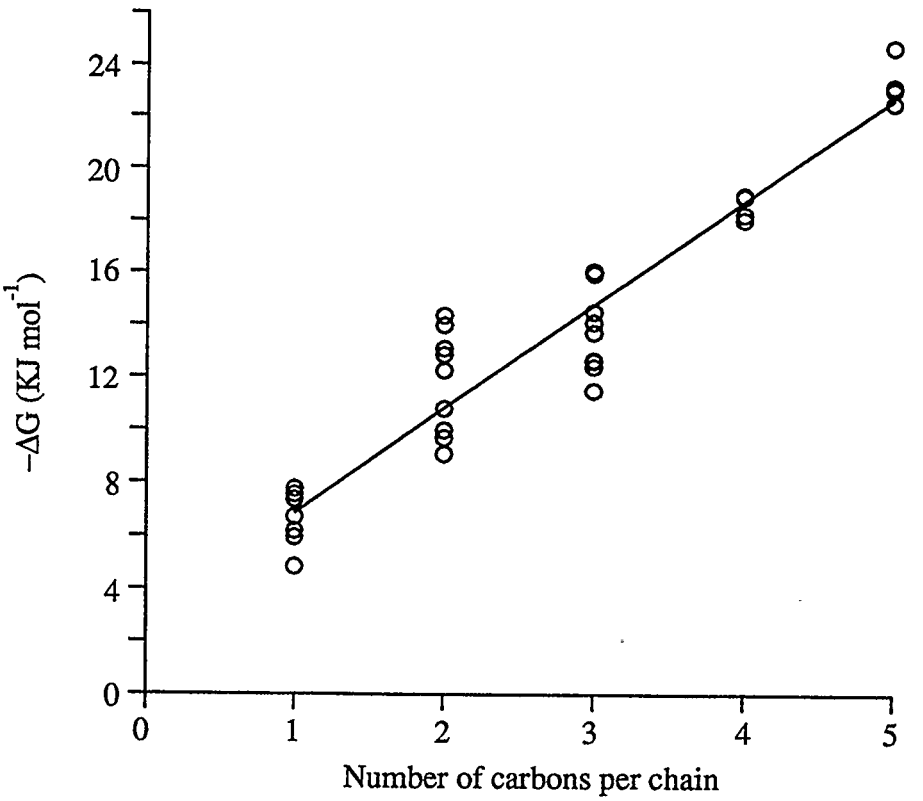
24
20
16
12
8
4
0
0
1
2
3
4
5
$-\Delta G$ (KJ mol^{-1})
Number of carbons per chain

B

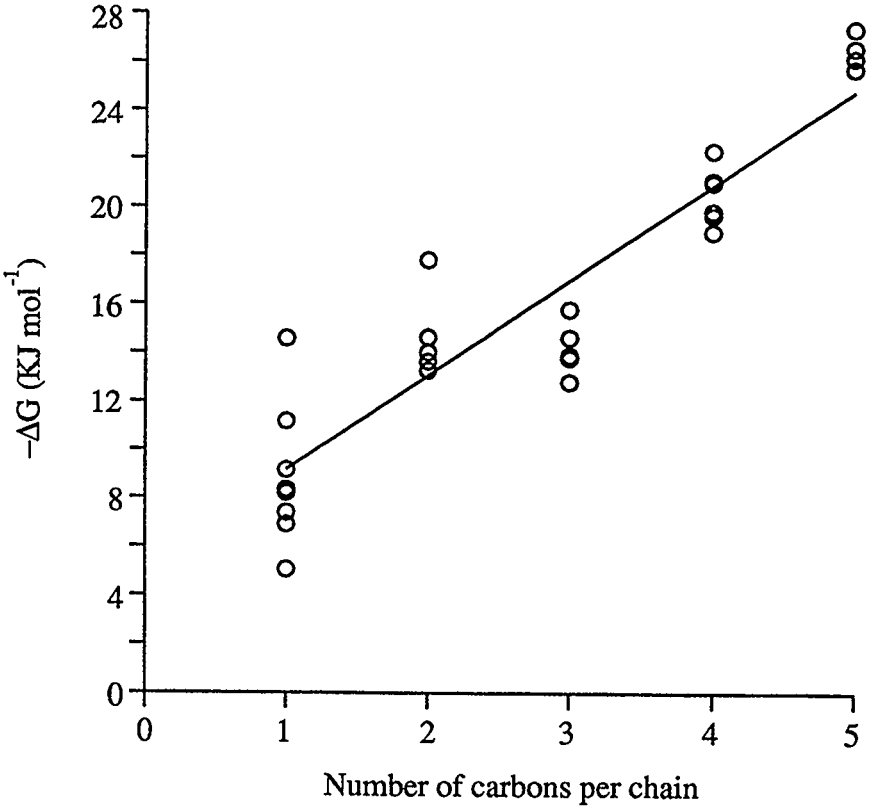
28
24
20
16
12
8
4
0
0
1
2
3
4
5
$-\Delta G$ (KJ mol^{-1})
Number of carbons per chain

Can the increase in binding energy with blocker size be accounted for by specific interactions?

To determine the relationship between blocker size and binding energy, the data in Fig. 11 were fit with linear regressions. As a carbon was added to each of the four chains of the blocker, binding energy increased by –3.97 KJ mol^{-1} (–950 cal mol^{-1}) within the cone and by –4.01 KJ mol^{-1} (–958 cal mol^{-1}) within the rod pore (values correspond to the slope of the linear regression). A statistical comparison of the slopes from the two linear regressions with a Student's t-test revealed that they are not significantly different. Therefore, the addition of a carbon to the length of the blocker side chain contributes the same amount of energy to binding whether the interactions are occurring in the cone or rod channel pore. The binding energy contributed by each carbon is consistent with additional van der Waal forces occurring between the ion channel pore and the longer TAA compounds. van der Waal forces are essentially dipole-dipole interactions containing less the 5 KJ mol^{-1} in energy. These forces can form between two polar molecules, a polar and non-polar molecule, or between two non-polar molecules (Serway & Faughn, 1989). Since the TAA blockers are all non-polar, they could be interacting with amino acids that are either polar or non-polar in nature.

Can the diameter of the internal channel mouth be determined?

Since TAA compounds up to the size of TPeA were able to block both the rod and cone channel in a voltage-dependent manner, the blocker carbon chains were increased in length once again. This time tetrahexylammonium (THxA) was found to block the cone (Fig. 12A) and rod (Fig. 12B) channel conductance in a voltage-independent manner.

Figure 12 Block of cGMP-gated channels by THxA is voltage-independent. Current-voltage relations were formed for cone (**A**) and rod (**B**) patches exposed to THxA. THxA, mixed in concentrations of 0.01, 0.02, and 0.05 mM, was found to decrease current through the channels equally across all voltages.

A

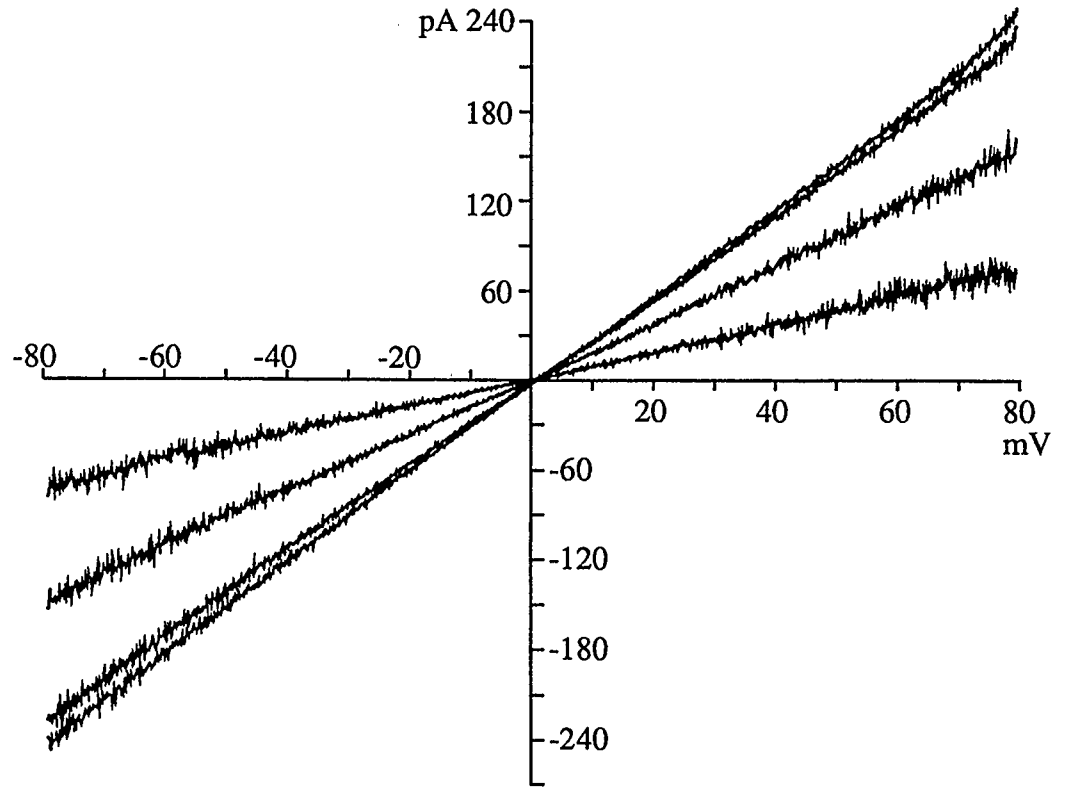
pA 240
180
120
60
-80
-60
-40
-20
20
40
60
80
mV
-60
-120
-180
-240

B

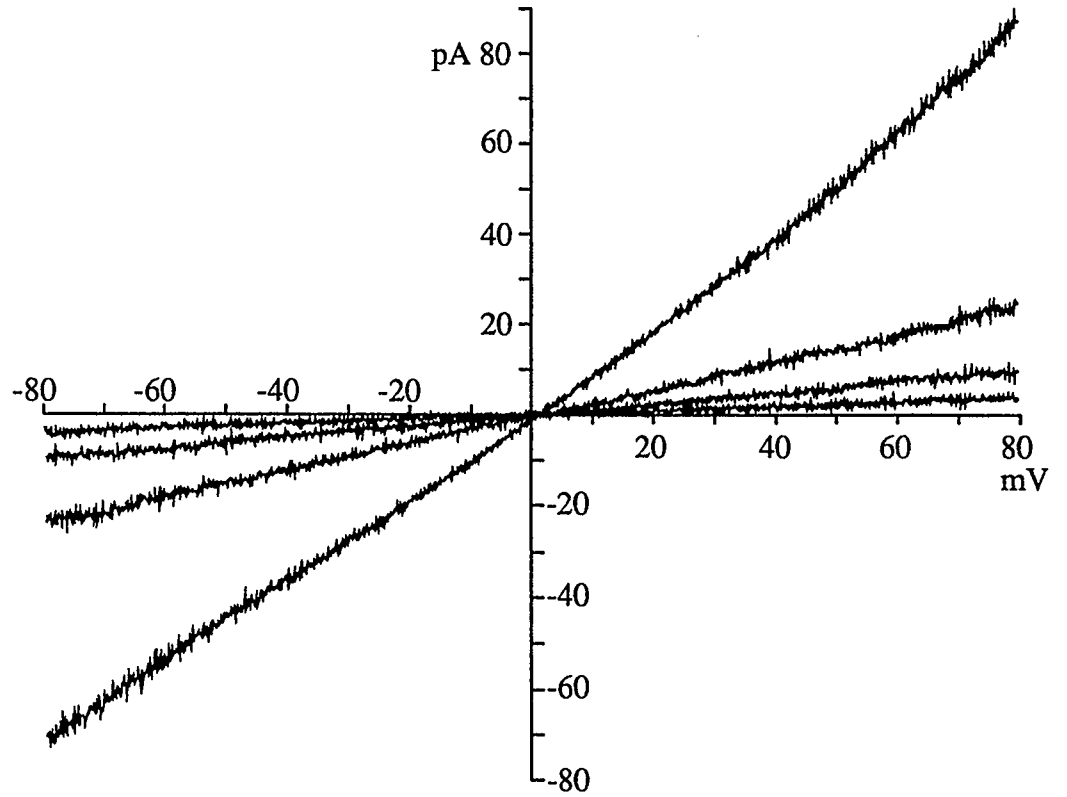
pA 80
60
40
20
-80
-60
-40
-20
20
40
60
80
mV
-20
-40
-60
-80

Voltage-independent block indicates that the blockers are interacting with the channel outside of the membrane electrical field. Physically, this suggests that the blocker is nolonger capable of entering the channel and is simply covering the pore. Therefore, the relative diameter of the cone and rod inner channel mouth can be deduced. Since TPeA blocks both channels in a voltage-dependent manner, the inner mouths of the channels must be slightly larger in diameter than this ion (~12 Å), but smaller than a THxA ion which cannot enter the transmembrane voltage drop. Since the alkyl chains of the larger TAA ions are quite flexible, with free rotation occurring around their carbon-carbon bonds, the actual shape and size of the ions in solution and as they interact with the channel is unknown. Until these factors can be determined, only the relative size of the inner channel pores will be known.

Internal block by hydroxyl group-containing blockers

Can the nature of the amino acids comprising the channel binding sites be deduced?

Data contributed by the TAA experiments has not indicated the nature of amino acids lining the blocker binding sites further than to show that they are capable of hydrophobic interactions with the blockers. It is possible that the amino acids present in these sites are also capable of forming hydrogen bonds with a hydrophillic blocker. If these amino acid groups contain hydroxyl or carboxyl side chains, then the addition of hydroxyl groups to blocker side chains should render these agents more effective than the TAA compounds in blocking channel conductance. However, if amino acids within the TAA compound binding site are non-polar, the presence of hydroxyl groups on the blocker will impede interactions. The two hydroxyl-containing ions chosen to probe the

characteristics of the blocker binding site were Tris and NMDG. These organic cations were selected because they are widely used in a variety of "physiological" and biophysical experiments. Tris is a compound similar in size to TEA, containing hydroxyl groups substituted for carbons on three of the four side chains. Tris is commonly used as a buffer in "physiological" solutions. NMDG is a larger compound formed through the single addition of a long hydrophillic tail containing five hydroxyl groups to a methylammonium head group. NMDG is frequently used as an "inert" substituting ion for sodium in concentration-conductance measurements.

Do Tris and NMDG block conductance in a manner similar to TAA compounds?

To determine if these hydroxyl-containing compounds interact with the channel in a manner similar to TAA compounds, patches containing cone cGMP-gated channels were exposed to different concentrations of Tris and NMDG. The I-V relations obtained in the presence of both blockers are shown in Fig 13A. In the Tris I-V plots, the data is presented with the blocker concentration as mixed. However, the Henderson-Hasselbalch equation predicts that the actual concentration of the blocker in its ionized form at pH 7.6 is 80% of that concentration. The apparent shift in reversal potential as the concentration of the blocker increased is predicted by the Nernst potential for sodium. As the concentration of blocker and the transmembrane voltage gradient is increased, the level of conductance blocked by Tris and NMDG also increased. The voltage- and concentration-dependence of block suggests that these compounds interfere with conductance by entering the open pore of a cone channel. This is the same manner of block elicited by the TAA compounds.

Figure 13 Cone cGMP-gated channels are blocked by non-symmetrical organic compounds from the cytoplasmic surface. The organic compounds chosen for this study, Tris and NMDG, contain hydroxyl groups available for hydrogen bond formation with the channel pore. In these experiments, solutions were mixed by substituting Tris or NMDG on an equimolar basis for sodium on the cytoplasmic side of the channel. Tris was mixed in concentrations of 0, 1, 5, 10, 20, and 50 mM and NMDG in concentrations of 0, 2, 5, 10, 20, and 50 mM.

A. I-V relations for Tris (left) and NMDG (right). Each plot represents data obtained from a single patch. These patches were chosen to illustrate the typical response of cone cGMP-gated channels to blocker. The shift in reversal potential observed in the I-V functions can be accounted for by the Nernst potential for sodium (see Data analysis).

B. Block as a function of voltage. Data contained in each plot was obtained from the corresponding I-V functions directly above. The fraction of conductance blocked by each concentration of blocker is represented by a distinct symbol (from lowest to highest O, □, △, ▽, and ☆). The solid lines represent a fit of the Woodhull equation to the data by method 1. The electrical constants ($K_{D(0)}$ and δ) describing block of each patch were 41 mM and 0.59 for Tris, and 188 mM and 0.84 for NMDG.

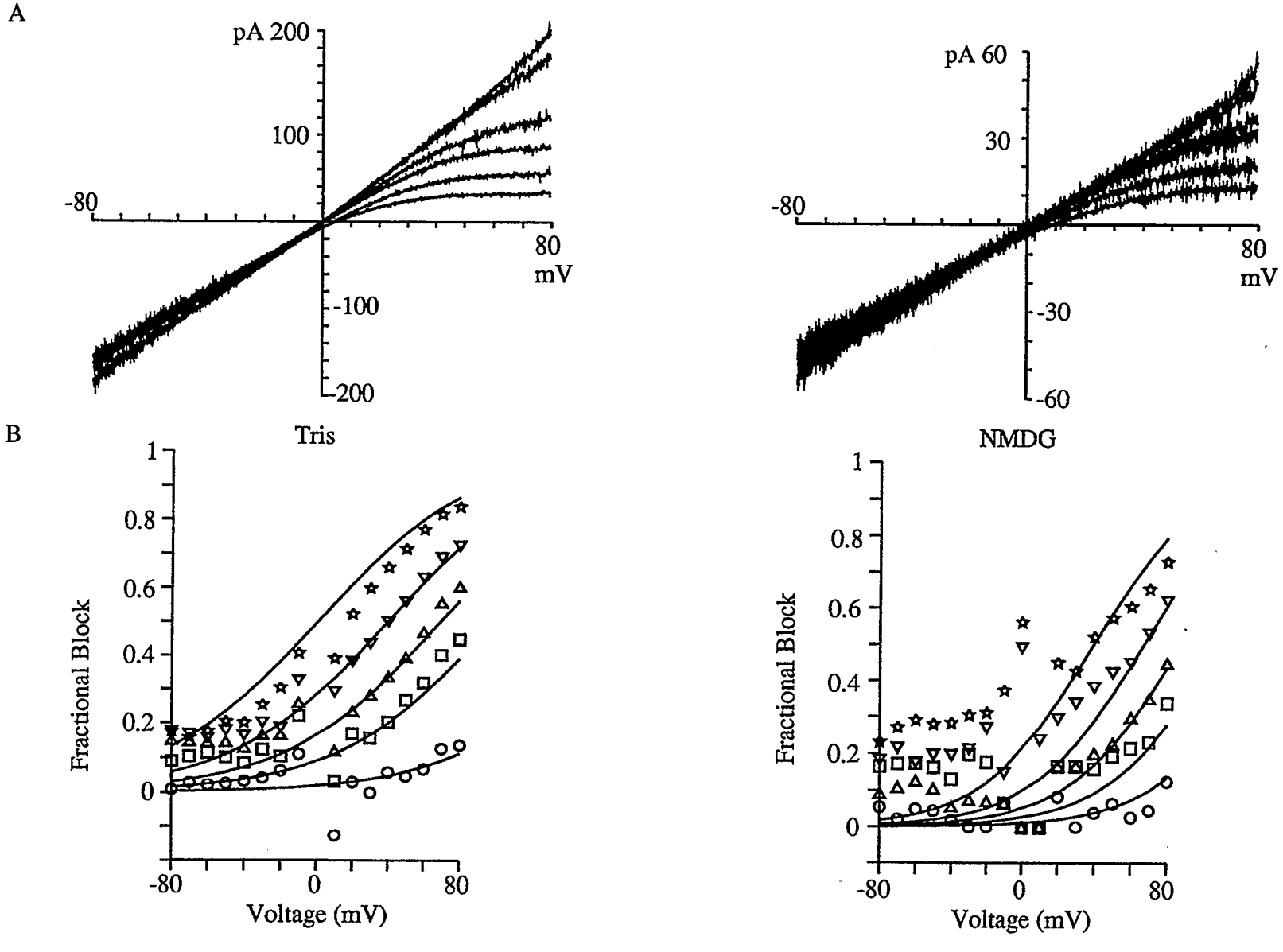
A
pA 200
100
-80
80
mV
-100
-200
pA 60
30
-80
80
mV
-30
-60
B
Tris
NMDG
1
0.8
0.6
0.4
0.2
0
Fractional Block
-80
0
80
Voltage (mV)

Do hydroxyl-containing blockers bind to the same sites as TAA compounds?

To clearly illustrate the voltage- and concentration-dependence of block, the fraction of conductance blocked by Tris and NMDG was calculated and plotted as a function of voltage in Fig. 13B. Each plot was fit with the Woodhull model according to method 1 (a simultaneous fit of the fractional block over all concentrations and voltages tested on a patch) to provide a summary view of how the blockers interact with the channels. In instances where voltage-independent block was evident, the data was fit with the Woodhull model at positive potentials only. The electrical values obtained from the fits are provided in Table II. A comparison of the mean δ values obtained for NMDG and Tris with those obtained for the TAA compounds indicate that Tris typically binds to a position indistinguishable from the average TAA binding site while NMDG binds to a position further into the membrane electric field. In fact, the mean position of NMDG binding is not significantly different from the cone channel's permeant ion binding site ($\delta = 0.61$; Haynes, 1995b). The ability of NMDG to enter so deeply into the channel pore is likely due to its structure. Ammonium is capable of permeating the cone channel (Haynes, 1995a). The presence of this unshielded head group may allow the compound access to the permeant ion binding site while the addition of a long hydrophillic tail acts as an anchor, preventing NMDG from passing through the channel.

Does the presence of hydroxyl groups effect binding in the pore?

A comparison of the mean $K_{D(0)}$ value obtained for Tris (32 ± 14) with that of TEA (11 ± 8) suggests that an increase in blocker hydrophillicity destabilizes interactions between the blocker and cone channel pore. Although these blockers are of similar size

and bind to similar locations within the transmembrane electric field, the $K_{D(0)}$ values describing Tris block are three times larger than those describing TEA block. A similar comparison of mean $K_{D(0)}$ values for NMDG and the TAA compounds reiterates the idea that increased polarity allows the blockers to dissociate with greater ease from the channel pore. This data would suggest that the amino acids comprising the blocker binding site are hydrophobic in nature. Assuming this deduction is correct, the interactions between the blocker and pore are achieved through the formation of hydrophobic interactions between non-polar groups.

External block by TMA

Do external TAA compounds block conductance through the cGMP-gated channel?

Since TAA compounds internally block the cone and rod cGMP-gated channels through interactions with regions of the cytoplasmic pore, it was of interest to determine whether the TAA compounds would effect conductance when presented externally. Figures 14A and 15 demonstrate the effect external TMA had on the current passing through open cone and rod channels respectively. Unlike internal TMA, which interfered with both cone and rod conductance in a voltage-dependent manner, external TMA only blocked conductance through open cone cGMP-gated channels in a voltage-dependent manner, having no effect on the conductance through the rod cGMP-gated channels (Fig. 15). As voltage was made more negative, block of the cone channel became more apparent (Fig. 14A). The voltage-dependence of block suggests that the blocker is experiencing the membrane electric field in a manner that effects its ability to impede

Figure 14 Cone cGMP-gated channels are voltage-dependently blocked by extracellular TMA.

A. Current-voltage relations obtained under conditions where TMA was substituted on an equimolar basis for part of the extracellular sodium concentration. The difference in reversal potential of 6.5 mV was used to estimate the concentration of blocker bathing the extracellular surface of the membrane patch, which in this experiment was approximately 35 mM TMA.

B. Voltage-dependence of block. The fraction of conductance blocked by the organic cation was plotted as a function of voltage. Fit of the data with the method 3 of the Woodhull equation determined that $K_{D(0)}$ = 100 mM and δ = 0.082 for this patch.

A

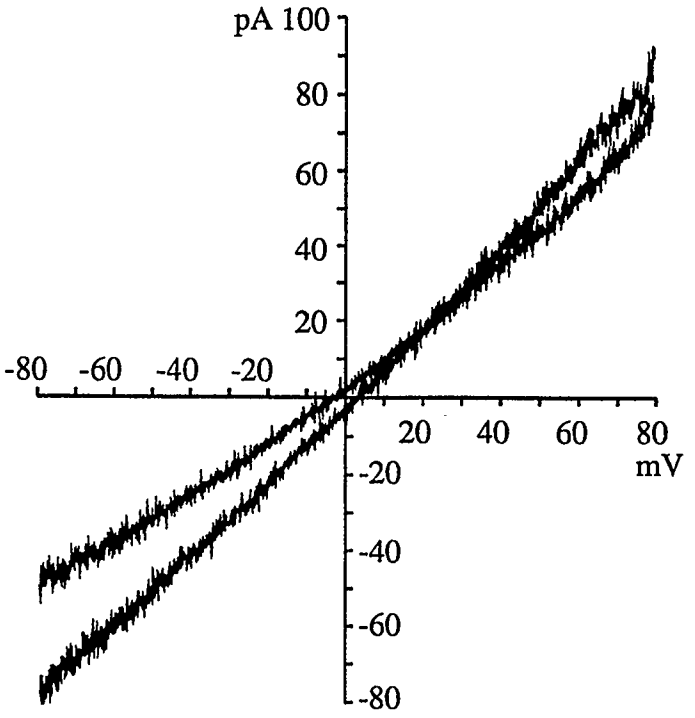
pA 100
80
60
40
20
-80 -60 -40 -20
20 40 60 80
mV
-20
-40
-60
-80

B

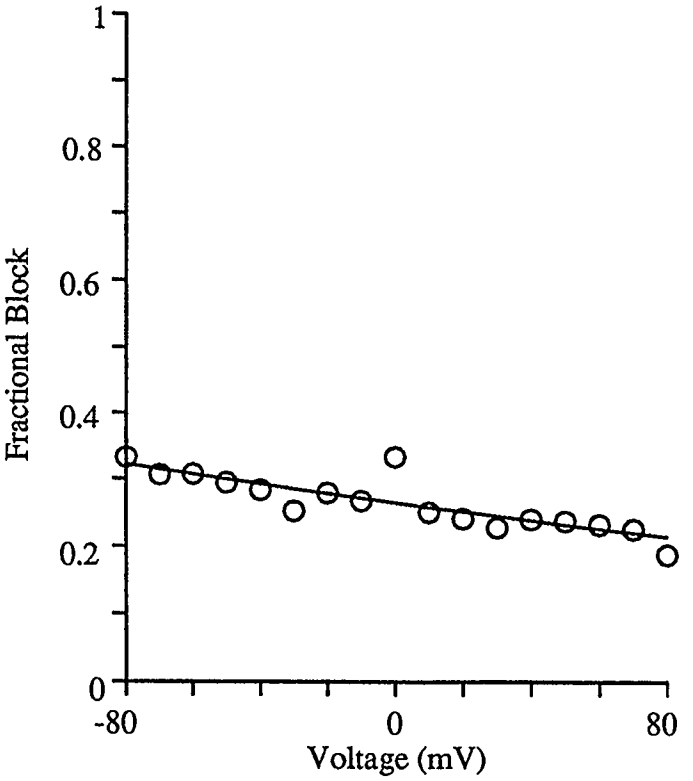
1
0.8
0.6
0.4
0.2
0
Fractional Block
-80
0
80
Voltage (mV)

Figure 15 Rod cGMP-gated channels are not blocked by extracellular TMA. Replacing external sodium with TMA caused a shift in the current reversal potential as predicted by the Nernst equation but did not block conductance. Based on the difference in reversal potential of 26 mV, external TMA concentration was approximately 90 mM.

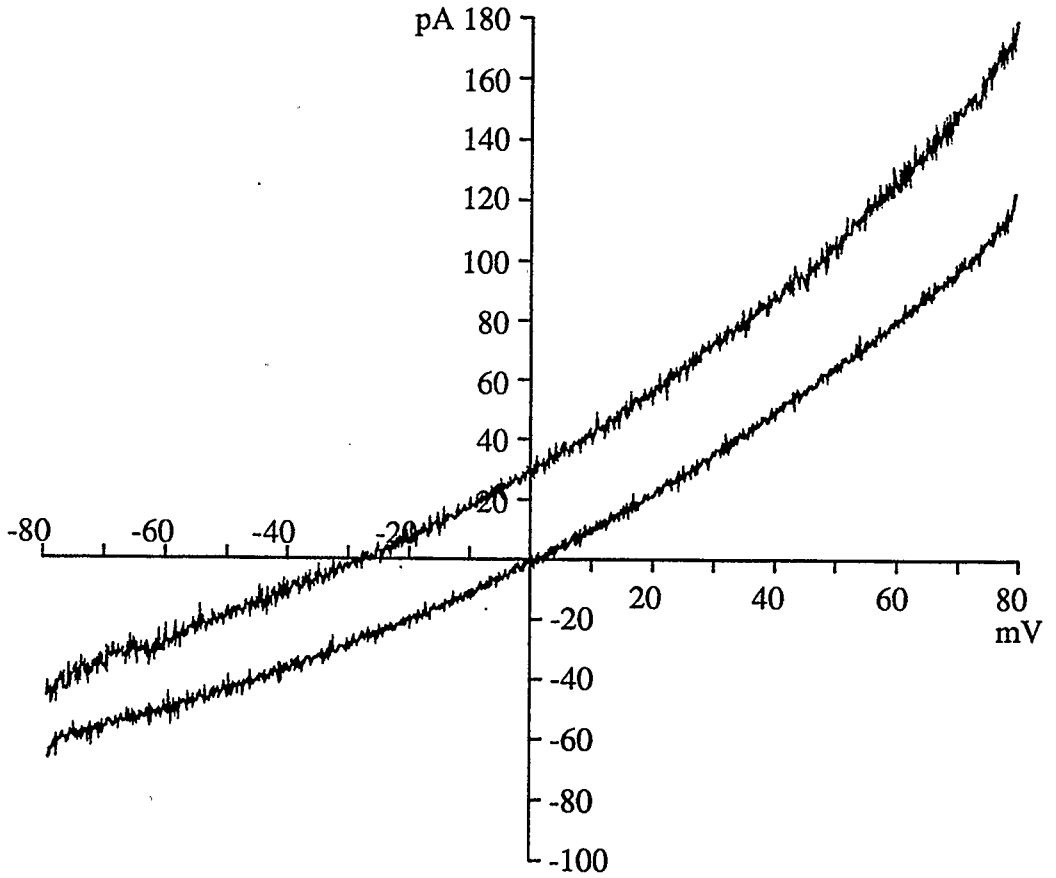
pA 180
160
140
120
100
80
60
40
20
-80
-60
-40
-20
20
40
60
80
mV
-20
-40
-60
-80
-100

conductance. As previously proposed, TMA is likely blocking current by entering the external pore of the cone channel.

Can the concentration of blocker bathing the external surface be estimated?

In the presence of external TMA, negative shifts in the reversal potential (V_{rev}) were observed as predicted by the Nernst equation to occur as the concentration of external sodium is decreased. It was hypothesized that based on the reversal potential shift the concentration of TMA reaching the outer surface of the patch after mixing with the contents of the pipet could be estimated. A set of internal solutions containing different concentrations of TMA were made and the shift in V_{rev} caused by each wasmeasured. A plot of V_{rev} as a function of calculated sodium concentration determined that a simple linear regression did not describe the relation between the two parameters (data not shown). When the sodium activity of the mixed solutions was measured with a sodium electrode, a significant difference between activity and calculated concentration was noted. Empirically, it was observed that the sum of the calculated TMA concentration and the measured sodium activity consistently yielded a constant value of 127. V_{rev} was plotted as a function of the natural logarithm of the measured sodium activity concentration (Fig. 16). This plot could be fit with the Nernst equation, indicating that the shift in reversal potential corresponded to the change in measured sodium concentration. A linear regression was fit to the plot, yielding values for slope equal to −22.07 and y-intercept equal to 105.54 with a confidence value of 95%. Based on the observed reversal potential, the sodium activity of the solution in the pipette could be calculated using:

$$[Na\ activity] = e^{\frac{V_m + y\text{-}intercept}{-slope}} \quad \textbf{(12)}$$

Once Na activity had been calculated, the concentration of TMA bathing the extracellular surface of the patch was estimated using

$$[TMA] = 127 - [Na\ activity] \quad \textbf{(13)}$$

Why isn't the rod cGMP-gated channel blocked by external TMA?

In contrast to the cone I-V relation, the rod I-V function (Fig. 15) established that even high concentrations of external TMA are unable to evoke voltage-dependent block. In seven of seven patches, conductance was unaffected by the presence of up to 90 mM external TMA. Physically, this data may indicate that TMA is too large to enter the external mouth of the rod channel, or that a TAA binding site does not exist in the external mouth. At this point, the two proposals are indistinguishable from each other. However, this data does indicate that structural differences exist between the external mouth regions of the cone and rod cGMP-gated channel pores.

Where within the external cone membrane electric field is TMA interacting?

To clearly illustrate the voltage-dependence of cone channel block by external TMA, fractional block was calculated and plotted as a function of voltage in Fig. 14B. As the membrane potential was made more negative, more conductance was blocked. Since block increases even at the most negative potentials tested, the data suggests that TMA is unable to pass through the open channels. Therefore, TMA is impermeant whether presented internally or externally to a patch containing cone cGMP-gated channels. The data were fit with the Woodhull model according to method 3 and the

Figure 16 Calibration curve for sodium reversal potential shifts. The solid line represents a linear regression of the data with a slope of -22.07, a y-intercept of 105.54 and an r value of 0.95. The dotted line represents the prediction of the Nernst equation based on the activity gradients.

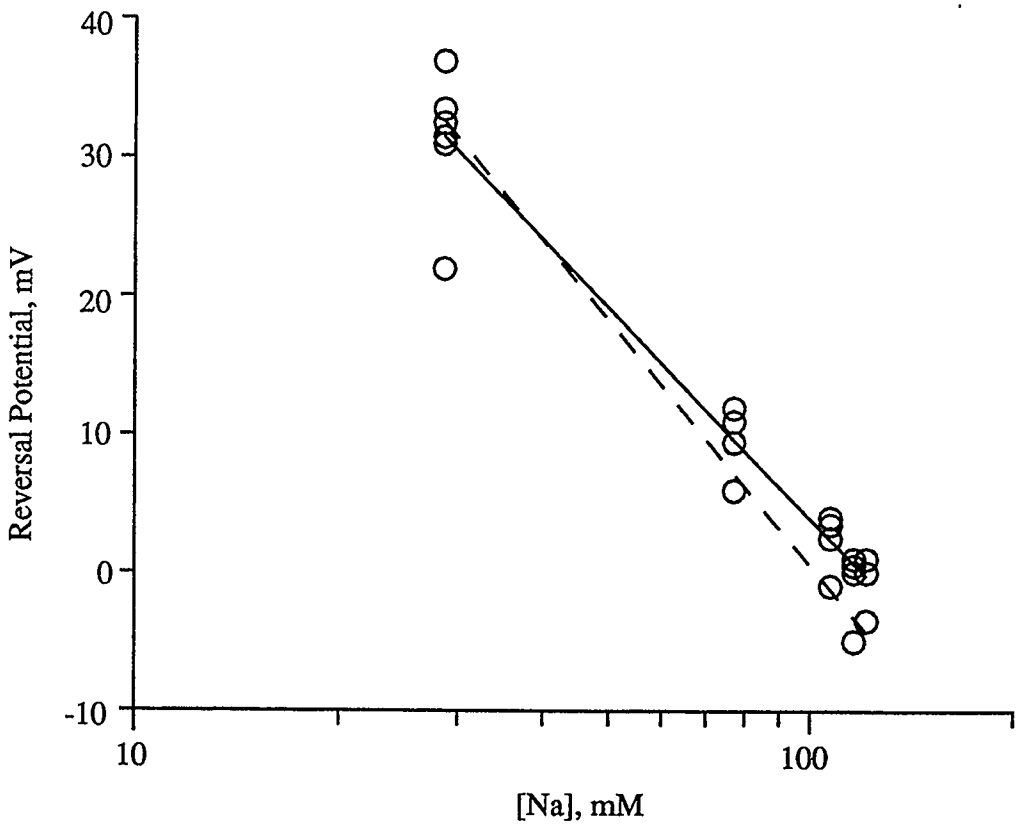
40
30
20
10
0
-10
Reversal Potential, mV
10
100
[Na], mM

resulting electrical values are recorded in Table II. A statistical comparison of the permeant ion binding site position ($\delta = 0.39$ from the outside, Haynes, 1995b) with the mean electrical position of the external TMA binding site determined that these two positions are significantly different from each other ($p < 0.05$). Based on this data, at least two TMA binding sites must lie at either end of the cone cGMP-gated channel pore. Since TMA presented to the cytoplasmic surface of the patch was incapable of accessing the second external binding site, and external TMA was incapable of accessing the cytoplasmic binding site, the two sites must be physically separated from each other. The intervening permeant ion binding site may obstruct blocker passage between sites. Whether this barrier restricts access to the second binding site through physical or electrical means is unknown.

Does TMA bind to the internal and external binding sites with the same affinity?

A statistical comparison of the internal and external blocking effect of TMA using the Student's t-test demonstrated that the affinity with which this blocker interacts with the cone cGMP-gated channel is not significantly different from either side of the membrane. This suggests that these TMA binding sites have similar chemical characteristics. To thoroughly characterize the external binding site would require probing with a series of TAA compounds. Upon completion of such a study the pore properties and mouth size could be deduced. The difficult nature of perfused pipet investigations however, has limited the extent to which the external mouth has been probed in this study.

Sodium Competition Experiments

What does voltage-dependent block really indicate?

Analysis of data obtained in the previous experiments has assumed that voltage-dependent block is the result of blocker interactions with the membrane electric field across the channel. These interactions have been physically interpreted to mean that the blocker is binding within the channel pore. However, blocker interactions with a voltage-sensitive channel process, such as gating, would also produce voltage-dependent "block". While studies of rod channel gating indicate that the overall process has slight voltage-dependence (Karpen *et al.*, 1988a, 1988b; Taylor & Baylor, 1995), which is absent in the cone channel (Haynes, 1995a). However, individual conformational changes that occur during the cone gating process may be voltage-sensitive. If the TAA compounds interfere with a voltage-sensitive stage of the gating process, then describing the resulting decrease in conductance with the Woodhull model is inappropriate and has no meaning.

Can block by TAA compounds be localized to within the channel pore?

To determine that the TAA compounds are interacting within the channel pores and not with a voltage-sensitive gating process, a study which would effect only the blocker within the channel pore was required. If internal TAA compounds block conductance through interactions with the channel pore, their occupancy would be determined in part by the voltage applied to the membrane and in part by competition with permeant ions from the extracellular solution. As the membrane potential is made positive the entry rate of cytoplasmic ions increases relative to the entry rate of extracellular ions, while the exit rate to the same side decreases, promoting channel

occupancy by internal ions. As the membrane potential is made negative the entry rate of extracellular ions increases and the exit rate decreases, promoting occupancy by external ions. With identical solutions on either side of the membrane at 0 mV, there is equal opportunity for the open channel to be occupied by ions from either the cytoplasmic or extracellular medium. However, previous experimental evidence, such as block described by a Hill coefficient of 1, has suggested that the cone and rod cGMP-gated channels can only be occupied by a single ion at a time. Under these conditions a competition develops between ions on either side of the membrane for occupancy of the pore. This competition can be eliminated if all the permeant ions in the extracellular solution are replaced with ions capable of maintaining tonicity and membrane surface potential but which in no way permeate or interact with the channel. Under these conditions, an applied membrane potential of 0 mV would find the channel occupied by ions from the intracellular solution only. If blockers in the intracellular solution are capable of entering the ion channel pore, then the apparent affinity of the channel for the blocker will increase, reflecting the decrease in competition. However, if the blocker is interacting with a voltage-sensitive channel process external to the membrane electrical field, the apparent affinity between the blocker and channel will be unaffected by the lack of competition for occupancy of the channel pore. Manipulating competition for occupancy of the open cGMP-gated channel pore and assessing the direct effects the change has on blocker binding affinity will distinguish the site of blocker action.

Does removing competition affect internal TBA block?

To test whether TAA compounds are entering the channel pore while blocking conductance, the concentration of permeant ions in the extracellular solution was manipulated. In the absence of a suitable inert substituting ion for sodium, sucrose was used to change the ionic composition of the external solution. The ability of internal TBA to block open channel conductance was assessed first in the presence of equal external and internal sodium, and then in the presence of high external sucrose, and consequently low external sodium. The resulting I-V relation is shown in Fig. 17A. The noticeable shift in reversal potential apparent in the presence of external sucrose is consistent with predictions made by the Nernst equation to occur as external sodium levels decrease. Currents measured in the presence of internal TBA were decreased in a voltage-dependent manner both in the presence and absence of sucrose. To determine whether the decreased ionic concentration of the external solution effected block elicited by TBA, the fraction of conductance blocked under both conditions was calculated and plotted as a function of voltage in Fig. 17B. The fractional block elicited by TBA in the presence of sucrose was greater than block elicited in the absence of sucrose. This observation is confirmed by a comparison of the resulting $K_{D(0)}$ values obtained by fitting each data set from other patches with method 3 of the Woodhull model. Those values are listed in Table VII. These results suggest that manipulation of the external ionic composition can effect the affinity of the channel for the intracellularily applied blocker.

Figure 17 Eliminating extracellular competition for pore occupancy increases blocker binding affinity. External sodium competing with internal ions for pore occupancy was reduced with sucrose via the perfused pipette technique.

A. Current-voltage relations. The effect of 0.2 mM TBA on cone cGMP-dependent currents were assessed in the absence and presence of sucrose. Under both conditions, TBA voltage-dependently blocked current. Reduction of extracellular sodium with sucrose caused a −50 mV shift in the reversal potential as predicted by the Nernst equation.

B. Voltage-dependence of block. The fraction of conductance blocked by 0.2 mM TBA in the absence and presence of sucrose was plotted as a function of voltage. The data were fit with method 3 of the Woodhull model. In the absence of sucrose, $K_{D(0)}$ was 1.70 and δ was 0.599. In the presence of sucrose, $K_{D(0)}$ was 0.903 and δ was 0.495.

A

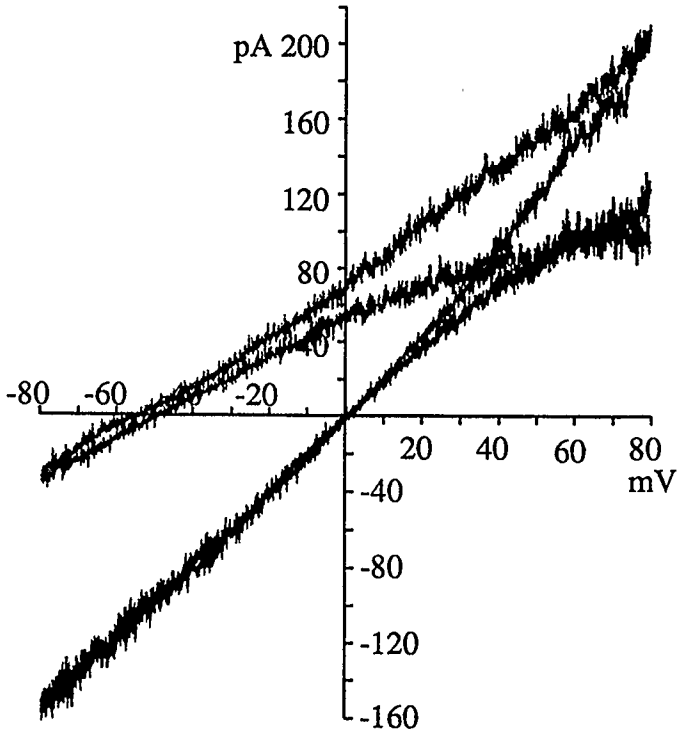
pA 200
160
120
80
-80
-60
-20
20
40
60
80
mV
-40
-80
-120
-160

B

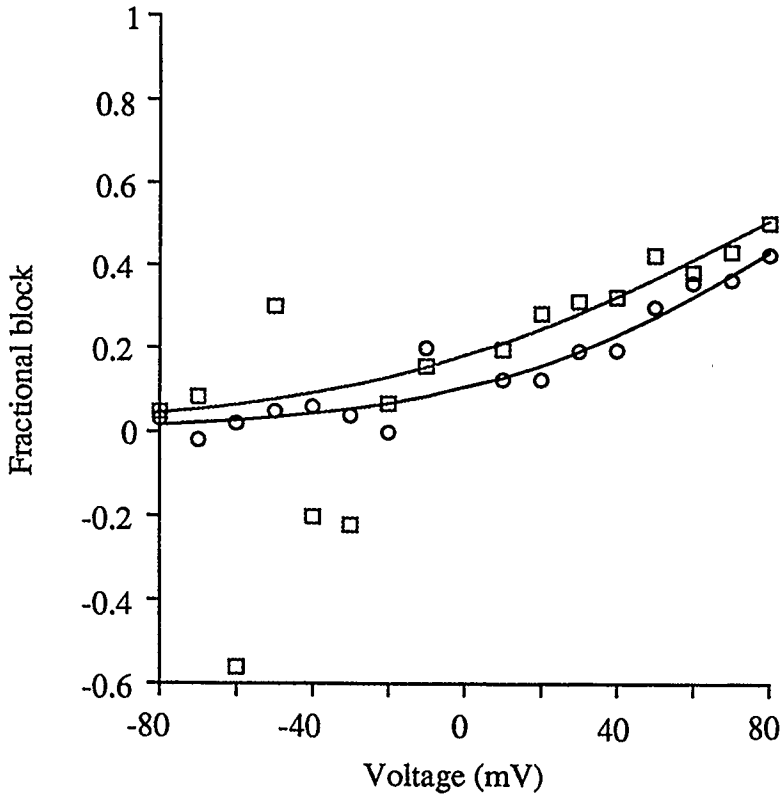
1
0.8
0.6
0.4
0.2
0
-0.2
-0.4
-0.6
Fractional block
-80
-40
0
40
80
Voltage (mV)

Table VII. Assessing the effect competition for channel occupancy has on electrical values describing cone cGMP-gated channel block by internal TBA.

	No sucrose		Sucrose	
Patch	$K_{D(0)}$	δ	$K_{D(0)}$	δ
040396a	1.697	0.599	0.903	0.495
040396b	0.791	0.519	0.148	0.252
010995a	1.033	0.518	0.26	0.311

Is the shift in $K_{D(0)}$ accounted for completely by competition?

Before this data could be interpreted as positive support that the TAA compounds are interacting within the channel pore, the effect that sucrose has on membrane surface charge had to be taken into account. To manipulate the ionic composition of the external solution, an inert and impermeable ion was required to replace sodium. As an impermeant molecule, sucrose is capable of maintaining the tonicity of solution without interfering with proper channel function. However, sucrose is an uncharged molecule. Replacing the charged sodium ion with an uncharged molecule exposes fixed negative charges on the membrane surface. Under conditions of equal ionic composition these negative charges, contributed by phospholipids and proteins, are normally shrouded in a cover of positive ions. The permeation model proposed for the cone cGMP-gated channel (Haynes, 1995b) predicts that the negative charges on the external membrane will create a local surface potential of −4.6 mV, while negative charges on the internal membrane will create a local surface potential of −30 mV. Therefore, even when the membrane potential is held at 0 mV, an ion permeating from the internal solution is experiencing a transmembrane voltage drop of 25.4 mV. When sucrose was perfused into the external solution, sodium dropped in concentration to approximately 10 mM. The lack of positive charges in solution exposed the negative charges on the external membrane surface, reducing the local surface potential to −14.6 mV. As the transmembrane gradient falls to 15.4 mV, the apparent binding ability of the blocker will increase as the negative voltage field stabilizes interactions with the positively charged ion. Therefore, based on the effect of sucrose on surface charge alone, the apparent $K_{D(0)}$ is expected fall by

approximately 21% in the presence of sucrose. However, replacement of sodium with sucrose actually evoked an average decrease in the apparent $K_{D(0)}$ of 68%, a significant difference from the prediction ($p < 0.05$). Although the effect sucrose has on membrane surface charge causes a change in the apparent binding affinity, the magnitude of the change attributable to this factor is smaller than observed. Therefore, the reduction of external solution ionic strength with sucrose increases the affinity with which TBA binds to the channel by reducing competition for occupancy. Since the lack of competition for occupancy affects blocker affinity, the TAA compounds must be interacting within the inner channel pore when evoking voltage-dependent block.

CHAPTER 5: DISCUSSION

TAA compounds interact with the open pore of cGMP-gated channels

The results described here confirm previous reports that cone and rod cGMP-gated channels are unable to conduct TAA compounds ((Hodgkin *et al.*, 1985; Furman & Tanaka, 1990; Menini, 1990; Picones & Korenbrot, 1992; Picco & Menini, 1993; Haynes, 1993). However, these results also reveal that the blockers interfere with conductance through binding interactions within the open channel pore. This was first inferred with the appearance of voltage-dependent block in the dose-response experiments. Voltage-dependent block suggests that the TAA compounds are interacting with the electrical potential that exists across the channel pore (reviewed in Yellen, 1987; Hille, 1992). Confirmation of these interactions was provided by the sucrose / sodium replacement experiments. When competition for pore occupancy was reduced, the affinity the blocker had for its binding site increased. This study, which manipulated the blocker's access to binding sites in the pore, provides substantial support for localizing the TAA compound effect to the mouth of the open channel.

Identifying the internal TAA compound binding site

Although each of the TAA compounds experienced a large range of the cone and rod electric field (evident in the large standard deviations associated with mean position), the data suggests that there is a single blocker binding site accessable from the cytoplasmic surface. This site is located approximately 40% of the way across the rod and cone electric fields (determined from mean δ values). To account for the variation in δ values, this single site must be continually changing its position in the field. This

constant change of binding position was observed while assessing electrical variability within a patch (Table V). Whether this continual transformation is an intrinsic characteristic of the channel or if modulation is involved has yet to be determined. Since excised patches contain active enzymes of the phototransduction cascade (Ertel, 1990), endogenous modulators within the patch may be responsible for changes in channel conformation. This modulation, rather than a continual channel process, might then be responsible for variability seen in binding position.

Characterizing the inner blocker binding site

To determine the nature of the amino acid groups forming the inner TAA blocker binding site, various organic cations were used as probes. Initially, a series of TAA compounds were presented to cone and rod patches. Using binding affinity to gauge the strength of interaction, the ability of these hydrophobic compounds to interact with amino acid residues in the binding site was assessed. As the carbon length of the TAA compound side chain increased, the binding affinity systematically increased. The amount of energy gained in binding as the carbon chain length expanded was consistent with additional van der Waal forces forming with the pore. Since van der Waal forces can form between non-polar molecules and polar molecules, blockers with hydroxyl groups available for hydrogen bond formation were used to assess the ability of hydrophillic compounds to interact with the binding site. Hydrophillic blockers were found to dissociate from the channel with greater ease, suggesting that the hydroxyl groups prevent rather than encourage interactions with residues in the binding site. Based on these

results, the amino acids contributing to the inner TAA compound binding site are likely hydrophobic in nature.

Characterizing the exterior TAA compound binding site

A second TAA compound binding site, accessible only from the external surface of the cone patch, was identified with the perfused pipette technique. Although experimental limitations prevented complete characterization of this cone blocker site, a comparison of internal and external binding affinities suggests that the two sites have similar properties. This binding site was not present in the external mouth of the rod channel, indicating that the two channel subtypes have structural differences. This site is either completely absent or unaccessible from the external surface of the rod. Primary sequence analysis of the pore-forming region in the cone and rod α subunit has shown that there is a sequence difference of only a single amino acid (Bönigk *et al.*, 1993). This residue, changed from an isoleucine in the cone to a valine in the rod, is thought to be located on the extracellular surface of the channel mouth (Bönigk *et al.*, 1993). It is possible that this change in sequence, combined with any structural differences that may exist between other pore contributors (such as the putative β subunits), may cause the rod external mouth to configure in a slightly different manner. Small changes in structure may be enough to obstruct accessability to the external TAA blocker binding site from the surface.

A model for the cGMP-gated channel structure

Using the electrophysiological data that has been accumulated through this investigation and from others, a basic model of the three-dimensional cone cGMP-gated

channel pore has been developed. Under physiological conditions, ions flow through the open channel from the extracellular medium into the cytoplasm. The external mouth region of the channel is the first to experience the permeating ions. This region is estimated to extend into the first 39% of the electric field, up to the permeant ion binding site. Although the width of the external mouth has yet to be determined, it contains a TAA blocker binding site which can accomodate at the very least TMA. This site, located at $\delta = 0.13$, is composed of amino acids purported to be hydrophobic in nature. The permeant ion binding site, located at $\delta = 0.39$ (Haynes, 1995b), acts as a barrier to impermeant ions. Permeability studies show that the cone cGMP-gated channel is easily capable of conducting alkali metal cations up to the size of cesium, suggesting that the cone selectivity filter has a diameter of at least 3.38 Å (Haynes, 1995a). The characteristic high permeability of the cone cGMP-gated channel (Picones & Korenbrot, 1992; Haynes, 1995a, 1995b) may be attributable to this wide pathway for ions through the channel (Unwin, 1989). After passing through the selectivity filter, ions enter a large internal vestibule. This inner mouth covers the last 61% of the cone transmembrane voltage drop, and is expected to be slightly wider than a TPeA ion. The depth and width of the inner mouth likely contribute to fast and efficient clearing of ions from the channel. This region also contains a hydrophobic TAA blocker binding site, located at $\delta = 0.59$. The data described here suggest that this site is flexible, changing location with the conformation of the channel. Collectively, these attributes of the cone cGMP-gated channel pore allow for the efficient flux of various cations across the plasma membrane of the photoreceptor, depolarizing the cell between photoresponses.

To produce an adequate model of the rod cGMP-gated channel pore, more structural information is required. At this time the diameter of the outer mouth remains a mystery, yet the external block experiments (the inability of external TMA to block) and previous conductance measurements (25 pS unitary conductance for rods: Haynes et al., 1986; Zimmerman & Baylor, 1986; Matthews & Watanabe, 1987; Matthews & Watanabe, 1988; 50 pS for cones: Haynes & Yau, 1990a; Haynes, 1995a) suggest that the rod outer vestibule would be smaller than the cone's. A comparison of primary amino acid sequence for the rod and cone α subunits has identified only a single substitution of a non-polar residue for another non-polar residue in the outer pore region, indicating that similar components can form structures of various conformation. The region containing the rod permeant ion binding site is proposed to be roughly 0.38×0.59 nm in diameter, the size of the largest permeant ion, methyl guanidinium (Picco & Menini, 1993). This wide selectivity filter is likely the reason for the high permeability of cations through the channel. The inner mouth of the rod channel shows the greatest similarity to the cone channel. This inner vestibule, with the diameter of a TPeA compound, contains a single flexible TAA compound binding site. The amino acid residues constituting the blocker binding site at $\delta = 0.36$ are hydrophobic in nature, capable of forming van der Waal interactions with TAA blockers. Nevertheless, amino acids forming the rod internal TAA binding site must be slightly different than the components of cones, for the blockers bind with greater energy to the rod pore. Hopefully, future structural studies will complete and confirm the characteristics of this model for the cGMP-gated channels.

Similarities in the pores of ligand- and voltage-gated channels

Characterizing the pore of the cGMP-gated channels with organic blockers has confirmed that similarities exist between the pore regions of these ligand-gated channels and those of the voltage-gated potassium channel family. Channels from both families contain a single TAA compound binding site within their inner vestibules. Characterization of both sites have found that the constituent amino acid groups are hydrophobic in nature (potassium channels, French & Shoukimas, 1981; Coronado & Miller, 1982). The relative size of both inner vestibules is also similar, each capable of holding the large TPeA blocker (potassium channels, French & Shoukimas, 1981). The diameter of the potassium channel is 0.3 nm at its narrowest region (Hille, 1973), far more restrictive to ion passage than either of the cGMP-gated channels. This difference in diameter may be responsible for the selective versus nonselective nature of these channel families (Hille, 1973; Gay & Stanfield, 1978; Reuter & Stevens, 1980; Yellen, 1987). Not all subtypes of the potassium channel family contain a separate external TAA compound binding site, and those that do selectively bind TEA (Villaroel *et al.*, 1988). Within the cGMP-gated channel family, only the cone subtype contains an external TAA compound binding site. This site, which bound TMA will need further characterization in order for comparisons to be made with the potassium channel site. Based on the data presented here, it would seem that the prediction of similarity between the cGMP-gated channel and voltage-gated potassium channel pores based on sequence analysis has borne out (Jan & Jan, 1990; Kaupp, 1991; Bönigk *et al.*, 1993).

BIBLIOGRAPHY

Ahmad, I., L.J. Redmond, and C.J. Barnstable. 1990. Developmental and tissue-specific expression of rod photoreceptor cGMP-gated ion channel gene. *Biochemistry and Biophysical Research Communications* 173: 463-470.

Aidley, D.J. 1989. The physiology of excitable cells. 3rd edition. Cambridge University Press. New York. Chapter 18.

Alberts, B., D. Bray, J. Lewis, M. Raff, K. Roberts, and J.D. Watson. 1983. Molecular biology of the cell. Chapter 18.

Armstrong, C.M. 1975a. Ionic pores, gates and gating currents. *Quarterly Review of Biophysics* 7: 179-210.

Armstrong, C.M. 1975b. Potassium channel pores of nerve and muscle membranes. *In* Membranes: A series of advances. G. Eisenman, editor. Marcel Dekker. New York. 3: 325-358.

Armstrong, C.M. & B. Hille. 1972. The inner quaternary ammonium ion receptor in potassium channels in the node of Ranvier. *Journal of General Physiology* 59: 388-400.

Armstrong, F.B. 1989. Biochemistry. 3rd edition. Oxford University Press. New York. Chapter 11 pp 208-209.

Attwell, D. 1990. The photoreceptor output synapse. *Progress in Retinal Research* 9: 337-362.

Attwell, D., F.S. Werblin, and M. Wilson. 1982. The properties of single cones isolated from tiger salamander retina. *Journal of Physiology* 328: 259-283.

Attwell, D., and M. Wilson. 1980. Behaviour of the rod network in tiger salamander retina mediated by properties of individual rods. *Journal of Physiology* 309: 287-315.

Bauer, P.J., and M. Drechsler. 1992. Association of cyclic GMP-gated channels and Na+/Ca2+-K+ exchangers in bovine retinal rod outer segment plasma membranes. *Journal of Physiology* 451: 109-131.

Baylor, D.A., G. Matthews, and B.J. Nunn. 1984. Location and function of voltage-sensitive conductances in retinal rods of salamander, *Ambystoma tigrinum. Journal of Physiology* 354: 203-223.

Beech, D.J., and S. Barnes. 1989. Characterization of a voltage-gated potassium channel that accelerates the rod response to dim light. *Neuron* 3: 573-581.

Biel, M., W. Altenhofen, R. Hullin, J. Ludwig, M. Freichel, V. Flockerzi, N. Dascal, U.B. Kaupp, and F. Hofmann. 1993. Primary structure and functional expression of a cyclic nucleotide-gated channel from rabbit aorta. *FEBS Letters* 329: 134-148.

Biel, M., X. Zong, M. Distler, E. Bosse, N. Klugbauer, M. Murakami, V.Flockerzi, and F. Hofmann. 1994. Another member of the cyclic nucleotide-gated channel family, expressed in testis, kidney, and heart. *Proceedings of the National Academy of Science* USA. 91: 3505-3509.

Bönigk, W., W. Altenhofen, F. Muller, A. Dose, M. Illing, R.S. Molday, and U.B. Kaupp. 1993. Rod and cone photoreceptor cells express distinct genes for cGMP-gated channels. *Neuron* 10: 865-877.

Bridges, C.D.B. 1976. Vitamin A and the role of the pigment epithelium during bleaching and regeneration of rhodopsin in the frog eye. *Experimental Eye Research* 22: 435-455.

Bridges, C.D.B., R.A. Alvarez, S.-L. Fong, F. Gonzalez-Fernandez, D.M.K. Lam, and G.I. Liou. 1984. Visual cycle in the mammalian eye: retinoid-binding proteins and the distribution of 11-cis retinoids. *Vision Research* 24: 1581-1594.

Cervetto, L., L. Lagnado, R.J. Perry, D.W. Robinson, and P.A. McNaughton. 1989. Extrusion of calcium from rod outer segments is driven by both sodium and potassium gradients. *Nature* 337: 740-743.

Changeux, J.-P., A. Devillers-Thiery, and P. Chemouilli. 1984. Acetylcholine receptor: an allosteric protein. *Science* 225: 1335-1345.

Chen, T.-Y., M. Illing, L.L. Molday, Y.T. Hsu, K.-W. Yau, and R.S. Molday. 1994. Subunit 2 (or beta) of retinal rod cGMP-gated cation channel is a component of the 240-kDa channel-associated protein and mediates calcium-calmodulin modulation. *Proceedings of the National Academy of Sciences* USA 91: 11757-11761.

Chen, T.-Y., Y.-W. Peng, R.S. Dhallan, B. Ahamed, R.R. Reed, and K.-W. Yau. 1993. A new subunit of the cyclic nucleotide-gated cation channel in retinal rods. *Nature* 362: 764-767.

Cobbs, W.H., A.E. Barkdol III and E.N. Pugh, Jr. 1985. Cyclic GMP has photocurrent and light sensitivity of retinal cones. *Nature* 317: 64-66.

Cohen, A.I., I.A. Hall, and J.A. Ferrendelli. 1978. Calcium and cyclic nucleotide regulation in incubated mouse retina. *Journal of General Physiology* 71: 595-612.

Colamartino, G., A. Menini, and V. Torre. 1991. Blockage and permeation of divalent cations through the cyclic GMP-activated channel from tiger salamander rods. *Journal of Physiology* 440: 189-206.

Cook, N.J., W. Hanke, and U.B. Kaupp. 1987. Identification, cloning and functional reconstitution of the cyclic GMP-dependent channel from rod photoreceptors. *Proceedings of the National Academy of Science* USA 85: 9806-9810.

Coronado, R. & C. Miller. 1982. Conduction and block by organic cations in a potassium-selective channel from sarcoplasmic reticulum incorporated into planar phospholipid bilayers. *Journal of General Physiology* 79: 529-547.

Darnell, J., H. Lodish, and D. Baltimore. 1990. Molecular Cell Biology. 2nd edition. W.H. Freeman & Co. New York. Chapter 2.

Deisenhofer, J., and H. Michel. 1989. The photosynthetic reaction from the purple bacterium *Rhodopseudomonas viridis*. *EMBO Journal* 8: 2149-2170.

Dhallan, R.S., J.P. Macke, R.L. Eddy, T.B. Shows, R.R. Reed, K.-W. Yau, and J. Nathans. 1992. Human rod photoreceptor cGMP-gated channel: amino acid sequence, gene structure, and functional expression. *Journal of Neuroscience* 12: 3248-3256.

Dhallan, R.S., K.-W. Yau, K.A. Schrader, and R.R. Reed. 1990. Primary structure and functional expression of a cyclic nucleotide-activated channel from olfactory neurons. *Nature* 347: 184-187.

Dizhoor, A.M., D.G. Lowe, E.V. Olshevskaya, R.P. Laura, and J.B. Hurley. 1994. The human photoreceptor membrane guanylyl cyclase, RetGC, is present in outer segments and is regulated by calcium and a soluble activator. *Neuron* 12: 1345-1352.

Dryer, S.E. & D. Henderson. 1991. A cyclic GMP-activated channel in dissociated cells of the chick pineal gland. *Nature* 353: 756-758.

Dwyer, T.M., D.J. Adams, and B. Hille. 1980. The permeability of the endplate channel to organic ions in frog muscle. *Journal of General Physiology* 75: 469-492.

Eisenman, G. & R. Horn. 1983. Ionic selectivity revisited: the role of kinetic and equilibrium processes in ion permeation through channels. *Journal of Membrane Biology* 76: 197-225.

Ertel, E.A. 1990. Excised patches of plasma membrane from vertebrate rod outer segments retain a functional phototransduction enzymatic cascade. *Proceedings of the National Academy of Sciences* USA 87: 4226-4230.

Fain, G.L., and J.E. Lisman. 1981. Membrane conductances in photoreceptors. *Progress in Biophysics and Molecular Biology* 37: 91-147.

Fesenko, E.E., S.S. Kolesnik, and A.L. Lyubarsky. 1985. Induction by cyclic GMP of cationic conductance in plasma membrane of retinal rod outer segment. *Nature* 313: 310-313.

Fong, S.L., and C.D. Bridges. 1990. Interstitial retinol-binding protein: Purification, characterization, molecular cloning, and sequence. *Methods in Enzymology* 189: 207-213.

French, R.J., and J.J. Shoukimas. 1981. Blockade of squid axon potassium conductance by internal tetra-n-alkylammonium ions of various sizes. *Biophysical Journal* 34: 271-291.

French, R.J., and J.J. Shoukimas. 1985. An ion's view of the potassium channel: The structure of the permeation pathway as sensed by a variety of blocking ions. *Journal of General Physiology* 85: 669-698.

Fung, B.K.-K., J.B. Hurley, and L. Stryer. 1981. Flow of information in the light-triggered cyclic nucleotide cascade of vision. *Proceedings of the National Academy of Sciences* USA 78: 152-156.

Fung, B.K.-K., & L. Stryer. 1980. Photolyzed rhodopsin catalyses the exchange of GTP for GDP in retinal rod outer segment membranes. *Proceedings of the National Academy of Science* 77: 2500-2504.

Furman, R.E. & J.C. Tanaka. 1990. Monovalent selectivity of the cyclic guanosine monophosphate-activated ion channel. *Journal of General Physiology* 96: 57-82.

Gay, L.A. and P.R. Stanfield. 1978. The selectivity of the delayed potassium conductance of frog skeletal muscle fibres. *Pflügers Archives* 378: 177-179.

Gorczyca, W.A., A.S. Polans, I.G. Surgucheva, I. Subbaraya, W. Baehr, and K. Palczewski. 1995. Guanylyl cyclase activating protein: A calcium-sensitive regulator of phototransduction. *Journal of Biological Chemistry* 270: 22029-22036.

Gorczyca, W.A., J.P. Van Hooser, and K. Palczewski. 1994a. Nucleotide inhibitors and activators of retinal guanylyl cyclase. *Biochemistry* 33: 3217-3222.

Gorczyca, W.A., M.P. Gray-Keller, P.B. Detwiler, and K. Palczewski. 1994b. Purification and physiological evaluation of a guanylate cyclase activating protein from retinal rods. *Proceedings of the National Academy of Science* USA 91: 4014-401

Gordon, S.E., D.L. Brautigan, and A.L. Zimmerman. 1992. Protein phosphotases modulate the apparent agonist affinity of the light-regulated ion channel in retinal rods. *Neuron* 9: 739-748.

Gordon, S.E., and W.N. Zagotta. 1995. Localization of regions affecting an allosteric transition of cyclic nucleotide-activated channels. *Neuron* 14: 857-864.

Goulding, E.H., G.R. Tibbs, and S.A. Siegelbaum. 1994. Molecular mechanism of cyclic-nucleotide-gated channel activation. *Nature* 372: 369-374.

Goulding, E.H., J. Ngai, R.H. Kramer, S. Colicos, R. Axel, S.A. Siegelbaum, and A. Chess. 1992. Molecular cloning and single channel properties of the cyclic nucleotide-gated channel from catfish olfactory neurons. *Neuron* 8: 45-58.

Hamill, O.P., A. Marty, E. Neher, B. Sakmann, and F.J. Sigworth. 1981. Improved patch-clamp techniques for high-resolution current recording from cells and cell-free membrane patches. *Pflügers Archives* 391: 85-100.

Hanke, W., N.J. Cook, and U.B. Kaupp. 1988. cGMP-dependent channel protein from photoreceptor membranes: single-channel activity of the purified and reconstituted protein. *Proceedings of the National Academy of Sciences* USA 83: 48-492.

Haynes, L.W. 1992. Block of the cyclic GMP-gated channel of vertebrate rod and cone photoreceptors by L-*cis*-diltiazem. *Journal of General Physiology* 100: 783-801.

Haynes, L.W. 1993. Mono- and divalent cation selectivity of catfish cone cGMP-gated channels. *Biophysical Journal* 66: A133. (Abstract).

Haynes, L.W. 1995a. Permeation of internal and external monovalent cations through the catfish cone photoreceptor cGMP-gated channel. *Journal of General Physiology* 106: 485-505.

Haynes, L.W. 1995b. Permeation and block by internal and external divalent cations of the catfish cone photoreceptor cGMP-gated channel. *Journal of General Physiology* 106: 507-523.

Haynes, L.W., A.R. Kay, and K.-W. Yau. 1986. Single cyclic GMP-activated channel activity in excised patches of rod outer membrane. *Nature* 321: 66-70.

Haynes, L.W., and S.C. Stotz. 1996. Modulation of cone photoreceptor cGMP-gated channels. *Biophysical Journal* 70: A138 (Abstract)

Haynes, L.W. & K.-W. Yau. 1985. Cyclic GMP-sensitive conductance in outer segment membrane of catfish cones. *Nature* 317: 61-64.

Haynes, L.W., & K.-W. Yau. 1990a. Single-channel measurements from the cyclic GMP-activated conductance of catfish retinal cones. *Journal of Physiology* 249: 451-481.

Haynes, L.W., & K.-W. Yau. 1990b. Kinetics of the cGMP-activated channel of catfish cones. *Neuroscience Research* 12: S161-S163.

Heginbotham, L., T. Abramson, and R. MacKinnon. 1992. A functional connection between the pores of distantly-related ion channels as revealed by mutant potassium channels. *Science* 258: 1152-1155.

Hill, R.W., and G.A. Wyse. 1989. Animal Physiology, 2nd edition. Harper Collins Publishers Inc. :439.

Hille, B. 1971. The permeability of the sodium channel to organic cations in myelinated nerve. *Journal of General Physiology* 58: 599.

Hille, B. 1973. Potassium channels in myelinated nerve. Selective permeability to small cations. *Journal of General Physiology* 61: 669-686.

Hille, B. 1975. Ionic selectivity of sodium and potassium channels of nerve membranes. *In* Membranes. A series of advances. G. Eisenman, editor. Marcel Dekker, New York. 3: 255-323.

Hille, B. 1992. Ionic channels of excitable membranes. 2nd edition. Sinauer Associates, Inc. Sunderland, Massachusetts. Chapters 8, 9.

Hodgkin, A.L., P.A. McNaughton, and B.J. Nunn. 1985. The ionic selectivity and calcium dependence of the light-sensitive pathway in toad rods. *Journal of Physiology* 358: 447-468.

Hsu, Y.-T. & R.S. Molday. 1994. Interaction of calmodulin with the cyclic GMP-gated channel of rod photoreceptor cells: Modulation of activity, affinity purification, and localization. *Journal of Biological Chemistry* 269: 29765-29770.

Hsu, Y.-T. & R.S. Molday. 1993. Modulation of the cGMP-gated channel of rod photoreceptor cells by calmodulin. *Nature* 361: 76-79.

Hubbard, R., & A. Kropf. 1958. The action of light on rhodopsin. *Proceedings of the National Academy of Science* USA 44: 130-139.

Huganir, R.L. and P. Greengard. 1990. Regulation of neurotransmitter receptor desensitization by protein phosphorylation. *Neuron* 5: 555-567.

Hurley, J.B., and L. Stryer. 1982. Purification and characterization of the γ regulatory subunit of the cyclic GMP phosphodiesterase from retinal rod outer segments. *Journal of Biological Chemistry* 257: 11094-11099.

Jan, L.Y. & Y.N. Jan. 1990. A superfamily of ion channels. *Nature* 345: 672.

Karlin, A., P.N. Kao, and M. DiPaola. 1986. Molecular pharmacology of the nicotinic acetylcholine receptor. *Trends in Pharmacological Science* 7: 304-308.

Karpen, J.W., A.L. Zimmerman, L. Stryer, and D.A. Baylor. 1988a. Gating kinetics of the cyclic GMP-activated channel of retinal rods: Flash photolysis and voltage-jump studies. *Proceedings of the National Academy of Sciences* USA 85: 1287-1294.

Karpen, J.W., A.L. Zimmerman, L. Stryer, and D.A. Baylor. 1988b. Molecular mechanics of the cyclic GMP-activated channel of retinal rods. *Cold Spring Harbor Symposium on Quantitative Biology* 53: 325-332.

Kaupp, U.B. 1991. The cyclic nucleotide-gated channels of vertebrate photoreceptors and olfactory epithelium. *Trends in Neuroscience* 14(4): 150-156.

Kaupp, U.B., T. Niidome, T. Tanabe, S. Terada, W. Bönigk, W. Stühmer, N.J. Cook, K. Kangawa, H. Matsuo, T. Hirose, T. Miyata,, and S. Numa. 1989. Primary structure and functional expression from complementary DNA of the rod photoreceptor cyclic GMP-gated channel. *Nature* 342: 762-766.

Kilbride, P. 1980. Calcium effects on frog retinal cyclic guanosine 3′:5′-monophosphate levels and their light-initiated rate of decay. *Journal of General Physiology* 75: 457-465.

Koch, K.-W. & U.B. Kaupp. 1985. Cyclic GMP directly regulates a cationic conductance in membranes of bovine rods by a cooperative mechanism. *Journal of Biological Chemistry* 260: 6788-6800.

Koch, K.W. & L. Stryer. 1988. Highly cooperative feedback control of retinal rod guanylate cyclase by calcium ions. *Nature* 334: 64-66.

Körschen, H.G., M. Illing, R. Seifert, F. Sesti, A. Williams, S. Gotzes, C. Colville, F. Müller, A. Dosé, M. Godde, L. Molday, U.B. Kaupp, and R.S. Molday. 1995. A 240K protein represents the complete β-subunit of cyclic nucleotide-gated channel from rod photoreceptor. *Neuron* 15: 627-636.

Krapivinsky, G.B., G.N. Filatov, E.A. Filatova, A.L. Lyubarsky, and E.E. Fesenko. 1989. Regulation of cGMP-dependent conductance in cytoplasmic membrane of rod outer segments by transducin. *FEBS Letters* 247: 435-437.

Kühn, H., S.W. Hall, and U. Wilden. 1984. Light-induced binding of 48-kDa protein to photoreceptor membranes is highly enhanced by phosphorylation of rhodopsin. *FEBS Letters* 176: 473-478.

Lagnado, L., L. Cervetto, and P.A. McNaughton. 1992. Calcium homeostasis in the outer segments of retinal rods from the tiger salamander. *Journal of Physiology* 455: 111-142.

Light, D.B., J.C. Corbin, and B.A. Stanton. 1990. Dual ion-channel regulation by cyclic GMP and cyclic GMP-dependent protein kinase. *Nature* 344: 336-339.

Lindstrom, J., R. Schoepfer, and P. Whiting. 1987. Molecular studies of the neuronal nicotinic acetylcholine receptor family. *Molecular Neurobiology* 1: 281-337.

Lolley, R.N., and E. Racz. 1982. Calcium modulation of cyclic GMP synthesis in rat visual cells. *Vision Research* 22: 1481-1486.

Ludwig, J., T. Marglit, E. Eismann, D. Lancet, and B. Kaupp. 1990. Primary structure of a cAMP-gated channel from bovine olfactory epithelium. *FEBS Letters* 270: 24-29.

MacKinnon, R. 1995. Pore loops: an emerging theme in ion channel structure. *Neuron* 14: 889-892.

Matthews, G. & S.I. Watanabe. 1987. Properties of ion channels closed by light and opened by guanosine 3′,5′-cyclic monophosphate in toad retinal rods. *Journal of Physiology* 389: 691-715.

Matthews, G. & S.I. Watanabe. 1988. Activation of single ion channels from toad retinal rod inner segments by cyclic GMP: concentration dependence. *Journal of Physiology* 403: 389-405.

McCarthy, M.P., J.P. Earnest, E.F. Young, S. Choe, and R.M. Stroud. 1986. The molecular neurobiology of the nicotinic acetylcholine receptor. *Annual Review of Neuroscience* 9: 383-413.

Menini, A. 1990. Currents carried by monovalent cations through cGMP-activated channels in excised patches from salamander rods. *Journal of Physiology* 424: 167-185.

Miller, C. 1982. Bis-quaternary ammonium blockers as structural probes of the sarcoplasmic reticulum potassium channel. *Journal of General Physiology* 79: 869-891.

Miller, J.L., A.M. Picones, and J.I Korenbrot. 1994. Differences in transduction between rod and cone photoreceptors: an exploration of the role of calcium homeostasis. *Current Opinion in Neurobiology* 4: 488-495.

Molday, L.L., N.J. Cook, U.B. Kaupp, and R.S. Molday. 1990. The cGMP-gated cation channel of bovine rod photoreceptor cells is associated with a 240 kDa protein exhibiting immunochemical cross-reactivity with spectrin. *Journal of Biological Chemistry* 265: 18690-18695.

Molday, R.S. & Y. Hsu. 1995. The cGMP-gated channel of photoreceptor cells: Its structural properties and role in phototransduction. *Behavioral and Brain Sciences* 18: 441-451.

Molday, R.S., L.L. Molday, A. Dose, I. Clark-Lewis, M. Illing, N.J. Cook, E. Eismann, and U.B. Kaupp. 1991. The cGMP-gated channel of the rod photoreceptor cell: Characterization and orientation of the amino terminus. *Journal of Biological Chemistry* 266: 21970-21922.

Morrison, D.F., M.A. Rider, and D.J. Takemoto. 1987. Modulation of retinal transducin and phosphodiesterase activities by synthetic peptides of the phosphodiesterase γ-subunit. *FEBS Letters* 222: 266-270.

Nakatani, K. & K.-W. Yau. 1986. Light-suppressible, cyclic GMP-activated current recorded from a dialysed cone preparation. *Investigations in Ophthalmology and Vision Research Supplement* 27: 300.

Nakatani, K. & K.-W. Yau. 1988a. Calcium and magnesium fluxes across the plasma membrane of the toad rod outer segment. *Journal of Physiology* 395: 695-729.

Nakatani, K. & K.-W. Yau. 1988b. Calcium and light adaptation in retinal rods and cones. *Nature* 334: 69-71.

Nawy, S. & C.E. Jahr. 1990. Suppression by glutamate of cGMP-activated conductance in retinal bipolar cells. *Nature* 346: 269-271.

Nizzari, M., F. Sesti, M.T. Giraudo, C. Virginio, A. Cattaneo, and V. Torre. 1993. Single-channel properties of cloned cGMP-activated channels from retinal rods. *Proceedings of the Royal Society of London* 254: 69-74.

Noda, M., Y. Furautani, H. Takahashi, M. Toyosato, T. Tanabe, S. Shimizu, S. Kikyotani, T. Kayano, T. Hirose, S. Inayama and S. Numa. 1983. Cloning and sequence analysis of calf cDNA and human genomic DNA encoding α-subunit precursor of muscle acetylcholine receptor. *Nature* 305: 818-823.

Numa, S. 1989. A molecular view of neurotransmitter receptors and ionic channels. *Harvey Lecture* 83: 121-165.

Perry, R.J. & P.A. McNaughton. 1991. Response properties of cones from the tiger salamander. *Journal of Physiology* 433: 561-587.

Picco, C. & A. Menini. 1993. The permeability of the cGMP-activated channel to organic cations in retinal rods of the tiger salamander. *Journal of Physiology* 460: 741-758.

Picones, A. & J.I. Korenbrot. 1992. Permeation and interaction of monovalent cations with the cGMP-gated channel of cone photoreceptors. *Journal of General Physiology* 100: 647-673.

Pittler, S.J., A.K. Lee, M.R. Altherr, T.A. Howard, M.F. Seldin, R.L. Hurwitz, J.J. Wasmuth, and W. Baehr. 1992. Primary structure and chromosomal localization of human and rod photoreceptor cGMP-gated cation channel. *Journal of Biological Chemistry* 267: 6257-6262.

Poulter, L., J.P. Earnest, R.M. Stroud and A.L. Burlingame. 1989. Structure, oligosaccharide structures, and posttranslationally modified sites of the nicotinic acetylcholine receptor. *Proceedings of the National Academy of Science* USA 86: 6645-6649.

Press, W.H., S.A. Teukolsky, W.T. Vetterling, and B.P. Flannery. 1992. Numerical recipes in C. 2nd edition. Cambridge University Press. Ch. 15: 683.

Pugh, E.N., & T.D. Lamb. 1993. Amplification and kinetics of the activation steps in phototransduction. *Biochimica et Biophysica Acta* 1141: 111-149.

Reuter, J. and C.F. Stevens. 1980. Ion conductance and ion selectivity of potassium channels in snail neurones. *Journal of Membrane Biology* 57: 103-118.

Schnapf, J.L. & R.N. McBurney. 1980. Light-induced changes in membrane current in cone outer segments of tiger salamander and turtle. *Nature* 287: 239-241.

Schwartzmann, G., H. Weigandt, B. Rose, A. Zimmerman, D. Ben-Haim, and W.R. Loewenstein. 1981. Diameter of the cell-to-cell junctional membrane channels as probed with neutral molecules. *Science* 213: 551-553.

Sekuler, R., and R. Blake. 1994. Perception. 3rd edition. McGraw-Hill, Inc. USA. Chapter 6.

Serway, R.A., and J.S. Faughn. 1989. College Physics. 2nd edition. Saunders College Publishing. Toronto.

Sesti, F., M. Straforini, T.D. Lamb, and V. Torre. 1994. Gating selectivity and blockage of single channels activated by cyclic GMP in retinal rods of the tiger salamander. *Journal of Physiology* 474: 203-222.

Stryer, L. 1983. Transducin and the cyclic GMP phosphodiesterase: amplifier proteins in vision. *Cold Spring Harbor Symposia on Quantitative Biology* 48: 841-852.

Stryer, L. 1986. Cyclic GMP cascade of vision. *Annual Review of Neuroscience* 9: 87-119.

Stryer, L., J.B. Hurley, and B.K. Fung. 1983. Transducin and the cyclic GMP phosphodiesterase of retinal rod outer segments. *Methods in Enzymology* 96: 617-627.

Sugimoto, Y., K. Yatsunami, M. Tsujimoto, H.G. Khorana, and A. Ichikawa. 1991. The amino acid sequence of a glutamic acid-rich protein from bovine retina as deduced

from the cDNA sequence. *Proceedings of the National Academy of Science* USA 88: 3116-3119.

Swenson, R.P. Jr. 1981. Inactivation of potassium currents in squid axon by a variety of quaternary ammonium ions. *Journal of General Physiology* 77: 255-271.

Takio, K., R.D. Wade, S.B. Smith, E.G. Krebs, K.A. Walsh, and K. Titani. 1984. Guanosine cyclic 3′, 5′-phosphate dependent protein kinase, a chimeric protein homologous with two separate protein families. *Biochemistry* 23: 4207-4218.

Taylor, W.R. and D.A. Baylor. 1995. Conductance and kinetics of single cGMP-activated channels in salamander rod outer segments. *Journal of Physiology* 483: 567-582.

Tessier-Lavigne, M. 1991. Phototransduction and information processing in the retina. *In* Principles of neural science, 3rd edition. Kandel, E.R., J.H. Schwartz, and T.M. Jessell, editors. Appleton & Lange. Connecticut. 28: 401-417.

Tomita, T., A. Kaneko, M. Murakami, and E.L. Pautter. 1967. Spectral response curves of single cones in the carp. *Vision Research* 7: 519-531.

Torre, V., H.R. Matthews, and T.D. Lamb. 1986. Role of calcium in regulating the cyclic GMP cascade of phototransduction in retinal rods. *Proceedings of the National Academy of Science* USA 83: 7109-7113.

Unwin, N. 1989. The structure of ion channels in membranes of excitable cells. *Neuron* 3: 665-676.

Villaroel, A., O. Alvarez, A. Oberhauser, and R. Latorre. 1988. Probing a calcium-activated potassium channel with quaternary ammonium ions. *Pflügers Archives* 413: 118-126.

Watson, J.D., M. Gilman, J. Witkowski, and M. Zoller. 1992. Recombinant DNA. 2nd edition. W.H. Freeman and Company. New York. Chapter 26.

Wolfart, P., H. Haase, R.S. Molday, and N.J. Cook. 1992. Antibodies against synthetic peptides used to determine the topology and site of glycosylation of the cGMP-gated channel from bovine rod photoreceptors. *Journal of Biological Chemistry* 267: 644-648.

Wolfart, P., H. Muller, and N.J. Cook. 1989. Lectin binding and enzymatic deglycosylation of cGMP-gated channel from bovine rod photoreceptors. *Journal of Biological Chemistry* 264: 20934-20939.

Woodhull, A.M. 1973. Ionic blockade of sodium channels in nerve. *Journal of General Physiology* 61: 687-708.

Woodruff, M.L. & G.L. Fain. 1982. Light-dependent ion influx into toad photoreceptor cells. *Annual Review of Neuroscience* 12: 289-327.

Yau, K.-W., & D.A. Baylor. 1989. Cyclic GMP-activated conductance of retinal photoreceptor cells. *Annual Review of Neuroscience* 12: 289-327.

Yau, K.-W. & K. Nakatani. 1984. Electrogenic Na-Ca exchange in retinal rod outer segment. *Nature* 311: 661-663

Yau, K.-W. & K. Nakatani. 1985. Light-induced reduction in cytoplasmic free calcium in retinal rod outer segment. *Nature* 313: 579-582.

Yau, K.-W., L.W. Haynes, and K. Nakatani. 1986. Roles of calcium and cyclic GMP in visual transduction. *In* Control of cellular activity. H.C. Lüttgau, editor. Fischer, Stuttgart, and Sinaur Associates, Inc. MA. :343-366.

Yellen, G. 1987. Permeation in potassium channels: Implications for channel structure. *Annual Review of Biophysics and Biophysical Chemistry* 16: 227-246.

Yellen, G., M.E. Jurman, T. Abramson, and R. MacKinnon. 1991. Mutations affecting internal TEA blockage identify the probable pore-forming region of potassium channels. *Science* 251: 939-942.

Zar, J.H. 1984. Biostatistical Analysis. 2nd edition. Prentice-Hall, Inc. Englewood Cliffs, N.J. Chapters 8, 17, and 18.

Zimmerman, A.L. & D.A. Baylor. 1986. Cyclic-GMP sensitive conductance of retinal rods consists of aqueous pores. *Nature* 321: 70-72.

Zimmerman, A.L., & D.A. Baylor. 1992. Cation interactions within the cyclic GMP-activated channel of retinal rods from the tiger salamander. *Journal of Physiology* 449: 759-783.

Zuckerman, R., B. Buzdygon, N. Philp, P. Liebman, and A. Litaramayya. 1985. Arrestin: an ATP/ADP exchange protein that regulates cGMP phosphodiesterase activity in retinal rod disk membranes. *Biophysical Journal* 47: 37a.